Western Graduate&PostdoctoralStudies

Western University
Scholarship@Western

Electronic Thesis and Dissertation Repository

4-25-2013 12:00 AM

# Climate Change Impact on Flood Hazard in the Grand River Basin, Ontario, Canada

Abhishek Gaur
*The University of Western Ontario*

Supervisor
Dr. Slobodan P. Simonovic
*The University of Western Ontario*

Graduate Program in Civil and Environmental Engineering
A thesis submitted in partial fulfillment of the requirements for the degree in Master of Engineering Science
© Abhishek Gaur 2013

Follow this and additional works at: https://ir.lib.uwo.ca/etd

 Part of the Other Civil and Environmental Engineering Commons

## Recommended Citation

Gaur, Abhishek, "Climate Change Impact on Flood Hazard in the Grand River Basin, Ontario, Canada" (2013). *Electronic Thesis and Dissertation Repository*. 1232.
https://ir.lib.uwo.ca/etd/1232

This Dissertation/Thesis is brought to you for free and open access by Scholarship@Western. It has been accepted for inclusion in Electronic Thesis and Dissertation Repository by an authorized administrator of Scholarship@Western. For more information, please contact wlswadmin@uwo.ca.

# CLIMATE CHANGE IMPACT ON FLOOD HAZARD IN THE GRAND RIVER BASIN, ONTARIO, CANADA

(Thesis format: Monograph)

by

Abhishek Gaur

Graduate Program in Civil and Environmental Engineering

A thesis submitted in partial fulfillment of the requirements for the degree of Master of Engineering Science

The School of Graduate and Postdoctoral Studies
Western University
London, Ontario, Canada

© Abhishek Gaur 2013

# ABSTRACT

Rapidly changing climatic conditions across the globe are believed to have an impact on key climate variables and the hydrologic cycle. Changes in magnitude and frequency of peak flow patterns have been noted in rivers worldwide. The associated risk is projected to increase many folds during the 21$^{st}$ century. Therefore, it is necessary to quantify these impacts for effective water resource planning and management in future. Methodology chosen to do so should be able to capture variations in climate variables at fine temporal, spatial and distributional scales. Also, it should be able to cover uncertainties associated with future climatic, socio-economic and physiographic projections. In this study, a methodology for making future flow projections has been presented and applied to the Grand River basin, Ontario, Canada. Results indicate consistent decreases in peak flows across the catchment for all the scenarios considered in the analysis.

**KEYWORDS**

Climate change, Uncertainty, Flood frequency, Global Climate Models

Dedicated to my *Teachers*, *Parents* and *Bhagwan*

# ACKNOWLEDGEMENTS

I want to express my immense gratitude towards my supervisor Dr. Slobodan P. Simonovic for his continued guidance and support over the past two years. His knowledge, experience and insights have led to this research. But more than that, he helped me immensely at a personal level during my "homesick-international-graduate-student" days. He has been very understanding, patient, kind and caring towards me. It is a privilege to be called as one of his students and i'm hopeful to receive his blessings in future as well.

I am also indebted to Dr. Hao Yu, who taught me the basics of R Programming language. Given the amount of work involved, this thesis would have remained a dream without his guidance. Also, i'd like to thank Dr. Gordon McBean who helped me realize the bigger picture of climate change and its impacts on society and Dr. Brian Luckman for providing useful guidance about report writing. I want to convey a special thanks to Dr. Nickolas Kouwen for providing the calibrated WATFLOOD model and being very helpful and responsive to my queries. Further, i want to thank Dr. S.E. Perkins and Dr. C. Piani for providing useful guidance during the research process. I'm also thankful to Tom Arsenault from Environment Canada for providing Grand River catchment shapefiles, Mr. Dwight Boyd and Miss Stephanie Shifflett from the GRCA for providing catchment datasets. Also, i want to acknowledge the guidance, love and encouragement offered by my professors back in India. Without their vision and blessings, i would not have been able to study at Western on the first place.

I cannot find words to express my gratitude towards my parents and my two lovely sisters who always find their entire world revolving around me. Their blessings and pristine love has always been a source of inspiration for me and i want to thank them for always being there whenever i needed them.

I want to thank my friends at FIDS and home for their support and friendship. A special mention to Angela, Vladimir, Roshan and Samiran for providing constant assistance at professional and personal levels. Also, want to thank Shubhajit, Shreyas, Tomo and Rahul for their friendship and for making my stay at Western a memorable one.

Lastly and most importantly, i want to thank my *Bhagwan* for blessing me with everyone mentioned before and i seek for his continued bliss in future.

## TABLE OF CONTENTS

## LIST OF FIGURES

## LIST OF TABLES

## List of Acronyms

| | |
|---|---|
| AET | Actual Evapo-Transpiration |
| AM | Annual Maximum |
| AR4 | Fourth Assessment Report (Issued by the IPCC) |
| CDCD | Canadian Daily Climate Data |
| CDF | Cumulative Distribution Function |
| CF | Change Factor |
| CMIP | Coupled Model Inter-comparison Project |
| DOS | Disk Operating System |
| ECDF | Empirical Cumulative Distribution Function |
| FORTRAN | (IBM Mathematical) FORmula TRANslating System |
| GCM | Global Climate Model |
| GHG | Green House Gas |
| GHM | Global Hydrologic Model |
| GPD | Generalised Pareto Distribution |
| GRCA | Grand River Conservation Authority |
| IEP | Interception EvaPoration |
| IPCC | Intergovernmental Panel for Climate Change |
| MME | Multiple Model Ensembles |
| NARR | North-American Regional Reanalysis |
| NCAR | National Centre for Atmospheric Research |
| NCDIA | National Climate Data and Information Archive |
| NCEP | National Centres for Environmental Protection |
| NetCDF | Network Common Data Forum |
| P | Precipitation |
| PDSI | Palmer Drought Severity Index |
| Pdf | Probability density function |
| PET | Potential Evapo-Transpiration |
| POT | Peak Over Threshold |
| PWM | Probability Weighted Moments |
| Q-T | flood magnitude (Q) – return period (T) |
| R | Range |
| RAOBS | RAdiOsonde database |
| RCM | Regional Climate Model |
| RMSE | Root Mean Square Error |
| SRES | Special Report on Emission Scenarios |
| T | Temperature |
| TAR | Third Assessment Report (Issued by the IPCC) |
| UNIX | UNiplexed Information Computing System |
| WG | Weather Generator |
| WCRP | World Climate Research Programme |
| WWF | World Water Forum |

# 1 INTRODUCTION

This chapter states the primary objective of this research and highlights contribution of this research towards the state of the art in climate change impact studies. Steps performed in a typical climate change impact study are presented and discussed. Climate change and its impact on key climate variables, for example temperature, precipitation, and on flow patterns are discussed on a global scale. Further, observed and projected impacts of climate change are discussed for the region of Canada with a focus on South-Western Ontario. A broad outline of the thesis is presented in the end.

## 1.1 Research objective

The primary objective of this research is to quantify the impacts that climate change has on flooding frequency for the Grand River, Ontario. To do so, a climate change impact study is performed on the Grand River catchment at Brantford. The Brantford catchment is selected because it encompasses major urban centres along the river; includes the majority of the catchment's population; is data rich; and covers an area of approximately 80% of the entire Grand River catchment.

## 1.2 Research contributions

Modelling climate change impact on water resources is a complex task. Uncertainties exist at each step in the climate change impact analysis process as shown in Figure 1. Broadly speaking, six different sources of uncertainty have been identified in literature. Uncertainties may arise from Global Climate Model structure, future greenhouse gas emission scenarios, downscaling of GCM outputs, hydrological model structure, hydrological model parameters and the internal variability of the climate system (Kay, Davies, Bell, & Jones, 2009). However, uncertainties may also exist outside the paradigm of these six primary sources. Chen, Haerter, Hagemann, & Piani, (2011) considered the decade used for deriving bias correction parameters as one of the three major sources of uncertainties associated. Hagemann et al., (2011) notes that uncertainty associated with bias correction step may be of an order equal to that associated with climate model projections. Climate model initial conditions, land-use change, natural variability of climate, choice of appropriate change factor methodology, choice of flood frequency analysis

methodology are only some of many other uncertainties associated with the climate change impact analysis process.

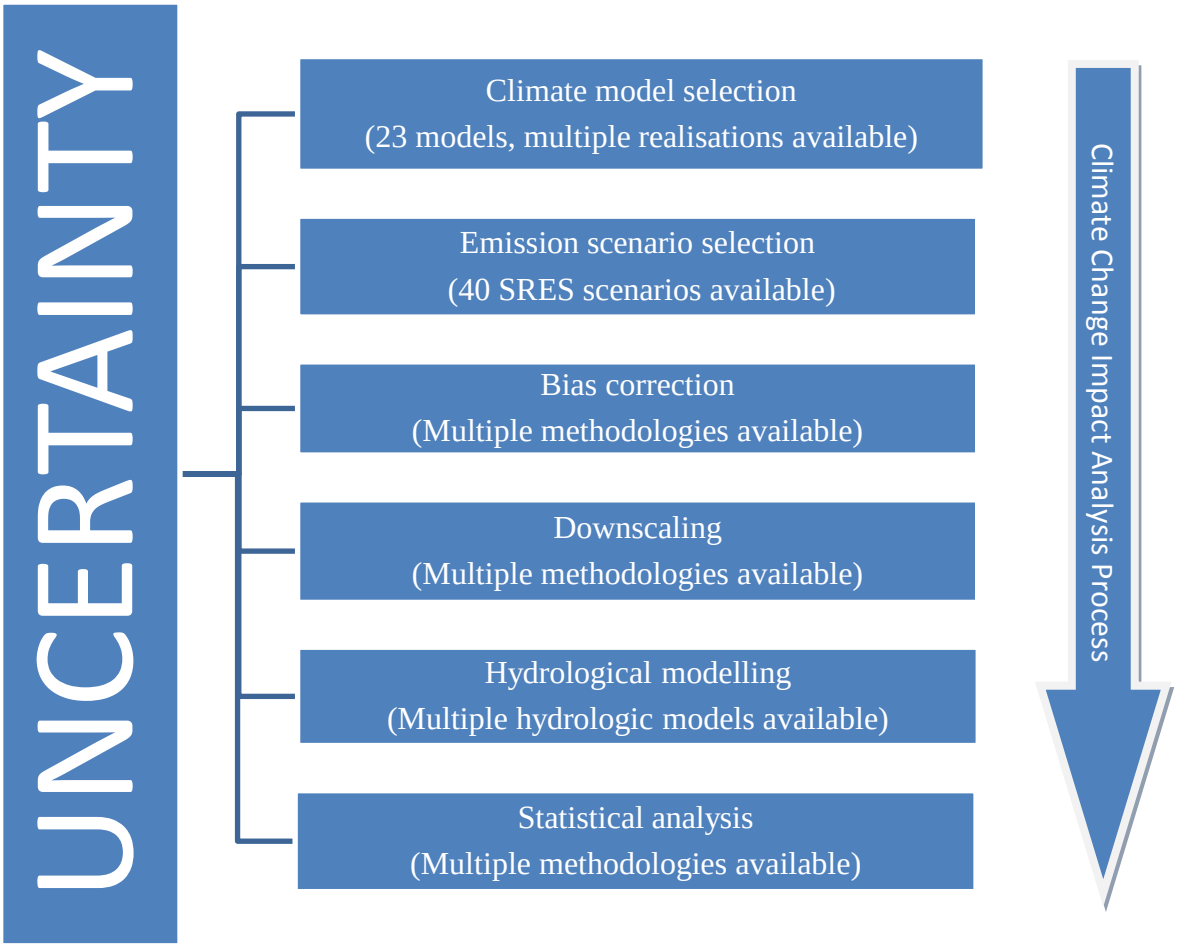


**Figure** 1. Steps and uncertainties involved in the climate change impact analysis process

Since it seems impossible to capture all the uncertainties associated with the process, identification and accounting for major sources of uncertainty seems a more pragmatic way of approaching the problem. Several studies have been performed to quantify relative contribution of different sources of uncertainty towards the total uncertainty. To this end, Jung, Chang, & Moradkhani, (2011) compared five sources of uncertainty viz. those related to GCM structures, future GHG emission scenarios, land-use change scenarios, natural variability and hydrologic model parameters to estimate their relative impact on flood frequencies across two catchments with different extents of urbanisation. Kay et al., (2009) analysed uncertainties contributed by GCM structure, downscaling methodologies, hydrological model structure, hydrological model parameters and internal variability of climate system and compared their impacts on flood

frequency across two catchments in England. Kingston & Taylor, (2010) compared uncertainties associated with GCM structures, climate variability and hydrologic parameterisation to quantify the impact of climate change on freshwater resources in the upper Nile basin in Uganda. Wilby & Harris, (2006) simulated future low flow scenarios for Thames River (UK) by using four GCMs, two GHG scenarios, two statistical downscaling techniques, two hydrological model structures and two sets of hydrological model parameters. In almost all of these studies, uncertainty associated with future climate projections has been identified as a prime contributor towards the total uncertainty associated with the climate change impact analysis process. Therefore, the *major focus of this study is towards encompassing future climate projection uncertainty* i.e. uncertainties contributed by GCM structure, future greenhouse gas scenarios and climate variability while other sources of uncertainty are neglected.

Another region of focus of this study is *to analyse whole distributions of climate data* instead of individual statistics. Changes in climate extremes have been projected to be many folds higher than climate normals in future (IPCC, 2012). An increase in the intensity and frequency of climate extremes is projected to have significant socio-economic and environmental impacts on society in future. Therefore, IPCC, (2012) emphasises on accurate predictions of future climate extremes. Probability distributions have been utilised to study past trends in climate extremes (Alexander et al., 2006; Kiktev, Sexton, Alexander, & Folland, 2003). Climate models have been evaluated by comparing entire distributions of model and observed data (Perkins, Pitman, Holbrook, & McAneney, 2007). Different bias correction methodologies correcting entire distributions of climate model data have been proposed and are found to perform better than traditional methods (Piani et al., 2010). Further, multiple change factors associated with specific percentiles of whole distribution have been found to be more effective in transferring changes projected by climate models than a single change factor (Anandhi et al., 2011). These methods and others available from literature are employed in this study for the synthesis of future climate variables in the best possible manner.

An appropriate temporal scale has been selected for this study based on the recommendations made in the past. Although majority of climate change studies have been performed on monthly or yearly timescales, the importance of evaluation of climate models on a daily temporal scale is highlighted in Perkins et al., (2007). Similar recommendations supporting the use of daily change

factors over monthly change factors is made in King, (2012). Therefore, a *daily temporal scale is adopted for use in the present study*.

## 1.3 The climate change impact analysis process

Flowchart of a typical climate change impact analysis process is provided in Figure 1. First, selection of climate models is made from a pool of climate models mentioned in IPCC, (2007) for regional climate change impact analysis. Atmosphere Ocean Global Climate Models (AOGCMs) are the approximate mathematical representations of physical processes occurring within the climate system. They provide us with the best possible estimates of historical and future climate data worldwide. Model performance is generally evaluated based on it's ability to simulate past and present regional climate. The ability of climate models towards replicating past and present climate has been found to vary spatially across the globe (Maxino, Mcavaney, Pitman, & Perkins, 2008). Therefore, quantification of their skills at the regional scale becomes important before a model is used in making future climate predictions. To consider the uncertainty involved in using climate models, an ensemble of outputs from a group of regionally skilled climate models (or Multiple Model Ensembles, MMEs) is preferred over a single model output (IPCC, 2007).

The selection of regionally efficient climate models is followed by the selection of future emission scenarios for analysis. Future emission scenarios are formulated based on future projections of global demographics, economics and technological advancements. Future climate data is generated based on these projected emission patterns. In the Third Assessment Report (TAR) issued by IPCC (IPCC, 2000), a group of forty Special Report on Emission Scenarios (SRES) scenarios are formulated from six scenario groups (A1F1, A1T, A1B, A2, B1 and B2) following four storylines (A1, A2, B1 and B2). The hierarchy of SRES scenarios and an explanation of different storylines is provided in Appendix A. Although each scenario mentioned in TAR has an equal probability of occurrence in future (IPCC, 2000), scenarios A2, B1 and A1B have been most widely used in climate change impact studies since they, more or less, cover the entire range of emission uncertainties exhibited by SRES scenarios (IPCC, 2007).

Climate data obtained from Global Climate Models (GCMs), as well as from higher resolution Regional Climate Models (RCMs), are associated with some time-independent

component of model errors called biases (Ehret, Zehe, Wulfmeyer, Warrach-Sagi, & Liebert, 2012). Several bias correction methodologies correcting single (Graham et.al. 2007), or multiple moments (Piani et al., 2010) of model data distribution have been proposed in literature. Corrections are generally made with respect to historically observed gauge data (Sharma, Das Gupta, & Babel, 2007) or reanalysis data (Piani et al., 2010) within the area of study. A more detailed discussion on bias correction methodologies is provided in section 2.1.4 of the report.

Coarsely gridded GCM data requires pre-processing before it can be used for catchment scale hydrologic analysis. Downscaling is method for improving the spatial resolution of Global Climate Model (GCM) outputs. There are two accepted methods of doing so. First method is known as the dynamic downscaling; where higher resolution Regional Climate Models (RCMs) are used in conjunction with GCMs to obtain more accurate regional climate data. Another less computationally demanding method for downscaling GCM data is known as statistical downscaling. It is based on the principal that regional data is dependent on large scale climate state as well as local physiographic features (IPCC, 2001). Information regarding large scale climate state is generally extracted from the GCMs while several parametric, semi-parametric and non-parametric methods are employed to transfer this large scale information to regional scales. A special class of downscaling tool called weather generator is very popular. They have been discussed in more detail in section 2.1.5 of this report.

Bias-corrected and downscaled GCM output is then used as input into a hydrological model to generate flow patterns for the area of study. Based on the spatial extents of the catchment under study, lumped, semi-distributed or distributed hydrologic models can be used to generate flow response from projected future climate variables. In a typical climate change impact study, statistical analysis is performed on the simulated future and historically observed flood peaks to infer probable changes in peak flow return periods in future.

## 1.4 Literature review

According to IPCC, (2012) any detectable change in the state of climate which persists over a considerable period of time (more than a decade) can be referred to as climate change. Both

natural (such as periodic changes in solar irradiance) and man-made (such as GHG emissions, changes in land-use patterns etc.) sources can be responsible for changes observed within the climate system. However, role of anthropogenic factors towards climate change has been found to be significant as compared to other sources (Huber & Knutti, 2011; IPCC,2007).

Carbon-di-oxide is an important greenhouse gas, which has increased significantly since the industrial revolution, primarily due to increased consumption of fossil fuels and rapid land use change. According to IPCC, (2007) atmospheric concentration of $CO_2$ in 2005 was higher than that experienced in the past 6,50,000 years and annual $CO_2$ growth rate continues to increase each passing year. Similar trends have also been recorded for other greenhouse gases such as methane and nitrous oxide. Due to the changes in environmental chemistry, changes in the mean, standard deviation and extremes of key climate variables are being observed. There has been an unprecedented increase in global mean temperature in the last 25 years (see Figure 2). Changes in precipitation patterns have also been noted worldwide. Figure 3 depicts changes in precipitation patterns observed indirectly using a Palmer Drought Severity Index (PDSI) which is calculated by analysing antecedent and current precipitation and evaporation data (calculated from mean temperature) at a location. In Figure 3a, red and orange areas are drier (or wetter) while green and blue areas are wetter (or drier) than normal when PDSI values are positive (or negative) in Figure 3b. A distinct post-1975 shift in PDSI regime can be noted from Figure 3b which suggests a subsequent change in spatial PDSI patterns across the globe (Figure 3a). A change in climate variables other than precipitation and temperature have also been reported (IPCC, 2007).

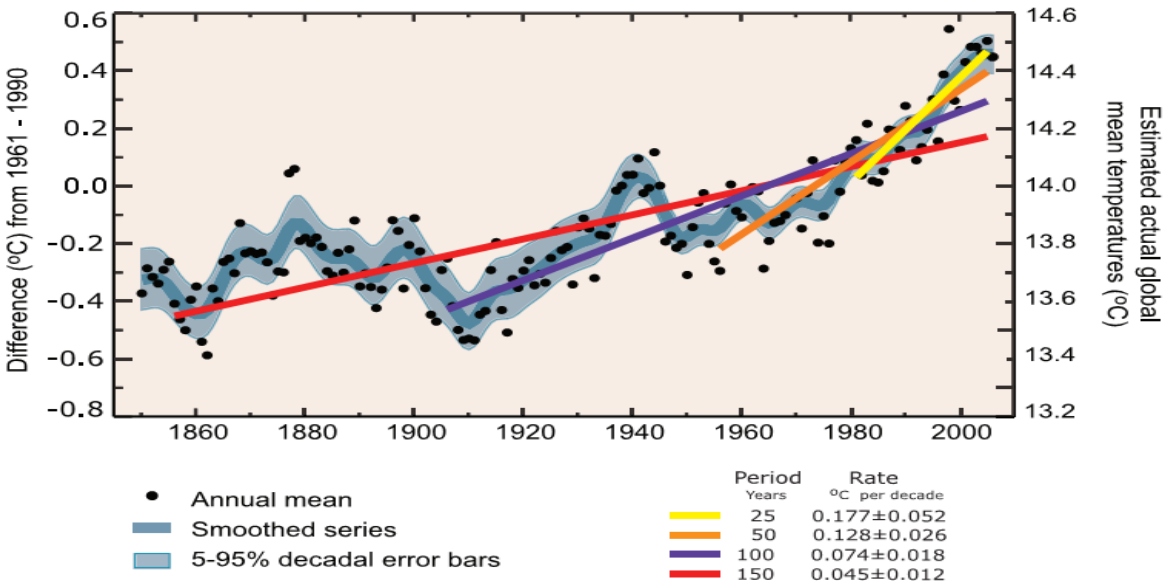


**Figure 2**.Global annual mean temperatures for the duration 1856-2005 (plotted in black dots). Left hand axis shows temperature anomalies with respect to average temperatures recorded in the period 1961-1990 while right hand axis shows absolute temperature values in degree celcius. Linear trend fits in yellow, orange, purple and red correspond to time-periods 1981-2005, 1956-2005, 1906-2005 and 1856-2005 respectively. (after IPCC, 2007)

Since hydrologic behaviour of a catchment is governed by feedbacks from various climatic and ecologic variables, relationships between them are difficult to formulate. An extensive Canada-wide study highlighting this relationship has been performed by Whitfield & Cannon, (2000). Changes observed in precipitation, temperature and streamflow between the decades 1976-1985 and 1986-1995 are grouped into different classes or clusters. After analysing the spatial distribution of these climatic and hydrologic clusters obtained from 210 temperature, 271 precipitation and 642 hydrology stations, they noted distinct linkages between climate variables, hydrologic responses of streams and ecozones within Canada. The study also highlights that even small changes in climate variables may result in significant changes in a region's hydrologic characteristics.

By reconstructing monthly discharges of the largest worldwide rivers, Labat, Godd, Probst, & Guyot, (2004) estimated a 4% increase in global runoff every 1ºC rise in global temperatures over the last century. Further, IPCC, (2007) projects a range of 1.8ºC (low emission scenario) to 4ºC (high emission scenario) in global mean temperature change (relative to temperatures

observed during 1980-1999) for the 21st century. It is anticipated that this change in global mean temperature will produce unprecedented changes in hydrologic regimes across the globe.

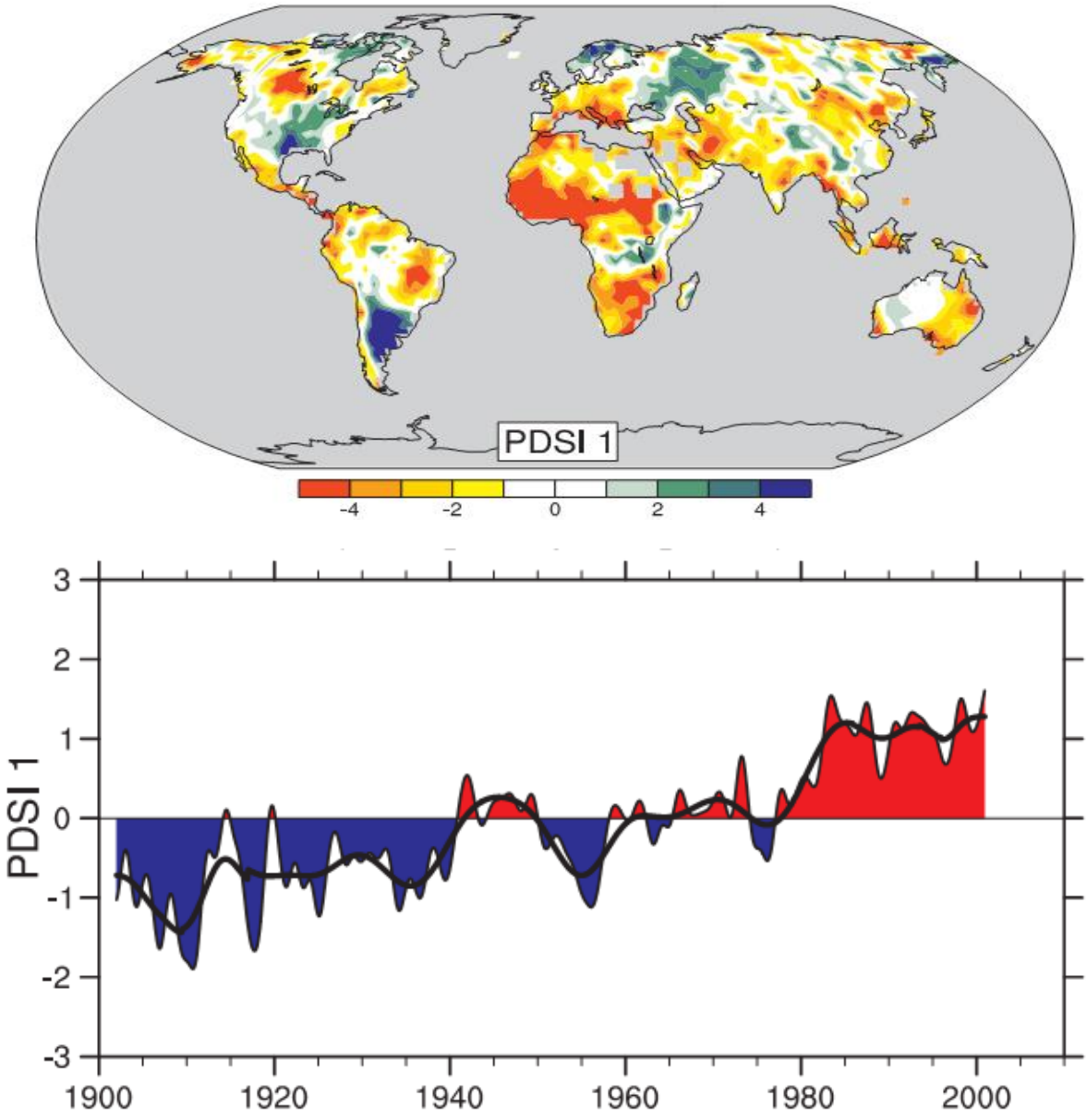


**Figure 3** (a) Spatial distribution of monthly Palmer Drought Severity Index (PDSI) for the duration 1900-2002. (b) Temporal variability in PDSI (after IPCC, 2007)

The impact of climate change has been identified on precipitation and temperature extremes. According to IPCC, 2012 there is a strong likelihood that since 1950, the number of cold days

and nights has decreased, whereas the number of hot days and nights has increased globally. An increase in anthropogenic emissions has been identified as the most likely cause for this change. Further, it has been projected following the SRES A2 and A1B scenarios that by the end of 21st century, a 1 in 20 year return period annual hottest day event may become 1 in 2 year return period event (except for high latitudes of Northern America where it will become a 1 in 5 year event). Changes in precipitation extremes have also been detected worldwide. Most consistent increases in precipitation extremes have been noted across the North American sub-continent. It has been projected that towards the end of 21st century, a 1 in 20 year return period annual maximum 24-hour precipitation rate event will change to 1 in 5 to 1 in 15 year return period event.

Change in frequencies of flood and drought events has also been reported. Since 1950, droughts have become more frequent and intense in southern Europe and western Africa, while they have become less frequent and intense in central North America and northwestern Australia (IPCC, 2012). In the case of flooding, precise identification of changes in historical flooding trends and their attribution to climate change has not been possible as of yet. However, there is evidence suggesting a shift in the timing of spring peak flows. Due to excessive warming and subsequent melting of winter snow accumulations, spring peak flows of the past have been detected to occur during winters or early springs. Further, global (Hirabayashi, Kanae, & Emori, 2009) and continental scale (Dankers & Feyen, 2009) studies project an increase in flood hazard worldwide, except for central to western Eurasia and northern parts of North America where a decrease in flood hazard is projected.

Changing climate has induced changes in temperature and precipitation patterns across Canada. These changes vary spatially, with frequency, duration and intensity of cold spells decreasing around western and increasing around eastern regions of Canada (Groisman et al., 2002; Shabbar & Bonsal, 2003). Winter warm spells are increasing in both frequency and duration across all of Canada, with one exception in the extreme north-eastern regions where warm spells are becoming shorter and less frequent (Shabbar & Bonsal, 2003). Precipitation has increased in almost all parts of Canada during the last 50 years. An average increase of 5% has been observed in annual total precipitation for the entire country, while an increment of 12% has been observed in southern Canada indicating that the changes in precipitation are not uniform

spatially. Further, precipitation has been found to increase during spring, summer and autumn while the ratio of snowfall to total rainfall has been decreasing in winter and spring especially along the western part of the country (Barrow, Maxwell, & Gachon, 2004). This observation is consistent with the warming trends observed along the western regions of Canada.

Changes in major climatic variables such as temperature and precipitation also affect the flow patterns of Canadian rivers. Annual maximum and mean daily flows are significantly increasing in northern British Columbia, Yukon Territory and southern Ontario. On the other hand, a decreasing trend is observed in the southern regions of British Columbia (Environment Canada, 2004). Studies also estimate a decrease of approximately 10% in annual river discharge in the period 1967 to 2003 for rivers situated in the northern regions of Canada (Déry, 2005). More recently, an extensive study analysing present and projected future flows of ten rivers with varying geography, ecosystem and drainage basins situated across Canada (Figure 4). They projected a steady and decreasing flow trends across all the selected rivers except River Nipigon ( WWF-Canada, 2009).

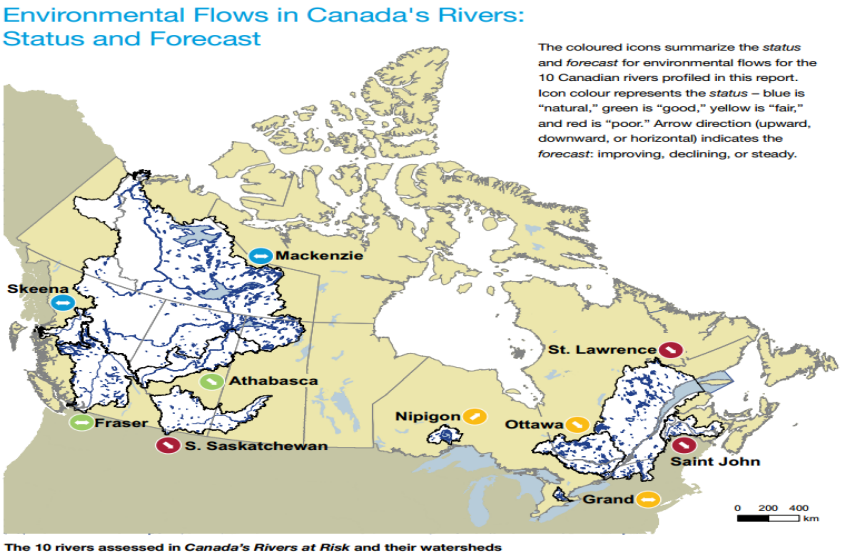


**Figure 4.** Present and future flow trends of ten Canadian rivers assessed in Canada's Rivers at Risk project (after WWF-Canada, (2009))

The number of flooding events has increased over the last 50 years, with 70% of flooding events occurring after 1959. It has also been estimated that 62% of these flood disasters have been caused by snowmelt runoff, storm rainfall or their combinations (Brooks *et al*., 2001). A detailed study of the 168 flood disasters between 1990 and 1997 revealed that most of these

occurred in densely populated areas. For example, it is found that 62% of these disasters occurred in four intensely populated provinces: Ontario (37 events), New Brunswick (26 events), Québec (23 events) and Manitoba (18 events) while relatively few disasters are observed in sparsely populated provinces of Northwest Territories (5 events), and Yukon (3 events) (Shrubsole, Lacroix, & Simonovic, 2003). This suggests that the amount of *flood risk* (defined as the product of flood probability or hazard, and exposure of capital and population to that hazard) is gradually increasing across Canada.

Historical records suggest a shift towards milder winter and warmer summers in the south-western regions of Ontario. This region experiences frequent precipitation extremes due to large amounts of water vapour in the atmosphere because of close proximity of the Great Lakes. Between 1979 to 2004, south-western Ontario experienced the greatest number of heavy rainfall events within the province of Ontario (Report of the Expert Panel on Climate Change Adaptation, 2009). Temperature and precipitation means and extremes are projected to further increase in future across south-western Ontario. A decreased annual runoff, increased winter and spring flows, lower summer and fall flows, and increased frequency of high flows is projected for the 21$^{st}$ century in this region (Lemmen et. al. 2008). Due to high population density and high industrialisation in the region, south-western Ontario is considered to be at highest degree flood risk in the entire province. This highlights the importance of an extensive climate change impact study for this region.

In this thesis, chapter 2 describes the methodology adopted for performing climate change impact analysis on Grand River at Brantford catchment. Procedure followed and results obtained when proposed methodology is applied to the Grand River at Brantford catchment are explained in Chapter 3. Conclusions established are given in Chapter 4, which is followed by references and appendices.

# 2 METHODOLOGY

The procedure followed while performing a climate change impact study on *Grand river at Brantford* catchment can be subdivided into three major sections: *(i)* future climate projections uncertainty analysis, *(ii)* hydrological modelling and *(iii)* statistical analysis of the simulated future flow series.

The process of encompassing future climate projection uncertainty is carried out by first selecting a group of regionally efficient Global Climate Models (GCMs). The Probability density function (Pdf) analysis approach is employed to rank GCMs. Above approach, originally proposed by Perkins et al., (2007), has been used to rank climate models in Australia and other regions of the world (Maxino et al., 2008). A slight modification is made in the methodology to promote the selection of GCMs projecting variable extremes accurately. A test of robustness in model rankings is performed by comparing model rankings obtained with and without using reanalysis data (alongside historically observed data) as the reference data. Future emission scenarios: A2, B1 and A1B are used to cover the uncertainty associated with future greenhouse gas emissions. All possible GCM-scenario combinations are evaluated and five combinations spreading across the entire range of future climate projections are selected for time slices 2045-2065 (2050s) and 2080-2100 (2090s) using percentile method. Historical and future GCM data, corresponding to selected GCM-scenario combinations is bias-corrected using statistical bias correction approach. Statistical downscaling is performed on bias-corrected GCM data using a non-parametric weather generator KNN-CAD (v4) and 50 plausible future precipitation and mean temperature timeseries are generated for future timelines 2050s and 2090s. Simulated future precipitation and temperature combinations most likely to produce hydrological extremes (i.e. Wet-Hot, Wet-Cold, Dry-Hot, Dry-Cold) are selected using scatter-plot method. Two extreme variability scenarios capturing sub-daily temperature variability are combined with selected hydro-climatic extreme scenarios to obtain eight scenarios capturing daily and sub-daily scale uncertainty associated with future climate projections.

Temperature and precipitation timeseries corresponding to selected scenarios are used as inputs into a semi-distributed hydrologic model WATFLOOD. Future flow series are generated by performing a continuous hydrological simulation on selected timeseries.

Statistical analysis is performed on the simulated future and historical observed flowseries. Flow peaks are selected using Peak Over Threshold (POT) method and a Generalised Pareto Distribution (GPD) is used to fit the selected flood peaks. Flood magnitude vs. return period plots are generated for historically observed and generated future flowseries. Obtained results are compared to identify possible impacts of climate change on peak flow frequencies across the Grand River catchment.

## 2.1 Future climate projections uncertainty analysis

This section describes the methodology adopted to encompass future climate projections uncertainty. Procedures followed for selection of Global Climate Models (GCMs), future emission scenarios, bias-correction and downscaling of GCM outputs and selection of extreme projected future scenarios for hydrological modeling have been explained in detail here.

### 2.1.1 Selection of regionally efficient Global Climate Models (GCMs)

Future climate projected by climate models continue to differ from each other significantly. Since future climate records are unavailable for comparison, climate models are generally evaluated based on their ability to replicate historically observed climate. Climate models have been evaluated based on observed climatology in the past (for example Tebaldi, 2004) and it is an established method for estimating model skill (IPCC, 2007). This test however, should be considered as a necessary, but not sufficient criterion for evaluation of model skill (Knutti, Furrer, Tebaldi, Cermak, & Meehl, 2010). Reasoning behind this is that climate models are generally calibrated on locally observed datasets and hence, their satisfactory replication of observed trends may not necessarily be a representative of their ability to project future climate well. However, models unable to pass this test should be deemed less reliable than other models performing well (Knutti et al., 2010).

Basic statistical measures (like mean and standard deviation) have been used in the past to evaluate climate models (IPCC, 2001). Recently, Pdfs have been utilised while studying climate change effects at a global (Alexander et al., 2006) and regional (Dessai, 2005; Maxino et al., 2008) scale. There are several advantages of using Pdfs as a scoring metric over other indices evaluating one or more statistical properties of the data distribution. It is a tougher check for

similarity of two distributions since entire distributions are compared to each other. Pdfs are much more robust statistic as compared to sample means which makes them less prone to observational errors (Perkins et al., 2007). Also, if a model is able to satisfactorily replicate the Pdf of historical datasets, it is very likely that it will also be able to simulate Pdfs for future climate as well, since the overlap between them is found to be very large (>90% in most cases) (Maxino et al., 2008; Perkins et al., 2007). Another advantage is that we can safely use datasets of different lengths to generate Pdfs for a particular region. This way, almost every single dataset lying inside the study area can be used in the analysis, which is extremely helpful at places where observed data is intermittent or scarce.

It has also been noted that the skill of GCMs vary spatially and across climate variables (Knutti et al., 2010; Maxino et al., 2008; Perkins et al., 2007; IPCC,2007). In this study, a Probability Density Function (Pdf) based comparison of observed and GCM precipitation and temperature data is performed for the period 1960-2000 to quantify model skills.

Climate variable (daily precipitation and daily mean temperature) gauging stations falling within the area of study and having climate data within the period of study (1960-2000) are used to generate Pdf plots. Similarly, precipitation and mean temperature data from GCM grids falling within the area of study are used to plot Pdfs for all the GCMs considered in the study. An appropriate bin size is selected while generating precipitation and temperature Pdfs. The selection of bin size should be made such that the variations inherent with climate variables are well captured. Figure 5 gives a comparison of changes between observed and modelled climate data, as reflected by Pdfs generated using different bin sizes. It can be noted that the differences between observed and modelled distributions are more accurately reflected by Pdfs generated with lower bin size. While plotting Pdfs for the Australian subcontinent, Perkins et al., (2007) used bin sizes of 1mm/day and 0.5ºC/day while generating Pdfs for precipitation and temperature respectively.

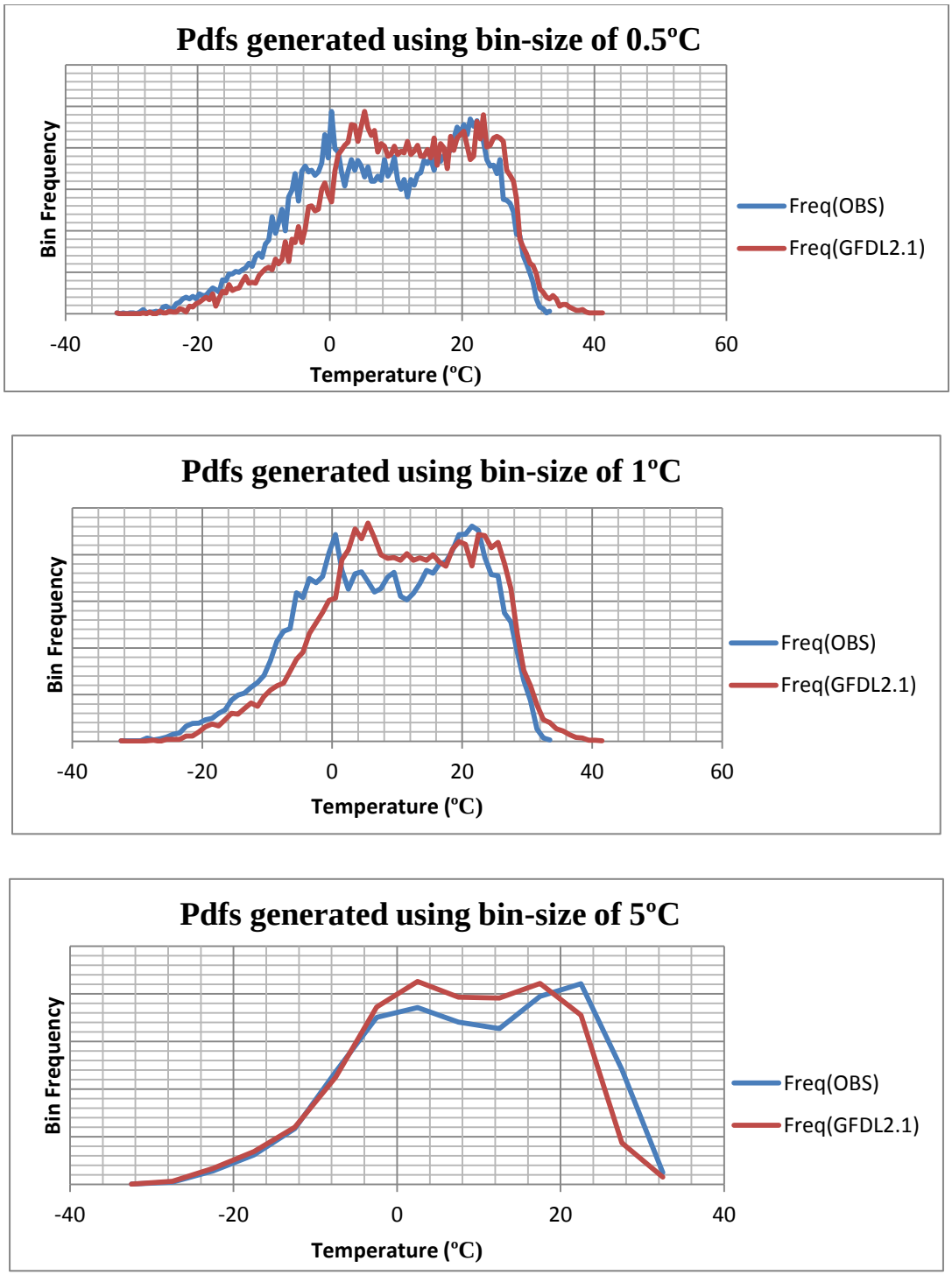


**Figure 5** Comparison of Probability Density Functions generated for historical observed and model data (GFDL2.1) at Apps Mills using bin sizes of 0.5ºC, 1ºC and 5ºC respectively

Skill scores are assigned to climate models based on the amount of overlap between Pdfs generated from historical climate model data and historical observed data. For the same, metric suggested in Perkins et al., (2007) was adopted. This metric calculates the cumulative minimum value of two Pdfs at each bin value, thereby measuring the common area between them. The formula for the metric is expressed as:

$$S_{score} = \sum_1^n min.(Z_m, Z_o) \quad (2.1)$$

Where,

$S_{score}$ is the score associated with a particular climate model. Its value lies between 0-1.

$n$ is the number of bins considered in the analysis

$Z_m$ is the frequency of climate model data in a particular bin

$Z_o$ is the frequency of historical data in a particular bin

Above metric allots a higher skill score to models replicating historical datasets more accurately than others which are unable to do so.

To make GCM rankings more relevant towards analysis of hydro-meteorological extremes, above methodology (taken from Perkins.et.al.2007) is modified by incorporating the concept of bin weights. Purpose of introduction of bin weights in the evaluation procedure is to make GCM rankings more problem-specific. A specific, user-defined weight is associated with each bin to influence the contribution of that bin towards the calculation of total skill score. Distribution of these bin weights is problem-oriented and user-dependent. For example, if GCMs are to be ranked for a future flood flow prediction problem, then a continuously increasing weight structure might be preferred for both precipitation and temperature to allot higher scores to GCMs replicating historical hot and humid conditions accurately. On the other hand, while selecting GCMs for analysing droughts, continuously decreasing weight structure might be preferred for precipitation while continuously increasing structure might be preferred for temperature. Likewise, different weight structures might be tried while analysing different climate problems. Selected bin-weights are multiplied with individual bin scores calculated before to establish the *total skill score* for each GCM.

### 2.1.2 Selection of extreme future GCM-scenario combinations

Model evaluation is carried out either to reduce or to encompass, the uncertainty associated with future climate projections. Reduction in uncertainty can be achieved by averaging outputs from selected climate models (Pierce, Barnett, Santer, & Gleckler, 2009). Uncertainty can be encompassed by considering ensemble of outputs projected by all climate models selected for analysis (Das & Simonovic, 2012). It is often argued if former approach is conceptually sound or effective in reducing model biases. Knutti et al., (2010) studied the effects of model averaging on biases associated with global near surface temperatures for the duration 1970-1999. They found that significant biases remain even after averaging model results from all Coupled Model Intercomparison Project-phase 3 models. This anomalous behaviour is reasoned to occur because of correlated structure of model errors in climate models, which stays unaffected even after averaging model outputs. Additionally, averaging of climate model projections may lead to a loss in signal of projected climate extremes (IPCC, 2007).

The SRES scenarios A2, A1B and B1 are outlined in the Third Assessment Report (TAR) as part of forty scenarios covering the total future emissions uncertainty. These scenarios have been employed in the CMIP3 to prepare "WCRP CMIP3 multi-model datasets" for future (Meehl et al., 2007). They represent "high", "medium" and "low" scenarios with regards to full range of emission forcings projected by the SRES scenarios (see Figure 6). Future projections made by regionally efficient GCMs following selected future emission scenarios are analysed to cover uncertainty associated with future emission scenarios.

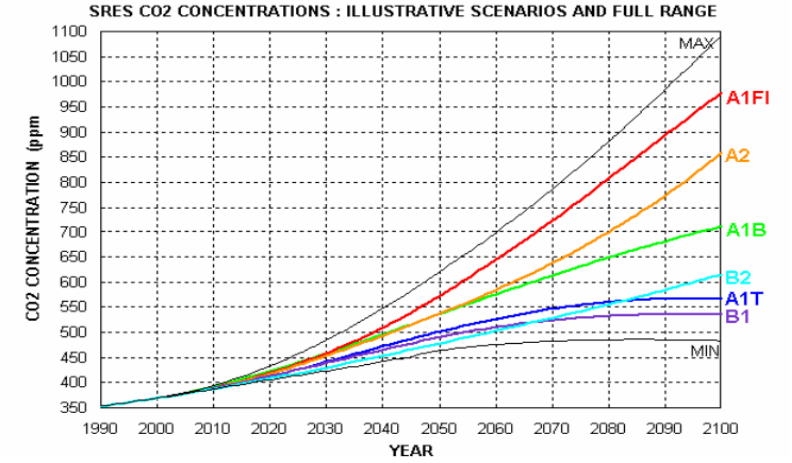


**Figure 6** SRES scenarios as mentioned in the TAR (after Taylor, 2004)

Firstly, a group of GCM-scenario combinations are selected for analysis out of the total number of combinations possible. The selection is made with an aim to capture the entire range of possibilities in future climate as depicted by regionally skilled GCMs. A workshop conducted by Environment Canada (EC) in Quebec (Mortsch, 2011) recommended to "use as many scenarios of climate change as possible to cover a wide range of potential outcomes be they due to the differences in climate model formulations or different emission scenarios driving the climate response. This point is crucial to developing an unbiased assessment and understanding the uncertainties surrounding future climate estimation". At the same workshop, two methods to select model-scenarios combinations representing widest range of future possibilities were discussed. They are referred to as *scatter plot method* and *percentile method*. Similar recommendations and conclusions are drawn by the Ministry of Natural Resources, Ontario at the Conservation Ontario Climate Change Workshop (Garraway, 2011).

Both methods mentioned above are used to cover climate uncertainty in numerous studies across Canada. While analysing future temperature and precipitation trends in Alberta (Barrow & Yu, 2005), five model-scenario combinations, i.e. coldest and wettest (NCARPCM-A1B), coolest and driest (CGCM2-B2), warmest and wettest (HadCM3-A2), warmest and driest (CCSR-A1FI) and the median conditions (HadCM3-B2) are chosen to capture uncertainty associated with future projections. In a similar study performed in the province of Saskatchewan (Lapp, Sauchyn, & Wheaton, 2008), model-scenario combinations projecting warmest-wettest, warmest-driest, coolest-wettest, and coolest-driest future climates around the South Saskatchewan river are selected.

## *Scatter-plot method*

In the scatter-plot method, GCM-scenario combinations most likely to produce hydro-climatic weather extremes in future are selected for analysis. Percent mean changes in precipitation and absolute temperature changes as projected in future by each GCM-scenario combination are plotted and extreme precipitation-temperature scenarios are selected. Figure 7 illustrates the selection of model-scenario combinations corresponding to wet-hot, wet-cold, dry-hot and dry-cold scenarios (Mortsch, 2011).

## *Percentile method*

In the percentile method, selection is made to capture the whole range of future climate projections made by selected GCMs. Percent changes in precipitation as projected by regionally efficient GCMs are plotted against absolute changes in temperature. Future GCM-scenario combinations corresponding to 5$^{th}$, 25$^{th}$, 50$^{th}$, 75$^{th}$ and 95$^{th}$ percentiles of changes in both climate variables are selected (Mortsch, 2011). Figure 8 illustrates the extreme GCM-scenario combination selection process using percentile method.

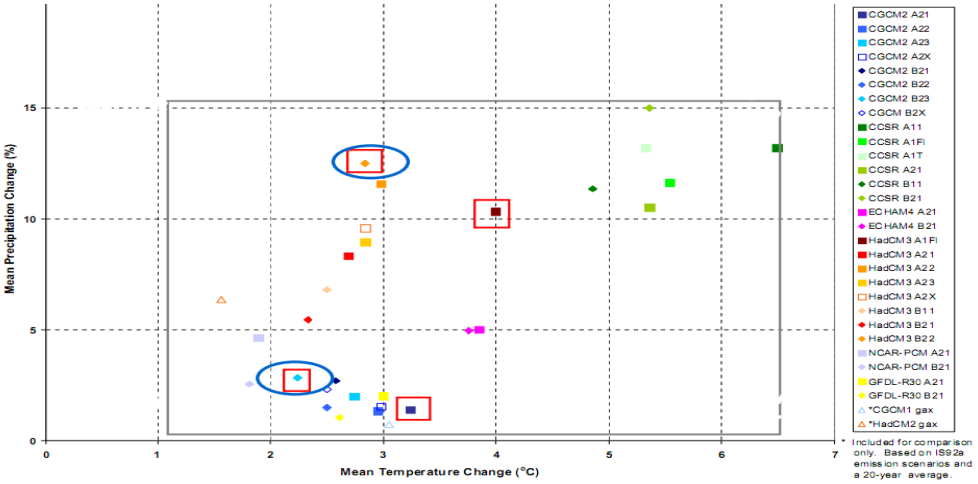


**Figure 7** Scenario selection using scatter plot method (after Mortsch, 2011)

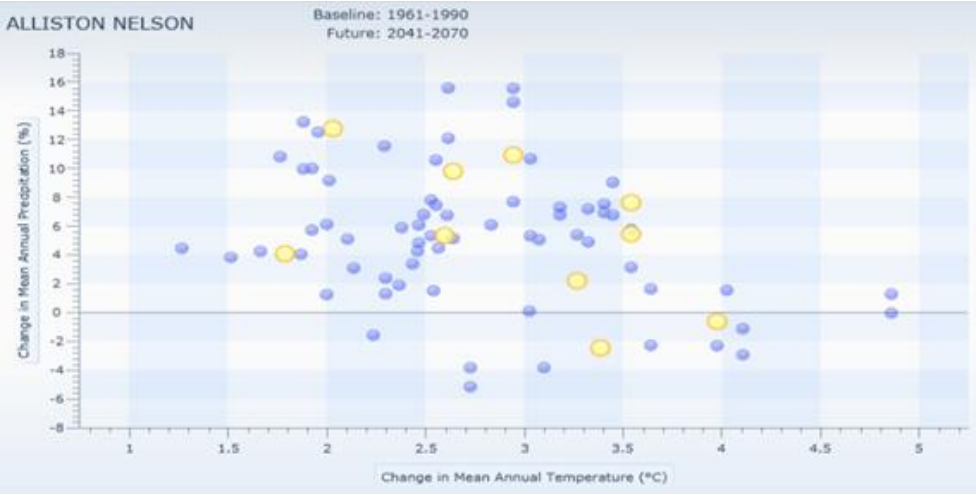


**Figure 8** Scenario selection using percentile method (after Mortsch, 2011)

### 2.1.3 Filling-in historical observed point data with spatially interpolated reanalysis data

The historically observed precipitation and temperature datasets are often found incomplete or intermittent over the period 1960 to 2000. Therefore, they are filled-in using spatially interpolated National Centres for Environmental Protection (NCEP)/National Centre for Atmospheric Research (NCAR) or North-American Regional Reanalysis (NARR) data. Interpolation of reanalysis data at a particular climate gauging station location was done using inverse distance square method. In this method, the distance of point of interpolation is found out from four nearest reanalysis data grid points surrounding it. A simple formula, shown in Equation 2.2 is then used to calculate weight associated with each grid point. Interpolated value at a particular location ($v_i$) is calculated by finding the sum of weighted means of climate data at all four grid points ($v_j$) using Equation 2.3.

$$w_j = \frac{{}^{1}/_{d_j^2}}{{}^{1}/_{d_1^2} + {}^{1}/_{d_2^2} + {}^{1}/_{d_3^2} + {}^{1}/_{d_4^2}} \tag{2.2}$$

$$v_i(t) = \sum_{j=1}^{4} w_j * v_j(t) \tag{2.3}$$

In above equation, $d_1$, $d_2$, $d_3$ and $d_4$ are the distances of the location of interpolation from four nearest grid points and $w_j$ is the weight calculated for $j^{th}$ grid point.

### 2.1.4 Bias correction of gridded GCM climate data

While performing climate change impact studies, bias associated with climate model data can be roughly but safely, defined as the time independent component of model error or the component of model error which remains constant throughout the length of datasets (Ehret et al. 2012, Chen et al. 2011). Major causes of these errors, as identified by IPCC, (2007) are: a) lack of computational power to study hydrological processes at a micro scale, b) limitations in our knowledge about few climate processes for example, in the representation and behaviour of clouds, and c) the inability to depict physical processes accurately in climate models.

The need for bias-correction step while performing climate change impact studies has been advocated by many researchers (for example, Muerth et al. 2012) and on the other hand, has

been criticised by some (for example, Vannitsem 2011). A major argument against the application of bias-correction is that most methods employed to do so are purely statistical in nature and lack a sound physical basis i.e. they are not governed by the laws of physics (Haerter, Hagemann, Moseley, & Piani, 2011). Therefore, it is argued if they should be used to bias-correct GCM outputs, which are prepared taking into consideration complex hydro-meteorological, atmospheric and land-surface interactions prevalent within earth's climate system.

Importance of this particular step and the methodology chosen to do so, can be realised by analysing the impact of bias-correction on projected future streamflow patterns. Sharma et al. (2007) applied bias-correction to spatially interpolated daily precipitation data in the Ping river basin and analysed its impact on the simulated discharge output. They found that the root mean square error (RMSE) between observed and simulated discharge series changed from 172 $m^3/s$ to 93 $m^3/s$. In another study, after bias-correcting gridded datasets from three GCMs for two scenarios and noting the changes in hydrological output from two Global Hydrologic Models (GHMs), Hagemann et al. (2011) concluded that bias correction step improves the simulated runoff patterns in most catchments considered in the analysis. It has also been pointed out that the uncertainty associated with bias-correction step can be of an order similar to that of GCM projections. These findings highlight the need for, and caution required, while selecting and applying a bias-correction methodology.

The purpose of bias correction step is to modify the climate model data in a way that its correlation with observed data improves. Methods employed to do so range from those correcting just the means (Fowler and Kilsby, 2007; Schmidli, Frei, & Vidale, 2006) to those correcting entire distributions of climate data (Ines & Hansen, 2006; Piani et al., 2010). Most recent efforts are towards including changes in bias correction parameter statistics between present and future (Watanabe et al., 2012), effects of multiple timescales (Haerter et al., 2011), correlation between multiple variables being corrected (Piani & Haerter, 2012).

Correction of probability density functions (Pdfs) of climate variables has been advocated in recent research (Haerter et al., 2011; Piani et al., 2010; Piani, Haerter, & Coppola, 2009). Methods used to do so are generally referred to as "quantile mapping", "histogram equalisation" or "rank matching" methods for correcting the GCM bias (Maraun et.al. 2010). Several studies

comparing effectiveness of multiple bias correction methodologies towards bias correction of climate model data have been performed. By comparing seven downscaling and bias correction methodologies, Jakob Themeßl, Gobiet, & Leuprecht, (2011) recommends the usage of quantile mapping methodology for bias correction, especially while analysing climate extremes. Teutschbein & Seibert, (2012) tests six bias correction methodologies of varying complexity in a non-stationary climate setting and concluded that distribution based methodologies perform best under a changing climate.

One such methodology called statistical bias correction method explained in Piani et al., (2010) is used in this study for bias correcting GCM precipitation and temperature data. In this method, climate model data ($X_{mod}$) is transformed so that the intensity histogram of corrected model data ($X_{cor}$) matches with the intensity histogram of observed data ($X_{obs}$) using transfer functions. Transfer functions for a particular climate variable are estimated by first calculating the Cumulative Distribution Function (CDF) of modelled and observed historical data and then, by finding correlation between them such that for each point in the distribution $CDF_{mod}(X_{mod}) = CDF_{obs}(X_{obs})$.

There are a few clear advantages of applying statistical bias correction methodology over traditional methods. The methodology can be used to correct a) mean only (when only additive transfer functions are used), b) mean and standard deviation only (when linear transfer functions are used) c) entire distributions (when exponential transfer functions are used) of model data. In other words, an appropriate level of complexity can be selected in transfer functions, to obtain the desired level of accuracy in results.

*Estimation of monthly bias correction parameters for precipitation data*

The transfer functions chosen for bias-correction should have minimal degrees of freedom so that they are robust and constantly valid over the period of analysis. Piani et al., (2010) suggested three transfer functions for bias-correcting daily precipitation data. Out of them, linear and exponential transfer functions (Equation 2.4 and 2.5) have been used in this study.

$$x_{cor} = a + bx \tag{2.4}$$

$$x_{cor} = (a+bx)\left(1 - e^{(-(x-x_0))/\tau}\right) \tag{2.5}$$

Where, $a$ is the additive correction factor

$b$ is the multiplicative correction factor

$\tau$ is the rate of approach of attaining the asymptote

$x_0$ is the dry day correction factor. It represents the maximum precipitation below which modelled precipitation is assumed to be zero. Also, $x_0=-a/b$.

It was suggested in Piani et al., (2010) that transfer functions are well approximated by linear functions (Equation 2.4) at higher precipitation intensities. However, to accommodate for a systematic change of slope at lower intensities, an exponential form of transfer function is also suggested (Equation 2.5). This function has an exponential tendency to the asymptote $(a+bx)$, where the rate of approach to the asymptote is $\tau$ and dry day correction factor is $x_0$. A combination of these two transfer functions is found to produce reasonable results in a global analysis performed in Piani et al., (2010). Similar results have been found by (Rojas, Feyen, Dosio, & Bavera, 2011) while correcting daily Regional Climate Model (RCM) precipitation and temperature time series over a pan-European scale. Therefore, a combination of linear and exponential transfer functions is used to bias-correct daily precipitation following these steps:

1) Month-wise daily observed and climate model precipitation data is extracted for the period of study.
2) Observed and modelled data is sorted in ascending order of intensities.
3) It is checked if at least 10% of the length of the observed record are contributed by wet days (>1mm of rainfall) and daily mean precipitation value is more than 0.01 mm/day. If any of these conditions are not met, a simple additive transfer function (equal to difference in means) is used to modify the modelled data.
4) If both the above conditions are met, for all wet days in observed record, linear transfer function (Equation 2.4) parameters are estimated by minimising Root Mean Square Error (RMSE) of the fit obtained between model and observed climate data.
5) If fitted parameters $a<0$ and $1/5<b<5$, transfer function obtained from linear fit is used to modify climate model precipitation.
6) If above conditions on parameters are not fulfilled, minimisation of RMSE is performed to estimate four parameters $a$, $b$, $\tau$ and $x_0$ of exponential transfer function (Equation 2.5).

*Estimating monthly bias correction parameters for temperature data*

It has been explained in Piani et al., (2010) that bias-correction of maximum temperature ($T_{max}$), minimum temperature ($T_{min}$) and mean temperature ($T_{mean}$) data directly results in large relative errors in temperature skewness ($T_{sk}$) and temperature range ($T_r$). Therefore, it is proposed that bias correction of $T_{max}$, $T_{min}$ and $T_{mean}$ values should be performed indirectly by correcting $T_{mean}$, $T_{sk}$ and $T_r$ values first and then calculating $T_{max}$ and $T_{min}$ values using equations 2.10 and 2.11 respectively. Usage of linear transfer functions (Equation 2.4) is recommended while correcting $T_{mean}$, $T_{sk}$ and $T_r$ time-series (Piani et al., 2010) and are used in this study for bias correcting climate model temperature data.

*Disaggregation of monthly bias correction parameters*

Monthly bias correction parameters estimated before are disaggregated into daily timesteps using methodology explained in Piani et al., (2010). If interpolation is being done for adjacent months with similar transfer functions (for example, both fitted with either linear or exponential transfer functions), Equation 2.6 is used to calculate transfer function parameters for a particular day *d* within the two months. The equation calculates transfer function parameters for each day by finding weighted average of parameters obtained at the middle days of surrounding months. Weight assigned to transfer function of a particular month varies inversely with the time difference between the day in consideration and middle day of that particular month.

$$TF_d = \propto TF_{m-1} + (1-\propto)TF_m \qquad (2.6)$$

Where,

$\alpha$ is the weight assigned to month *m-1*. It depends on the distance of day *d* (in units of month) from middle day of month *m*

$TF_d$ represents transfer function for day *d*

$TF_{m-1}$ and $TF_m$ represent transfer functions at middle days of months adjacent to day *d*

The process of disaggregation with dissimilar transfer functions in adjacent months (for example, with linear and exponential transfer functions) is a bit complex since it involves transition between different functional forms. An approximate solution for disaggregation of mixed transfer functions has been proposed in Piani et al., (2010) (Equation 2.7 to 2.9)

$$x_{cor,l} = a_l + b_l x \tag{2.7}$$

$$x_{cor,e} = (a_e + b_e(x - x_0))(1 - e^{(x-x_0)/\tau}) \tag{2.8}$$

$$x'_{cor} = (a' + b'(x - x'_0))(1 - e^{((x-x'_0)/\tau')}) \tag{2.9}$$

In the above equations,

$a' = (1 - \alpha)a_e$

$b' = (1 - \alpha)b_e + \alpha b_l$

$x'_0 = (1 - \alpha)x_0 + \alpha(-\frac{a_l}{b_l})$

$ln\ \tau' = (1 - \alpha)\ell n\tau + \alpha \ln(0.5)$

Where,

$a_l$, $b_l$ denotes the additive and multiplicative correction factor for linear transfer function

$a_e$,$b_e$,$x_0$,$\tau$ denote the additive, multiplicative, dry day correction factor and correction factor for exponential transfer function

a′,b′, $x'_0$, $\tau'$ denotes the additive, multiplicative, dry day correction factor and correction factor for interpolated transfer function

$\alpha$ is the parameter which assumes values from 0 to 1. It is 0 when day in question falls in the middle of the month with exponential transfer function and is 1 when it falls in the middle of the month with linear transfer function.

*Bias-correction of GCM climate data using daily transfer functions*

The disaggregated daily transfer functions are used to bias-correct historical and future daily temperature and precipitation time series. Appropriate additive, linear or exponential transfer functions are applied on each day to correct model precipitation data. In the case of temperature, estimated daily linear transfer functions are used to bias-correct daily $T_{mean}$, $T_{sk}$ and $T_r$ timeseries. Timeseries of $T_{max}$ and $T_{min}$ is subsequently calculated using Equations 2.10 & 2.11,

$$T_{min}^{bc} = T_{mean}^{bc} - (T_{sk}^{bc} \times T_r^{bc}) \tag{2.10}$$

$$T_{max}^{bc} = T_{mean}^{bc} + T_r^{bc} \times (1 - T_{sk}^{bc}) \quad (2.11)$$

### 2.1.5 Statistical downscaling

The process of statistical downscaling can be sub-divided into two parts: *i)* calculation of future scaled climate variables and, *ii)* generation of future climate variable timeseries using a weather generator.

Historically observed climate variables are modified to include changes projected by climate models in future. These changes are incorporated into the observed data by using change factors (CFs) calculated from bias-corrected historical and future GCM data. CFs can be applied on different temporal scales (daily, monthly, seasonally or annually), can have different mathematical formulations (additive or multiplicative) and can vary in numbers (same or unique for different percentiles of a climate variable). Anandhi et al., 2011 gives a comprehensive overview of different change factor methodologies used in climate change impact studies. After performing a comparative analysis of different CFs, usage of multiple CFs over single CF, and of additive CFs over multiplicative CFs (unless the variable is bounded, in which case multiplicative CFs are to be used) has been recommended. This is because multiplicative change factors can give unrealistically high or low values in cases where the variable's value is very low. However, they found that usage of large number of bins (>=25) eliminates this difference (Anandhi et al., 2011). Keeping above factors in mind, following steps are followed for generating future scaled climate variable data for precipitation and temperature:

1) Number of bins and distribution of variable percentiles across the bins is decided. Number of bins is kept >25. The distribution of variables can be uniform as well as non-uniform across selected bins.
2) Monthly empirical cumulative distribution functions (ECDFs) are calculated for bias-corrected historical and future GCM data.
3) For each month, means of the historical and future values falling within each bin is calculated.
4) Additive and multiplicative CFs are calculated for temperature and precipitation respectively for each month, at each bin, using equations 2.12 and 2.13.

$$CF_{add,b} = GCM_{f,b} - GCM_{h,b} \quad (2.12)$$

$$CF_{mult,b} = GCM_{f,b}/GCM_{h,b} \quad (2.13)$$

5) The historical observed data is distributed into an equal number of bins as the GCM data. CFs calculated for each bin are added or multiplied to the distributed observed values to obtain future scaled climate variable values.

Weather generators (WGs) are tools that generate synthetic series of climate data having characteristics similar to input data. They can be classified into three basic types i.e. parametric, semi-parametric and non-parametric WGs. Parametric weather generators typically employ Markov chains to simulate the occurrence of dry and wet days, and use probability distributions to calculate the amount of precipitation, temperature and other climate variables. The problem with this kind of weather generator is that they are heavily reliant on the statistical properties of the input data and generate climate series based on it. Since the statistical properties of historical and future climate data are expected to be different from each other, usage of parametric WGs for generating synthetic future climate series is clearly arguable. Semi-parametric WGs have both empirical as well as parametric components, which are used together in different ways to produce synthetic climate variable time series (King, 2012). Most of these WGs are single-site, single-variable WGs, so the correlation between different climate stations as well as between different climate variables is lost in the generated future climate series. Non-parametric WGs are based on the nearest neighbour resampling approach as introduced first by Young, 1993 and they overcome some of these limitations. KNN-CAD weather generator is a non-parametric multi-site, multiple variables WG. It has been used and validated at multiple sites in the past (King, Mcleod, & Simonovic, 2012; Raje & Mujumdar, 2011) and has been found to perform reasonably well in simulating historically observed precipitation and temperature data.

*KNN-CAD (v4) Weather Generator*

The KNN-CAD is a stochastic weather generator which has been developed by Yates (2003). It is based on the principal that past weather is representative of the future weather. It reshuffles and perturbs the historical observed multi-site data in a way that spatial and temporal correlation of the observed data remains preserved in the simulated data. First, a set of "potential

neighbours" are selected from the historical observed record. Their length depends on the width of temporal window chosen for analysis and number of years of observed record available. Regional averages of all the stations under study are then compared with regional average of current day weather using Mahalanobis distance (Yates 2003; Sharif and Burn, 2006) as the distance metric. First K nearest neighbours are selected out of the *N* potential neighbours and based on their ranks, a cumulative probability distribution is formed. Next day's weather is selected by generating a random number between 0 and 1 and by selecting the day closest to it in the cumulative probability distribution. The methodology proposed by Yates, (2003) described above was improved by Sharif and Burn, (2006) by incorporating a perturbation step in the weather generation process. The amount of perturbation for a variable at a particular location was defined as follows:

$$y_{i,t+1}^{j} = x_{i,t+1}^{j} + \lambda \sigma_i^{j} z_{t+1} \tag{2.14}$$

To prevent the occurrence of negative precipitation values, a threshold of $\lambda_a = \frac{x_{3,t+1}^{j}}{1.55 \times \sigma_3^{j}}$ is specified. Prodanovic and Simonovic, (2008) incorporated a leap year modification to the weather generator. Eum and Simonovic, (2008) added principal component analysis to account for more than one variable in the analysis without increasing computational demand.

However, it has been found that the perturbation scheme proposed by Sharif and Burn (2006) produced significantly high and low temperature values than the historical record (Eum and Simonovic, 2011). Also, temporal correlations between simulated weather variables are lost when only one of the K nearest neighbours is selected to represent next day's weather. Above shortcomings were addressed in KNN-CAD version 4, which is detailed below:

1) Computation of daily regional means of $p$ variables ($x_i$) across all q stations from the historical record using the Equation 2.15

$$\overline{X_t} = \left[\overline{x_{1,t}}, \overline{x_{2,t}}, \ldots . \overline{x_{p,t}}\right] \qquad \text{for } t = \{1,2,\ldots \mathrm{T}\}$$

$$\text{Where, } \overline{x_{\iota,t}} = \frac{1}{q} \sum_{j=1}^{q} x_{i,t}^{j} \qquad \text{for } i = \{1,2,\ldots \mathrm{p}\} \tag{2.15}$$

2) A suitable temporal window is chosen and a set of potential neighbours of length $L = N * (w + 1) - 1$ are selected from the historical record. Here, *w* is the size of temporal window and *N* is the number of years of historical data available. For each day, temporal window numbers of days surrounding it are selected as potential neighbours. Yates (2003) recommended a value of *w*=14 for the Great Lakes region.
3) Daily regional means are calculated across all *q* stations for potential neighbour number of days.
4) The covariance matrix $C_t$ of size *[L x p]* for t$^{th}$ day is created using values of climate variables on all potential neighbour number of days.
5) Weather on the first day is chosen randomly from all the values of *p* variables present for that day in the historic record at all *q* stations.
6) Mahalanobis distance between the current ($t^{th}$ day) and all other days comprising the potential neighbours ($i^{th}$ day) is calculated using Equation 2.16

$$d_i = \sqrt{(\overline{X_t} - \overline{X_\iota}) C_t^{-1} (\overline{X_t} - \overline{X_\iota})^T} \quad (2.16)$$

Where, $C_t^{-1}$ is the inverse of covariance matrix calculated for day *t* and *T* denotes the transpose operation.

7. Choose a size of *K* nearest neighbours to be selected out of all the potential neighbours for resampling. A value of K=$\sqrt{L}$ has been recommended by Yates et.al. 2003 and Rajagopalan and Lall (1999) and has been used in this thesis.
8. Sort the potential neighbours in increasing order of their Mahalanobis distance and select first *K* neighbours. Based on their ranks, a cumulative probability distribution is allotted to the K nearest neighbours using Equations 2.17 and 2.18

$$w_k = \frac{1/k}{\sum_{n=1}^{k} 1/n} \quad \text{for } k=\{1,2,\ldots K\} \quad (2.17)$$

$$p_n = \sum_{n=1}^{m} w_n \text{ for } m=\{1,2,\ldots K\} \quad (2.18)$$

9. A random number between 0 and 1 is generated and *B* number of days for which the cumulative probability is closest to it, are resampled to get the next day's weather across all stations in the region.

10. Steps (6) to (9) are repeated for each day in the historical record to produce a synthetic series equal in length to the historic series. In case, required synthetic time series is larger than the historic, multiple ensembles of synthetic data are produced.
11. To produce values of climate variables outside the observed range, a modified perturbation step is used. It perturbs precipitation variable *i*, station *j* and $(t+b)^{th}$ day (where $b$=1,2,..B) using Equation 2.19. The random variate $Z_t$ is calculated using Equation 2.20.

$$y_{j,t} = \lambda_{ppt} x_{j,t} + (1 - \lambda_{ppt}) Z_t \tag{2.19}$$

$$Z_{j,t} = \exp\left(Am_{j,t} + Bm_{j,t} * z_t\right) \tag{2.20}$$

Here, $y_{j,t}$ and $x_{j,t}$ are the perturbed and unperturbed values of precipitation at station *j* on time *t*. $\lambda_{ppt}$ is an interpolation coefficient chosen between 0 and 1. $Z_t$ value is extracted from a two parameter lognormal distribution having mean equal to unperturbed precipitation $x_{j,t}$ and standard deviation calculated from nonzero precipitation values from potential neighbours. Method of moments as proposed in Singh (1998) is employed to estimate parameters $B_m$ and $A_m$ of the log-normal distribution for each individual site, whereas $z_t$ is a random normal variable which is kept constant for all the sites in analysis to ensure inter-site correlation.

Temperature perturbation for temperature variable *i*, station *j* and $(t+b)^{th}$ day (where $b$=1,2,..B) is calculated by using a similar equation 2.21.

$$y_{j,t+b} = \lambda_{temp} x_{j,t+b} + (1 - \lambda_{temp}) Z_{t+b} \tag{2.21}$$

Here, $y_{j,t}$ and $x_{j,t}$ are the perturbed and unperturbed values of temperature at station *j* and time *t*. $\lambda_{temp}$ is an interpolation coefficient chosen between 0 and 1. $Z_{t+b}$ value is a random normal variable having mean equal to unperturbed temperature $x_{j,t}$ and standard deviation calculated from K nearest neighbours corresponding to a particular day. Same value of random component is chosen for $T_{max}$ and $T_{min}$ to ensure that former is always greater than the latter.

Multiple realisations of future temperature and precipitation are generated to capture uncertainty contributed by daily climate variability. Realisations corresponding to extreme hydro-climatic scenarios are selected from the generated realisations for further analysis.

### 2.1.6 Selection of appropriate climate variable time-series for hydrological modeling

Four combinations of precipitation and temperature time-series, most likely to produce hydro-climatic extremes, are selected for each time-slice. Future realisations obtained from the KNN-CAD weather generator projecting extreme wet-cold, wet-dry, dry-hot and dry-cold scenarios are selected using scatter plot method. The selected realisations correspond to climate data most probable of producing hydro-climatic extremes in future.

### 2.1.7 Introduction of sub-daily temperature variability scenarios

To capture sub-daily level uncertainty associated with downscaled future climate data, two "variability scenarios" are included in the analysis. These are named as "high variability" and "low variability" scenarios. Together with four extreme hydro-climatic scenarios, these variability scenarios produce a group of eight extreme future scenarios for each timeline. Temperature and precipitation combinations corresponding to these eight scenarios (presented in Figure 9) are used to estimate the range of flow projections possible in future.

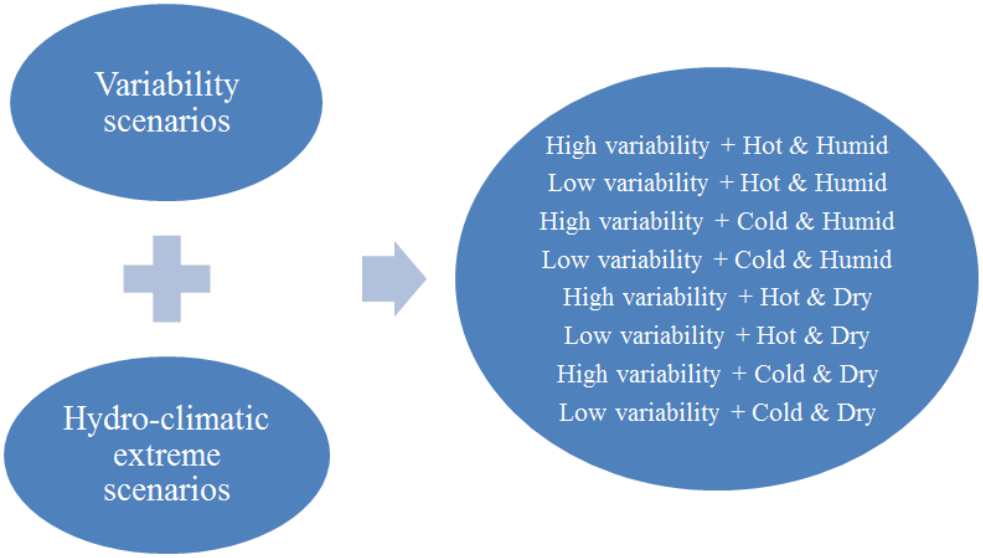


**Figure 9** Schematic diagram of combinations of hydro-climatic and variability scenarios considered in the study

## 2.2 Hydrological modeling

Runoff models predict the temporal distribution of runoff based on effective rainfall and catchment characteristics. Lumped hydrological models consider entire system under study as a single unit and represent state variables as averaged values across the system. Due to this, lumped models fail to represent catchment scale hydrological processes accurately especially for medium and large catchments (>100 $Km^2$ in area). On the other hand, distributed models divide the catchment into uniform grid cells and are much more complex systems than the lumped models. Lack of fine resolution climate data, as required by fully distributed models, makes their calibration process difficult. Also, defining initial values for hydrological parameters across the catchment grids is difficult for fully distributed hydrological models (Gosling, Taylor, Arnell, & Todd, 2011). Semi-distributed models are less complex than distributed models and have a higher spatial resolution of hydrological processes than a lumped model. Here, the catchment is distributed to a degree that hydrological properties of the catchment are satisfactorily, if not precisely, simulated by the model. They are generally divided into areas of similar hydrological responses. Hydrological processes within each of these areas are simulated as lumped processes within each sub-catchment and are routed downstream to get flow patterns at the catchment outlet. Semi-distributed and distributed hydrologic models have been found to perform better

than the lumped models in simulating hydrological response to climate variables especially for large catchments (Khakbaz, Imam, Hsu, & Sorooshian, 2012).

Continuous hydrological modelling is necessary while estimating peak runoff from a catchment. Unlike event based modelling, it accounts for the state of catchment prior to flood-producing rainfall event, in the modelling procedure. Lack of this antecedent information has been found to produce significantly underestimated peak flows in 45 catchments across the Murray Darling basin (Pathiraja, Westra, & Sharma, 2012). Similar results are noted when Berthet & Andr, 2009 analysed peak flow response of 178 French catchments to event and continuous hydrologic simulations. In their study, Pathiraja et al., 2012 also noted that usage of continuous simulation is even more important in catchments where there is a significant lag between rainfall and runoff peaks. Since a significant portion of flooding in the Grand river basin occurs due to snow accumulation and melt (Boyd, Smith, & Veale, 2000), continuous hydrological modelling using a semi-distributed model WATFLOOD is performed to model changes in runoff characteristics between present and future climate. This model has been found to simulate the hydrologic behaviour reasonably well for the catchment under study as well as for many other regions across the globe (Bingeman, Kouwen, Asce, & Soulis, 2006; Kouwen, Soulis, Pietroniro, Donald, & Harrington, 1993).

### 2.2.1 WATFLOOD hydrological model

WATFLOOD hydrologic model is based on the concept of Grouped Response Units (GRUs), where units of similar hydrological response (or Hydrological Response Units) within the catchment are modelled together to calculate overland flow, interflow and baseflow within the area of study. The resolution of computational grids is chosen keeping in mind the resolution of available meteorological data (generally from numerical weather models or radars) as well as the size of smallest catchment to be modelled. Using remotely sensed land-cover data, these computational grids are sub-divided into sections of unique land-cover classes. The hydrological response from each individual land-cover section is calculated and routed downstream to calculate the runoff response of the catchment under study (Kouwen et al., 1993). For instance, in Figure 10, land-cover image has four classes: A, B, C and D. Hourly runoff is first calculated for each individual class and then, combined together to get total runoff at each grid. Runoff

calculated at each grid is routed downstream using physiographic information of the catchment (Figure 10).

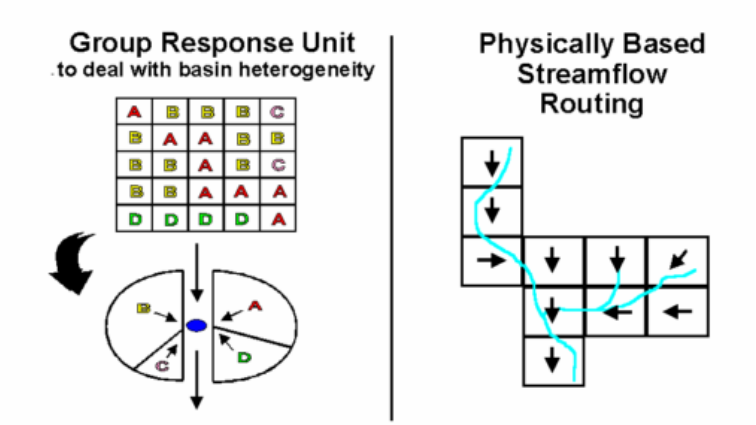


**Figure 10** Flow calculation and routing concept used in WATFLOOD

In this setting, hydrological parameters are associated with individual land-cover classes and they remain constant regardless of the composition of different grids existing within the basin area. Therefore, same set of parameters can be used without recalibration in another catchment with similar physiographic characteristics. Also, model need not be recalibrated if land-use within the catchment changes over time. An updated land-use file for the catchment will be sufficient to include changes in the calibrated model.

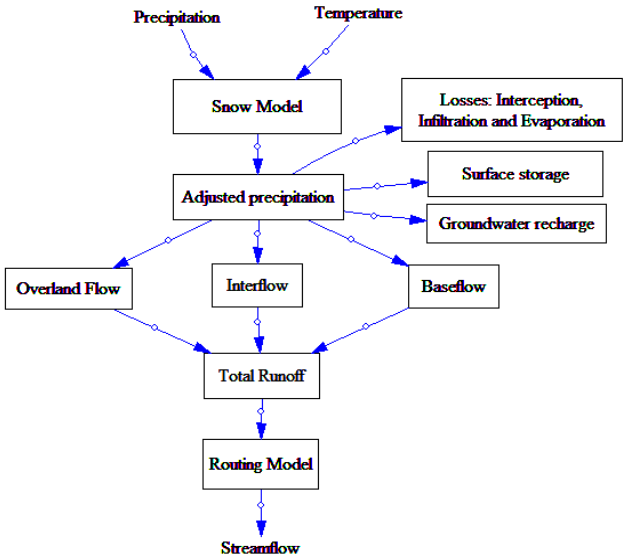


**Figure 11** Flowchart of processes involved for streamflow generation in WATFLOOD

**Table 1** Description of important input, outputs and subroutines in the WATFLOOD hydrological model

| Database | Files | Description |
|---|---|---|
| *Drainage input* | *.map | Watershed map file: has information such as stream elevation, drainage direction, land-cover information etc. |
| | *.shd | Basin file generated from the map file using programme bsn.exe |
| | *.par | Parameter file |
| | *.str | Contains stream gauge and reservoir locations |
| *Meteorological input* | *.rag | Contains precipitation gauging station locations and historical records |
| | *.tag | Contains temperature gauging station locations and historical records |
| *Event input* | event.evt | Contains information about the duration for which the simulation will run |
| *Output (imp)* | spl.txt | Provides a summary of the modelling parameters, the initial soil moisture, the total precipitation on each element, the runoff at each streamflow gauge station and the errors |
| | spl.plt | Provides hydrograph plots from the run |
| | stg.plt | Provides stage plots from the run |
| | spl.csv | Observed and simulated flow history in *.csv format for import to other programmes |
| *Useful subroutines* | radmet.exe | Converts the radar data file into SPL compatible format |
| | ragmet.exe | Distributes point precipitation data using distance weighting technique |
| | calmet.exe | Fills-in missing radar data with point precipitation data |
| | snw.exe | Distributes snow coarse data using distance weighting technique |
| | moist.exe | Distributes soil moisture data using distance weighting technique |
| | tmp.exe | Distributes point temperature data using distance weighting technique |
| | spld.exe | Compiles the model in debug mode with maximum error diagnostics |
| | splx.exe | Compiles the model with faster speed and lesser error diagnostics |
| | stats.exe | Calculates a number of statistics for the run |

The model is aimed at flood forecasting and long-term hydrologic simulation. It include processes like interception, infiltration, evaporation, snow accumulation and ablation, interflow, recharge, baseflow, overland flow and channel routing (Kouwen et al., 1993). A flowchart depicting the role of these processes in generation of streamflow from climate variables is provided in Figure 11. Hourly precipitation and temperature data is used as input into a snow

model and value of adjusted precipitation is obtained. Adjusted precipitation is reduced by losses from interception, infiltration and evaporation. A fraction of water is stored on the surface while some contribute towards groundwater recharge and baseflow. Remaining water flows overland and combines with baseflow to form total runoff. Generated total runoff is routed downstream to generate streamflow patterns for the catchment under study. A description of major processes involved in WATFLOOD hydrologic model is provided below (Kouwen et al., 1993):

- Interception is calculated using the approach suggested in Linsley et.al. 1949. According to it, total interception is equal to the sum of total canopy storage and the Interception Evaporation (IEP) occurring during a storm event.
- Infiltration processes are accounted for in the model using the Philip formulae (Philip, 1959), which also accounts for surface detention of water. Initially, infiltration rate is high due to large pressure gradient in the surrounding region. The same decreases with time as the gradient decreases.
- Potential Evapo-Transpiration (PET) can be calculated using different methods in WATFLOOD. When radiation (shortwave and longwave) data is available, the Priestly-Taylor equation can be used. When only temperature data is available, Hargreaves equation can be used. If both radiations as well as temperature data are unavailable, PET is estimated using published values from the literature. Estimation of AET involves consideration of water transpired from vegetation and water evaporated from open soils and open water.
- The calculation of snow-melt is performed using degree day approach as described in National Weather Service River Flow Forecast system by Anderson (1973).
- Interflow is the flow of infiltrated water (contributing towards Upper Zone Storage) in the surrounding space. Downward movement of water has been ignored in the model and total interflow is expressed as a linear function of water stored in the upper zone.
- Baseflow is estimated at each sub-division using measured hydrograph at the basin outlet. The magnitude of baseflow is made to recede with time using a recession constant. However, the contribution of baseflow has been found to be negligible with respect to overland flow during the flooding events.

- Overland flow is the component of flow exceeding the depression storage. It is estimated in the model using a modified form of manning's formula. Total runoff is calculated by adding up overland flow contributions from different land-use classes to the baseflow.
- Routing of overland flow across the channel cross-section is carried out using simple storage-routing technique. Relationship between overland flow and channel storage is expressed using Manning's formula.

The WATFLOOD is a compilation of FORTRAN codes and can be run on DOS and UNIX platforms. Its main advantage is that it is very fast, robust, can run with minimal (precipitation and temperature) inputs and its transferability to other watersheds without recalibration. Although model runs are performed in hourly temporal scale, meteorological inputs (except temperature) can be provided in daily time steps as well. If provided in daily timesteps, climate data is temporally disaggregated internally using standard climate variable disaggregating procedures and are used to generate streamflow response. Table 1 provides a list of major input files, output files and set of programmes that define WATFLOOD with their short descriptions.

### 2.2.2 Preparation of hourly temperature input data for WATFLOOD

As discussed before, WATFLOOD performs modeling simulations in hourly temporal scale. However, apart from temperature, datasets can be provided in the model in daily timesteps as well. In which case, WATFLOOD performs an internal disaggregation procedure to obtain datasets in hourly time-scale. To obtain hourly temperature series, generated future daily $T_{max}$ and $T_{min}$ series are used as inputs in the cosine function formula. This method has been employed to disaggregate daily temperatures in the past and has been found to be effective in doing so (Debele, Srinivasan, & Yves Parlange, 2007). A generalized expression of cosine formulae is expressed as,

$$T_t = \frac{T_{max} - T_{min}}{2} * \cos\left(\frac{\pi(t-14)}{12}\right) + \left(\frac{T_{max} + T_{min}}{2}\right) \quad (2.22)$$

Where, *t* denotes hour of the day at which temperature is being calculated.

Following procedure is adopted to prepare hourly temperature datasets corresponding to eight combinations of hydro-climatic and variability scenarios:

1. Generate multiple realizations of future time-series of $T_{max}$ and $T_{min}$ for selected GCM-scenario combinations.
2. For each timeline, GCM-scenario combination associated with selected $T_{mean}$ extremes is identified.
3. Daily averaged range ($R_{av}$) is calculated for all realizations of $T_{max}$ and $T_{min}$ associated with that particular GCM-scenario combination. Values of maximum ($R_{av,max}$) and minimum ($R_{av,min}$) range are identified. These ranges correspond to scenarios with maximum and minimum sub-daily temperature variability.
4. Selected $T_{mean}$ extreme scenarios timeseries, $R_{av,max}$ and $R_{av,min}$ are used to generate $T_{max}$ and $T_{min}$ timeseries corresponding to combinations of hydro-climatic and variability extreme scenarios using equations 2.23 and 2.24 respectively.

$$T_{max} = T_{mean} + f * R_{av} \quad (2.23)$$

$$T_{min} = T_{mean} - (1 - f) * R_{av} \quad (2.24)$$

   Where, $f$ is a random number between 0 and 1 following uniform distribution.
5. Once $T_{max}$ and $T_{min}$ timeseries are established for each hydro-climatic and variability extreme scenario, disaggregated hourly temperature values are calculated using Equation 2.22.

## 2.3 Statistical analysis

Flood frequency analysis is performed to develop relationships between flood magnitude and flood recurrence interval. The same is achieved by performing a statistical analysis on time-series of peak flows. There are two methods of extracting peak flow data from a discharge series, namely Annual Maximum (AM) and Peak Over Threshold (POT) method. In AM method, yearly maximum discharge values are selected while in POT method, discharge events larger than a specified threshold are considered for analysis. Major limitation of AM method is that the values extracted may not be representative of actual peaks in the entire discharge series. For example, the second largest discharge in a high-flow year may be higher than peaks of many other low-flow years in the discharge series, but will be ignored by the AM method since only one (maximum) value is selected per year. Another limitation is that sample size of peak flows

obtained from the AM method is small (equal to the number of years of discharge series data) and hence, reliable statistical inferences are hard to be drawn from it. POT method, on the other hand, overcomes these limitations and is extremely useful especially when the available discharge series is short.

The flood magnitude-return period relationship for POT model is:

$$1 - F(Q_T|Q_T > q_0) = \frac{1}{\lambda T} \tag{2.25}$$

Where *F()* is the cumulative distribution of the discharges exceeding the threshold $q_0$ and λ is the no. of peaks selected per year.

While selecting values for analysis using POT method, it should be ensured that they are independent and don't belong to the recession curves of previous flow peaks. Further, selection of an appropriate threshold value is of utmost importance. Although no strict rules are existent for selection of this threshold, guidelines for doing so have been summarised in Lang & Bobe, 1999. They identified three criterions to be considered while selecting a threshold value. These are related to a) "mean number of over-threshold events", b) "mean exceedence of threshold" and c) "dispersion index" obtained from the selected values. Mean exceedence over threshold criterion is based on the objective of stabilisation of POT distribution parameters. It has been found that choosing a threshold value within an interval where a linear relationship between threshold value and mean exceedence is observed, increases the stability of distribution parameters. Hence, recommendations have been made to locate this range and then test different threshold values within this range for their dispersion characteristics. First and third criterions aim to select peaks following characteristics of a Poisson's process or in other words, are randomly distributed over time. To account for it, a value of $\lambda$>2 or 3 is recommended for usage.

Flow peaks crossing a threshold can be fitted using a Generalised Pareto Distribution (GPD). The cumulative distribution function *F(x)* for the GPD can be given by the following equations:

$$F(x) = 1 - (1 - k\frac{(q-q_0)}{\beta})^{1/k} \qquad \text{if } k \neq 0 \tag{2.26}$$

$$F(x) = 1 - exp(-\frac{(q-q_0)}{\beta}) \qquad \text{if } k=0 \tag{2.27}$$

Where, $q_0$ is the threshold, $\beta$ is a scale parameter and $k$ is shape parameter. When $k=0$, it represents an exponential distribution.

The inverse form of the GPD is:

$$q(F) = q_0 + \frac{\beta}{k}[1 - (1 - f)^k] \qquad \text{if } k \neq 0 \qquad (2.28)$$

$$q(F) = q_0 - \beta \ln[1 - F] \qquad \text{if } k = 0 \qquad (2.29)$$

Method of L-moments is most frequently used for parameter estimation in hydrological studies. This parameter estimation method has been found to perform better than other traditional methods like method of moments and maximum likelihood, particularly when the sample size is small (Chin, D.A., 2006). The method has also been found robust against outliers present in datasets (Hosking, 1989). In this method, L-moments are expressed as the linear combinations of Probability Weighted Moments (PWM). The expressions for calculating PWMs and L-moments are summarised in Table 2.

As mentioned in Das and Simonovic, (2012), two different approaches can be taken while estimating parameters of GPD using L-moments.

i. An initial value of threshold $q_0$ is fixed and data values crossing it are picked from the data sample (say $M$ nos.). In this case, only two parameters $\beta$ and $k$ need to be estimated.
ii. An initial value of $\lambda$ is fixed and a total $(\lambda \times N)$ number of values are picked from the entire timeseries. Peak $M$ flows are then selected out of those values and parameters $q_0$, $\beta$ and $k$ are estimated.

For *(i)* parameters $\beta$ and $k$ are given by Hosking and Wallis, (1997)

$$k = ((l_1 - q_0)/l_2) - 2 \qquad (2.30)$$

$$\beta = (1 + k)(l_1 - q_0) \qquad (2.31)$$

For (ii) parameters $q_0$, $\beta$ and $k$ are given by Hosking and Wallis, (1997)

$$k = (l_1 - 3t_3)/(1 + t_3) \quad (2.32)$$

$$\beta = (1 + k)(2 + k)l_2 \quad (2.33)$$

$$q_0 = l_1 - (2 + k)l_2 \quad (2.34)$$

Where $l_1$is the 1st L-moment, $l_2$ is the 2nd L-moment and $t_3$is L-skewness.

**Table 2** Expressions for calculation of L-moments and L-moment ratios (Chin, D.A.,2006)

| **Population quantile** | **Sample estimates** |
|---|---|
| 1st PWM ($b_0$) | $\frac{1}{N}\sum_{i=1}^{N} x_i$ |
| 2nd PWM ($b_1$) | $\frac{1}{N(N-1)}\sum_{i=2}^{N}(i-1)x_i$ |
| 3rd PWM ($b_2$) | $\frac{1}{N(N-1)(N-2)}\sum_{i=3}^{N}(i-1)(i-2)x_i$ |
| 4th PWM ($b_3$) | $\frac{1}{N(N-1)(N-2)(N-3)}\sum_{i=4}^{N}(i-1)(i-2)(i-3)x_i$ |
| 1st L-moment (L1) | $b_0$ |
| 2nd L-moment (L2) | $2b_1-b_0$ |
| 3rd L-moment (L3) | $6b_2-6b_1+b_0$ |
| 4th L-moment (L4) | $20b_3-30b_2+12b_1-b_0$ |
| L-Coefficient of Variation | *L2/L1* |
| L-Skewness | *L3/L2* |
| L-Kurtosis | *L4/L2* |

(Note: Sampling data needs to be arranged in ascending order before calculating the values of PWMs).

# 3 CASE STUDY: GRAND RIVER AT BRANTFORD CATCHMENT

## 3.1 Introduction of the basin

Grand River has the largest drainage area among all southern Ontario rivers. It originates in Dundalk and grand valley region (525 masl) and flows 128 km southwards to drain into Lake Erie (100 masl) at Port Maitland. It crosses urban centres of Kitchener, Waterloo, Cambridge, Guelph etc. on its way to the summit (Stadnyk-Falcone, 2008).

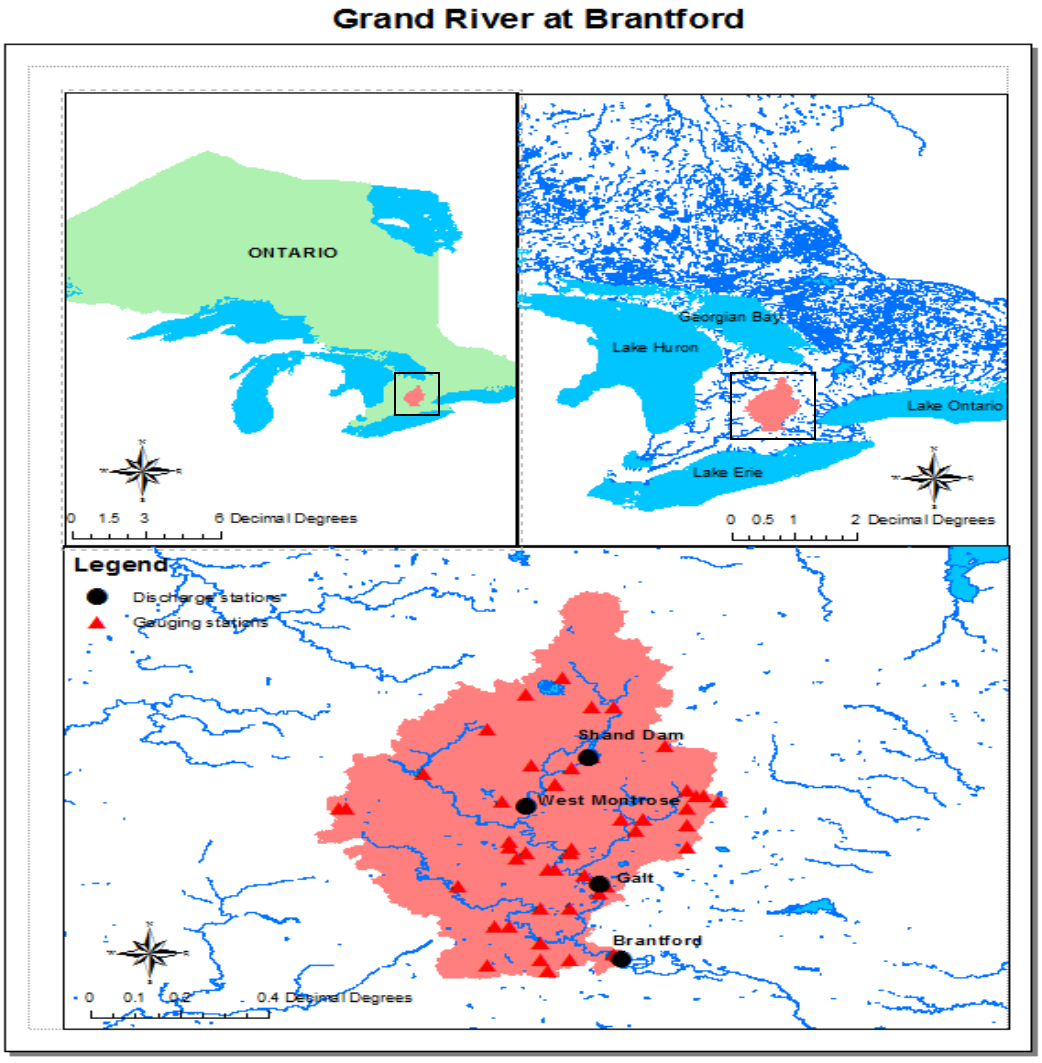


**Figure 12** Geographic settings of the Grand River at Brantford

The Grand River watershed is home for more than 787000 people, who depend on the river for fulfilling their needs of water for agriculture, transportation, drinking and power generation. A major section of the population resides in the central regions of the watershed with northern and southern regions generally used for agricultural purposes (Boyd et.al. 2009).

Based on the geologic setting, Grand River watershed can be roughly classified into three sections of upper Grand watershed (flat with poorly drained clayey soil), central Grand watershed (steep with well-drained soil) and lower Grand watershed (flat and low-lying with a mix of silty and clayey soil) (Grand River Conservation Authority, 2005). Catchment of Grand River at Brantford, with an area of 5210 $km^2$ roughly encompasses the upper and central Grand River catchments. There is a heterogeneous land-cover spread throughout the catchment. A major portion of the catchment is used for agricultural purposes. Northern regions are abundant with surface water and moraines due to the presence of clayey soil and thus, contribute heavily towards total surface-runoff from the catchment (Boyd et.al. 2009). Big urban centres Kitchener, Waterloo, Cambridge etc. are present in the central and south-eastern regions of the catchment promoting urban land-use in the area. Southern portion of the catchment is dominated by vegetation and forests.

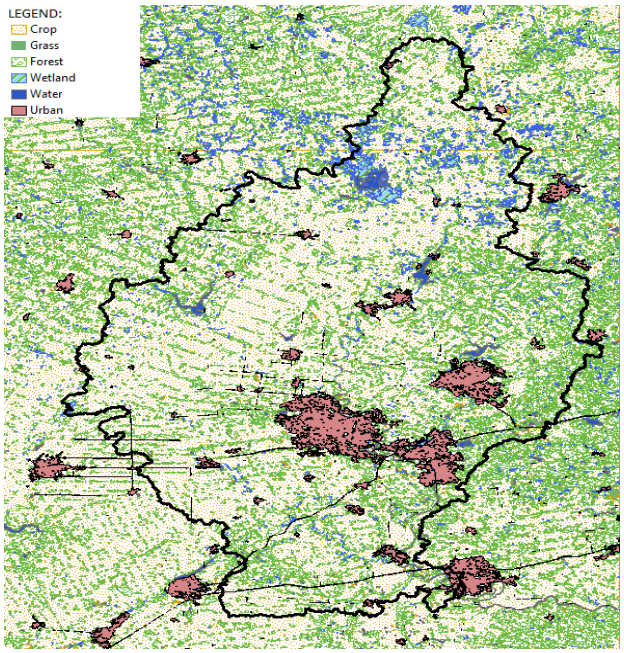


**Figure 13** Land-use classification of the Grand River at Brantford

Average annual precipitation across the catchment is approximately 900 mm though it shows significant spatial and temporal variations. For instance, average annual precipitation for gauging stations Monticello, Elmira and Falkland, located in the northern, central and southern regions of the catchment is 960 mm, 750 mm and 710 mm respectively. Significant temporal variations in precipitation patterns are observed as well. A major fraction of annual precipitation occurs in the summer months of April to August and relatively smaller precipitation is experienced in other months.

The annual average flow at Brantford (for the duration 1960-2000) is 57.83 $m^3/s$. Monthly variations in flow patterns are also noted. As shown in Figure 14, peak discharges are observed in March and April and low flows are observed in the summer months. Further, relatively higher values of discharges are noted in all the winter months. These observations suggest higher possibilities of snowmelt runoff, ice on flood or ice jam floods in the catchment than the storm rainfall floods.

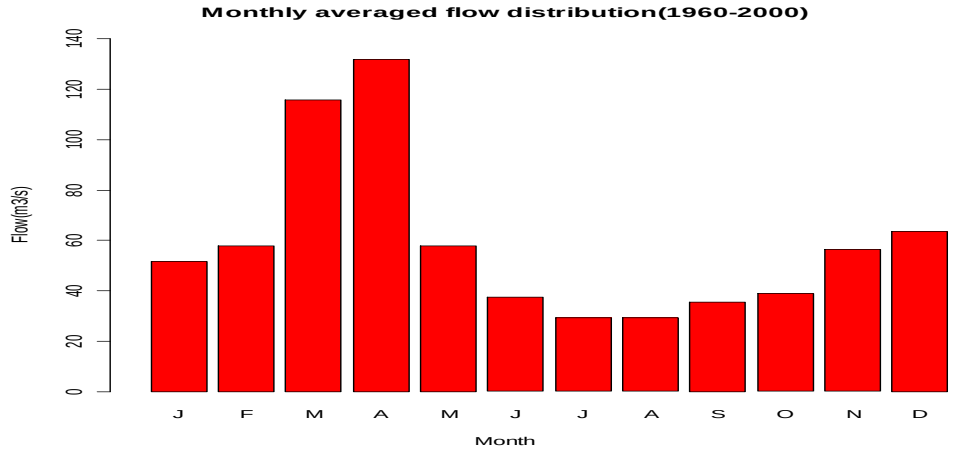


**Figure 14** Monthly variability of average flows recorded at Brantford

Flow is regulated at several locations along the Grand River to ensure continuous, necessary and sufficient supply of water for the communities living downstream. Luther dam, Damascus dam, Conestogo dam, Woolwich dam, Laurel dam, Shand dam, Guelph dam and Shade's Mills dam are the major dams existing within this catchment. In addition to them, a series of dykes also protect parts of Kitchener, Cambridge and Brantford from high flows. However, with continued deforestation, growing urban population and changing climate, runoff patterns within

the catchment are expected to change in the future. Authorities will face the challenge to frame appropriate water management policies for managing flow extremes within the catchment (Farwell, Boyd, & Ryan, 2008).

## 3.2 Data collection

A suit of different climate datasets are collected from several sources for this study. Datasets and their respective sources are discussed below.

### 3.2.1 Observed daily climate data

Historical observed precipitation and temperature (maximum, minimum and mean) data for the period 1960-2000 is collected from the National Climate Data and Information Archive (NCDIA) using Canadian Daily Climate Data (CDCD) software at 52 precipitation and temperature gauging stations falling within the Grand river catchment and having data within the period 1960-2000. A list of gauging stations at which climate data is collected, is provided in Appendix B. The CDCD software can be used to download observed daily temperature, precipitation and snow-on-the-ground data, and is downloadable for free from the NCDIA website.

### 3.2.2 Daily historical and future GCM data

Programme for Climate Model Diagnosis and Inter-comparison (PCMDI) archive offers a collection of historical and future daily, monthly and yearly climate datasets for all climate models mentioned in IPCC, (2007) to facilitate diagnosis and inter-comparison between them (Meehl et al., 2007). These multi-model datasets are the product of Coupled Model Inter-comparison Project phase 3 (CMIP3) of the World Climate Research Programme (WCRP).

Gridded historical GCM data corresponding to *Climate of the Twentieth Century* simulations are downloaded for a total of 49 different realisations from all the models mentioned in IPCC, (2007). Future GCM data corresponding to selected model-scenario combinations is also downloaded from the PCMDI archive. A list of climate models for which data is downloaded is provided in Appendix C. These datasets are available in NetCDF (*.nc) file format and are

accessed and analysed using R statistical programming language (R Development Core Team, 2008).

### 3.2.3 Historical observed hourly precipitation data

Hourly precipitation datasets for the duration 1960-2000 are obtained from the Grand River Conservation Authority (GRCA) at 21 stations located across the Grand River catchment. A list of these stations has been attached in Appendix D.

### 3.2.4 Historical observed daily streamflow data

Historical observed stream-flow data is collected at four discharge stations: Brantford, Galt, West Montrose and Shand dams located within the Grand River basin. These discharge stations are spread out widely across the catchment and have historical discharge data available for the period 1993-2000 (period chosen for hydrological model validation). Figure 15 shows the spatial distribution of discharge stations across Grand River at Brantford.

### 3.2.5 Historical reanalysis daily climate data

Reanalysis datasets are produced by combining a numerical model, capable of simulating one or more aspects of the earth's system, with climate observations made from several sources as ships, satellites, ground stations, radiosonde databases (RAOBS) and radars. They provide reliable climate data that extends from earth's surface to the stratosphere. NCEP/NCAR I provides gridded reanalysis data throughout the world, from 1948 till present, on a 2.5ºx2.5º and 2ºx2º Gaussian spatial scale (Kalnay et al.1996). NARR reanalysis is a relatively recent effort to produce high resolution reanalysis datasets (with a spatial resolution of 32 km) for North America (Mesinger et al., 2006). Inputs of both these reanalysis products are similar, but NARR output is obtained by using a lower resolution climate model and hence, is more accurate. Datasets from both the projects are used in this analysis. Wherever possible, NARR datasets are preferred over NCEP/NCAR I for their high accuracy. However, since NARR data is only available since 1979, NCEP/NCAR I datasets are used for period before it (1960-1979).

### 3.2.6 Catchment boundary for Grand River at Brantford discharge station

Catchment boundary for Grand River at Brantford discharge gauging station is obtained from the Environment Canada.

### 3.2.7 Historical reservoir release data

Daily historical reservoir release datasets for reservoirs at Conestoga, Luther, Shades, Guelph, Laurel, Woolwich and Shand dam for the duration 1984-present is provided by the Grand River Conservation Authority (GRCA). Hourly release data for the year 2012 at these reservoirs is also provided by the GRCA.

## 3.3 Analysis

As discussed before, skill of climate models for making climate predictions vary spatially. Therefore, first step towards performing model evaluations is to choose an appropriate spatial scale for analysis. To ensure effective evaluation and selection of GCMs for regional climate change impact analysis, we divided the spatial extents of Ontario into three distinct sections and performed model evaluations at each individual section. The division of Ontario into three parts is done keeping in mind the following factors:

- *Climate variability*: It seems more probable that regions with distinct climate trends will have different sets of efficient GCMs across them. Therefore, regions with distinct climate types (in terms of climate variables considered in the study, here mean temperature and precipitation) are first identified within Ontario. Same is done using plots of spatial variability in mean annual precipitation and temperature across Ontario as shown in Figure 16.
- *Spatial distribution of observed and GCM data*: Distribution of precipitation and temperature gauging stations as well as distribution of climate model grids across the province is also considered to ensure that sufficient amount of observed and model data falls within each section. This is reasoned to have a significant impact on the rankings since the methodology we were employing for ranking climate models is data-driven. The distribution of gauging stations within Ontario is found to be highly variable, with southern regions having much greater station densities than the

northern and central regions. Further, data grid sizes of GCMs selected for this analysis are found to vary from 1.125º to 5 º longitude and 1.125º to 4º latitude in terms of spatial resolution. Therefore, it is concluded that a) each individual section should be big enough to contain multiple climate model grids and b) that the central and northern regions should be larger than the southern region in terms of area to account for spatial variability in the distribution of climate gauging stations.

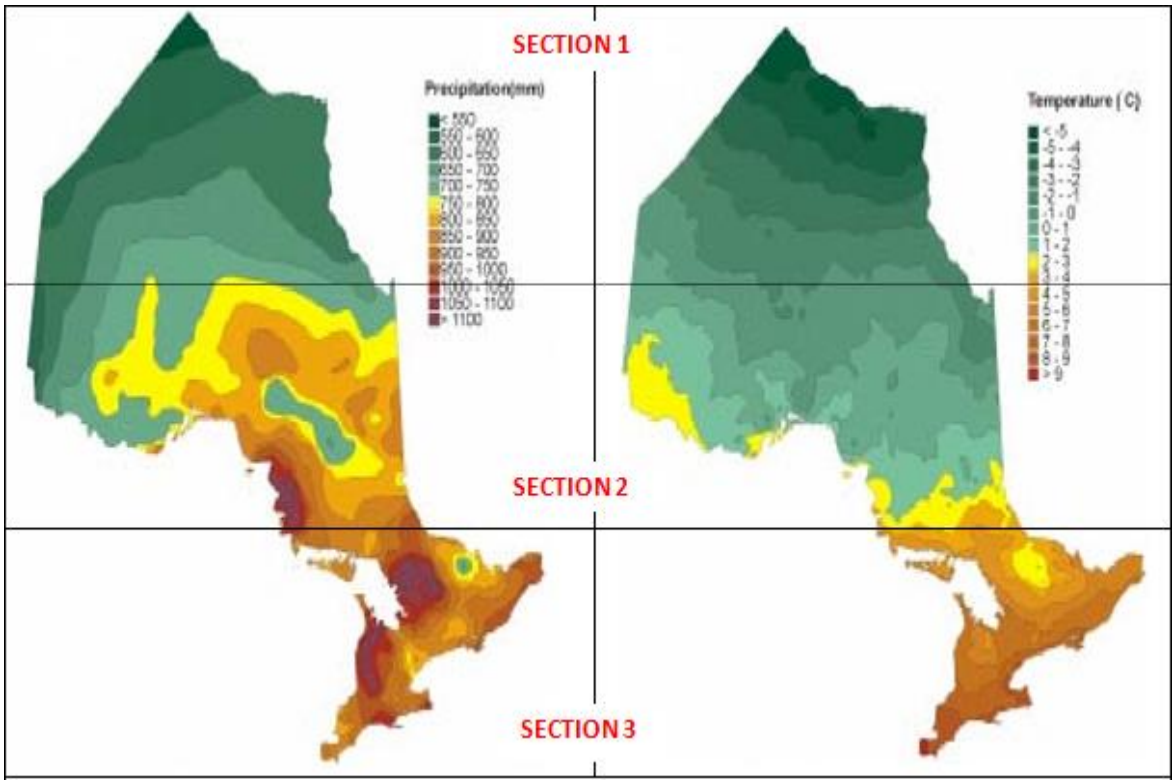


**Figure 15** Annual mean daily precipitation and temperature across Ontario (after Baldwin, Desloges, & Band, 2000)

Keeping above factors in mind, Ontario is divided into three sections as shown in Figure 16. Catchment selected for this study is located in section three of the divided province. However, in this study rankings are established for all the three sections of Ontario. This is done to be able to compare their results across the three sections and subsequently, make inferences about model skills.

Out of 1112 precipitation gauging stations having data with the period 1960-2000 or a part of it, 26 are located in part 1, 227 are located in part 2 and 866 stations are located in part 3. Likewise, out of 774 temperature recording stations, 22 are located in part 1, 175 are in part 2

and 577 are located in part 3. Historical observed point datasets at climate recording stations falling within each individual section are lumped together. Using a bin size of 1mm/day and 0.5ºC/day for daily precipitation and temperature, Pdfs are obtained for historical observed data. Missing datasets within the observed series are ignored while doing so. Similarly, historical daily precipitation and mean temperature gridded climate model data falling within each section are lumped together and Pdfs are generated for each GCM under study. Data obtained from different GCM runs are lumped together, without averaging, while analysing a particular GCM since it is found that differences in Pdfs are negligible across realisations. All Coupled Model Intercomparison Project Phase-3 (CMIP3) Atmosphere-Ocean General Circulation Models (AOGCMs) (Meehl et.al, 2007) are evaluated at a system level and rankings are obtained for climate variables precipitation and temperature. Results obtained are used to select six climate models simulating observed regional climate best in each section.

The distribution of climate stations is uneven across Ontario. The methodology used to rank GCMs in this study is data-driven and may produce groundless results for regions with sparse distribution of climate recording stations (for example, sections 1 and 2 of Ontario). Therefore, a check for robustness of rankings is performed prior to their further usage in the analysis. Many high resolution gridded reanalysis datasets are available across the globe. Although some bias does exist in these datasets (Decker et al., 2012), they have been found to replicate historically observed climate variables reasonably well (Kalnay et al.1996; Mesinger et al., 2006). Therefore, in the data sparse regions, reanalysis datasets are utilised in conjunction with the observed data for calculating GCM rankings.

Climate models are evaluated by performing three sets of experiments. Rankings are calculated by a) traditional approach considering observed data as baseline data b) weighted bin approach considering observed data as the baseline data and c) weighted bin approach considering both reanalysis and observed data as the baseline data. Linearly increasing bin weights are selected while adopting the weighted bin approach. Model rankings and skill scores obtained for temperature and precipitation in all three sections using above three approaches are provided in Appendix E. Top six climate models for each climate variable are highlighted in blue. Major inferences drawn by comparing GCM rankings in the three sections are:

- *Skill of climate models vary spatially*: It can be noted from climate model rankings obtained for three sections that the group of regionally efficient GCMs is different in different sections. Although there are instances where one single model is able to represented climatology really well over the entire Ontario province (for example, ECHAM5/MPI-OM in case of temperature), such instances are very rare and hence, there is no denying the fact that their skill does vary spatially. It also justifies our decision to make sections within Ontario while performing model evaluations.
- *Skill of climate models vary across climate variables*: It can be noted that the set of efficient climate models also vary with climate variable under study. Climate models performing well in simulating one climate variable, doesn't always simulate other climate variable well.
- *Skill of climate variables vary with the statistic under study*: A distinct change in rankings can be noted when traditional and weighted-bin approaches are considered, especially in case of precipitation. This highlights the importance of bin-weights used in this study, which make GCM rankings more problem-specific.
- *Adequate amount of baseline data is required for robust model evaluations*: This inference becomes evident if we compare model rankings under the approaches (b) and (c) for all the three sections under study. It can be noted that model rankings are more stable and robust in sections 2 and 3 as compared to section 1. It can be reasoned that gauging station density is significantly more in sections 2 and 3 than that in section 1 and hence, more robust model rankings are obtained in section 2 and 3 than in section 1. This finding highlights the importance of using sufficient amount of baseline data while performing model evaluations as well as justifies our usage of reanalysis datasets as part of baseline data while performing ranking experiments using approach c).

After comparing the rankings obtained from three approaches, a set of six most efficient GCMs are selected for section three, corresponding to each individual climate variable. Climate models ECHAM5/MPI-OM, GISS-ER, GISS-EH, FGOALS-g1.0, GFDL-CM2.1 and MRI-

CGCM2.3.2 are selected for temperature while GISS-ER, GISS-EH, ECHAM5/MPI-OM, UKMO-HadCM3, IPSL-CM4 and INGV- ECHAM4 are selected for precipitation.

Future data corresponding to selected GCMs is collected for scenarios A2, B1 and A1B from the PCMDI archive. Historical and future data grids falling within section three are selected and daily average temperature and precipitation change corresponding to each GCM-scenario combination is calculated. Since GCMs selected for precipitation and temperature are different and could not be plotted under the same graph, a modified version of percentile method is used. Daily average precipitation and temperature change is plotted and GCM-scenario combinations corresponding to (or close to) $5^{th}$, $25^{th}$, $50^{th}$, $75^{th}$ and $95^{th}$ percentiles of total range of changes, are selected for precipitation and temperature. Figures 17 presents GCM-scenario combinations selected for temperature and precipitation for future timelines. Similar procedure is followed to select GCM-scenario combinations for precipitation in 2050s and 2090s. GCM-scenario combinations selected for precipitation and temperature in 2050s and 2090s are summarised in Table 3.

**Table 3** GCM-scenario combinations selected for temperature and precipitation in section 3

| **Temperature** | | **Precipitation** | |
|---|---|---|---|
| **2050s** | **2090s** | **2050s** | **2090s** |
| GFDL-CM2.1(B1) | GFDL-CM2.1(A2) | GISS-ER(A1B) | GISS-ER, USA(A1B) |
| GISS-AOM(A1B) | GFDL-CM2.1(B1) | GISS-ER(A2) | GISS-ER, USA(A2) |
| GISS-AOM(B1) | GISS-ER(A2) | IPSL-CM4(B1) | IPSL-CM4(B1) |
| MPI- ECHAM5(A1B) | IAP-FGOALS(B1) | MPI-ECHAM5(A2) | INGV-ECHAM4(A1B) |
| MRI-CGCM2.3.2(B1) | MPI-ECHAM5(A1B) | INGV-ECHAM4(A2) | MPI-ECHAM5(B1) |

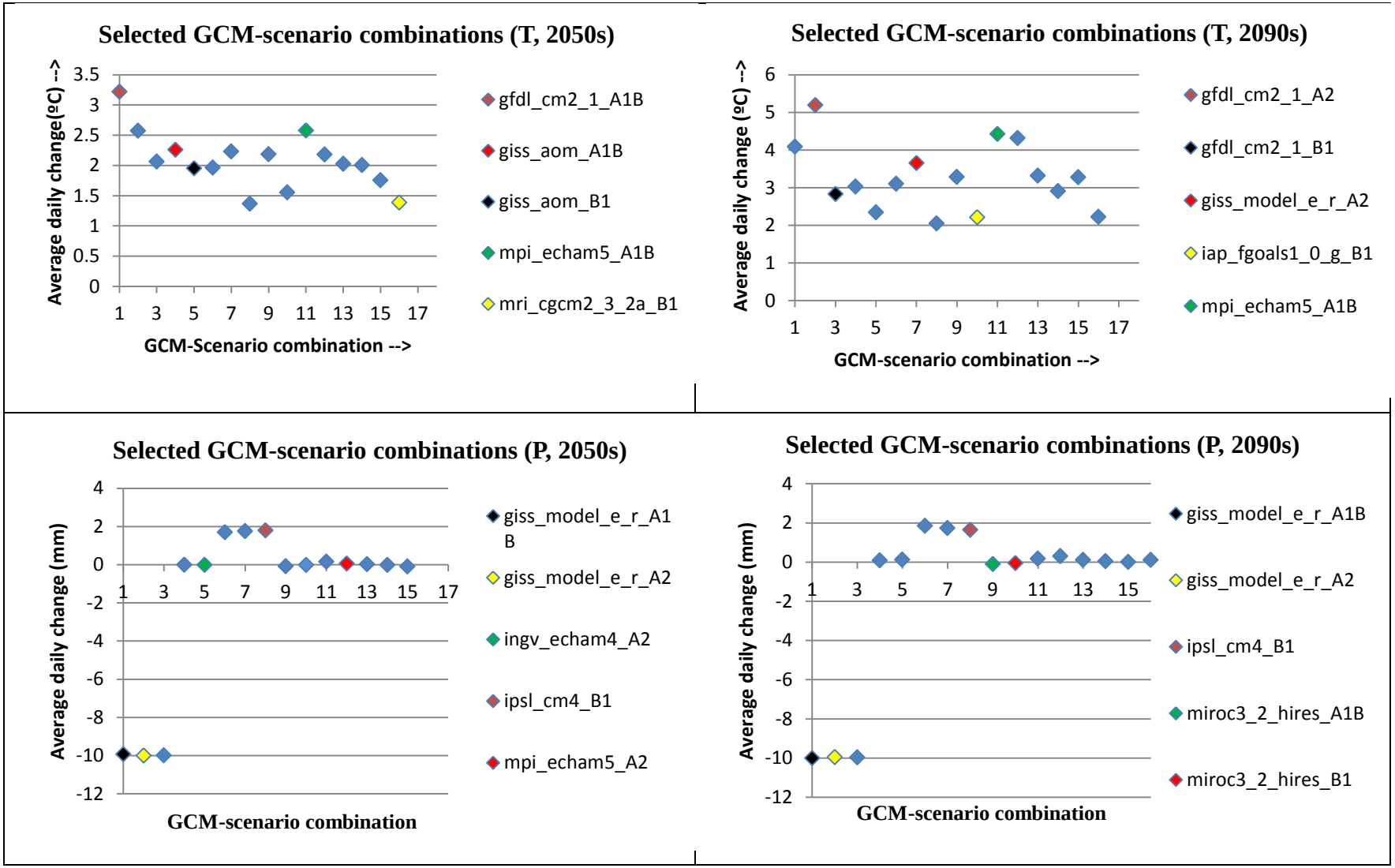


**Figure 16.** Selected GCM-scenario temperature and precipitation combinations for future timelines in section 3. Changes have been plotted for all the scenarios for which data is available from the CMIP3 archive.

Gridded daily historical climate model data corresponding to selected GCM-scenario combinations is spatially interpolated at 52 gauging stations lying within the Grand River catchment using Inverse Distance Square method. Further, historical observed data is filled-in with spatially interpolated reanalysis data to produce a continuous series of precipitation and temperature over the period of study (1960-2000). NCEP/NCAR daily precipitation data are available for the duration 1948-present while NARR precipitation data are available from 1979-present. Owing to their higher resolution, NARR datasets are preferred over their NCEP/NCAR counterparts. Maximum and minimum temperature data is available only for the NCEP/NCAR data product. Therefore, daily NCEP/NCAR gridded reanalysis datasets are used to fill in gaps in the observed $T_{mean}$, $T_{max}$ and $T_{min}$ data for the entire period of study. For precipitation, interpolated daily NCEP/NCAR and NARR reanalysis precipitation datasets are used to fill-in the missing observed data for the period 1960 to 1978 and 1979-2000 respectively.

Using interpolated GCM and filled-in observed historical data (for the duration 1960-2000) at each gauging station, daily bias-correction transfer functions are established selected GCMs. Obtained transfer functions are used to bias-correct historical and future GCM data at all 52 gauging stations using statistical bias correction approach. For bias-correction of GCM precipitation data, Piani et al., (2010) provided reasonable limits ($a<0$ and $1/5<b<5$) for linear transfer function parameters 'a' and 'b'. As explained in section 2.1.4, exponential transfer functions are used in case these thresholds are exceeded. However, few exceptionally high or low values of parameters 'a' and 'b' are obtained while fitting the exponential transfer function, which (in most cases) produce anomalous peaks in the corrected precipitation series. Therefore, to ensure precise estimation of bias-corrected precipitation extremes, an additional step of validation of bias correction parameters is included in the precipitation bias correction process.

The objective of transfer function validation step is to decide upon a threshold level to select or reject transfer function parameters for precipitation. At instances where transfer function parameter for a particular day crossed the threshold level, simple additive transfer functions (differences in means) are used in place of linear/exponential transfer functions. Different upper limit threshold levels are tried for parameter 'a' and daily transfer functions are estimated corresponding to each level. Obtained transfer function series is used to correct historical GCM precipitation data at all stations lying within Grand River catchment. Precipitation extremes

obtained from the bias corrected historical GCM data are compared with the extremes of the observed precipitation data and these steps are repeated for different threshold values of parameter 'a'. The threshold level, and corresponding transfer function series for which closest resemblance between bias-corrected and observed precipitation extremes is observed, is selected to bias correct historical and future GCM precipitation values across all gauging stations within the catchment.

**Table 4** Upper limit threshold levels tested for parameter 'a' in the transfer function validation step

| **Threshold level** | **IPSL_CM4** | | **MPI_ECHAM** | | **GISS_ER** | | **INGV_ECHAM4** | |
|---|---|---|---|---|---|---|---|---|
| | BC-GCM | OBS | BC-GCM | OBS | BC-GCM | OBS | BC-GCM | OBS |
| 100 | 89.06023 | 135.6 | 83.01382 | 135.6 | 97.87032 | 135.6 | 101.3427 | 135.6 |
| 150 | 128.0686 | 135.6 | 83.01382 | 135.6 | 97.87032 | 135.6 | 141.1488 | 135.6 |
| 200 | 163.7529 | 135.6 | 83.01382 | 135.6 | 97.87032 | 135.6 | 196.4013 | 135.6 |
| 250 | 205.4543 | 135.6 | 83.01382 | 135.6 | 97.87032 | 135.6 | 239.3878 | 135.6 |

Results obtained from the transfer function validation step are summarised in Table 4. As explained before, different threshold levels (here 100, 150, 200, 250) are tried for parameter 'a' and precipitation extremes (here $P_{max}$) of bias-corrected GCM data (denoted as BC-GCM) are compared with those obtained from observed data (denoted as OBS). From the obtained results, a threshold value of 150 is chosen for bias-correcting GCM precipitation data. It can also be inferred from the results that the transfer function validation step is not a necessary step in the bias-correction process. In fact, it is only required to screen the results from two out of four GCMs (i.e. for GCMs IPSL-CM4 and INGV-ECHAM4**).** Therefore, usage of this step rests with discretion of the user, if or not the obtained bias-corrected climate data seems reliable. In case of temperature, this transfer function validation step is not used as the bias-corrected values obtained are found to be within the limits.

Monthly bias correction transfer functions obtained at each gauging station are disaggregated into daily timesteps using methodology explained in section 2.1.4. Daily transfer functions are used to modify historical and future GCM data. Procedure followed is found effective in correcting bias associated with all moments of the GCM data. Same can be noted

from Figure 18, where bin frequency distributions of observed, raw GCM and bias-corrected GCM historical precipitation data have been compared. It can be noted that resemblance between frequency distributions of model and observed precipitation data is significantly improved using this methodology. Significant changes in statistical properties of future raw GCM precipitation and temperature data are also noted. Figures 19 compares the annual maximum values of precipitation and mean temperature as depicted by raw and bias-corrected GCM data, at gauging station: Apps Mills for periods 1980-2000, 2045-2065 (2050s) and 2081-2100 (2090s). Significant decreases in precipitation maximums and increases in temperature maximums can be noted, which highlights the importance and impact of bias-correction step in the climate change impact analysis process.

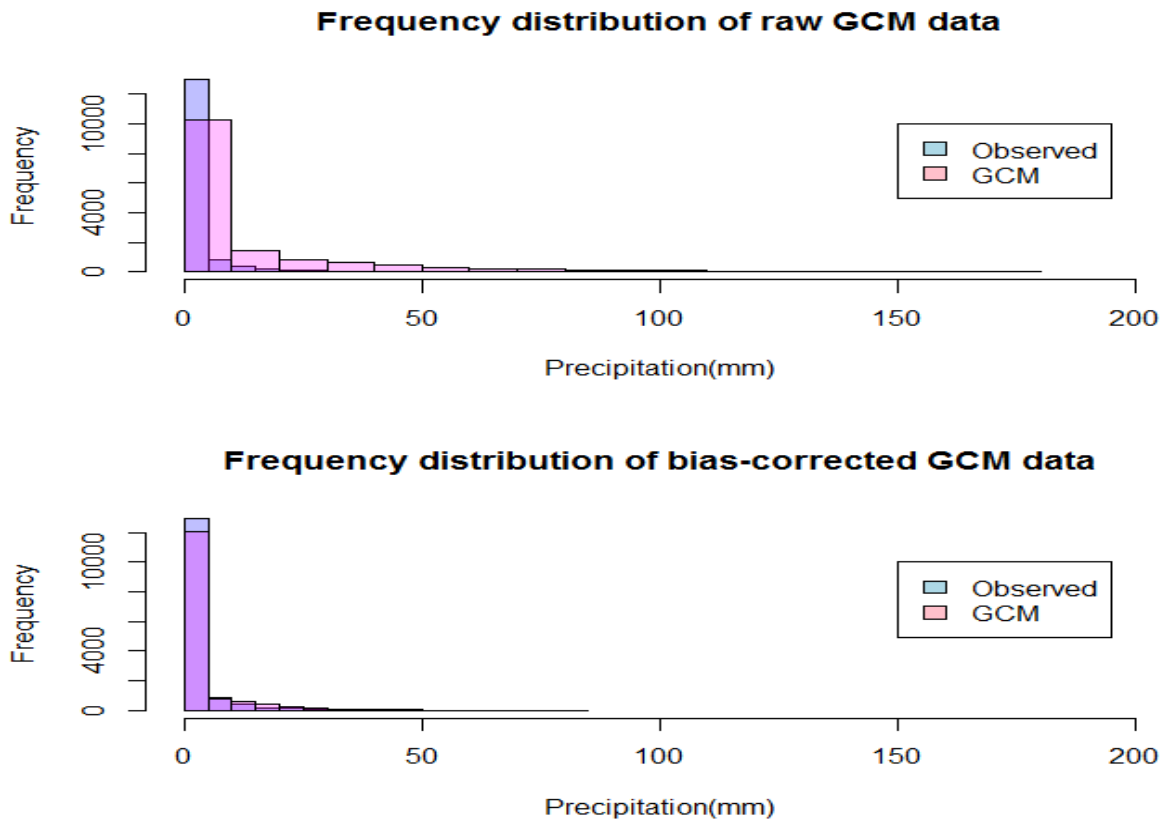


**Figure 17** Change in bin distribution of climate model (GISS-ER) precipitation data after bias correction

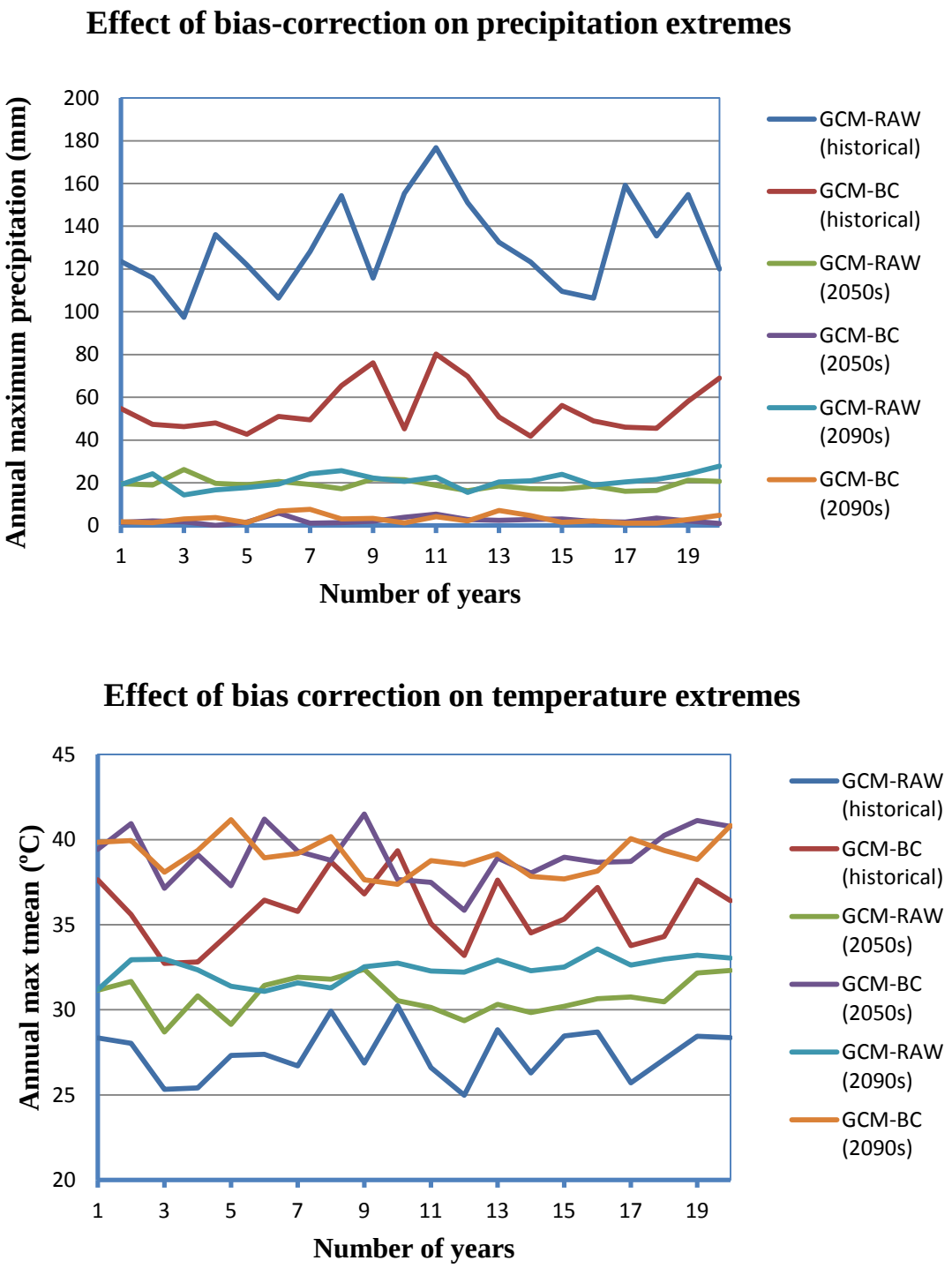


**Figure 18** Impact of application of bias correction on annual maximum precipitation and temperature climate model (MPI-ECHAM5) values. Here, Years=1 to 20 correspond to the periods 1981-2000, 2046-2065 and 2081-2100 for historical, 2050s and 2090s data respectively

Historically observed and bias-corrected historical and future GCM data are used together to downscale future climate projected by GCMs. Following the methodology explained in section 2.1.5, multiple additive and multiplicative CFs are used to generate future scaled temperature and precipitation data respectively. Total number of bins is chosen to be 100 and variable distribution is kept uniform across them. Generated future scaled data is imported in the KNN-CAD weather generator to generate ten different sets of future downscaled climate data for each GCM-scenario combination selected for analysis. In other words, fifty different future realisations of daily precipitation and mean temperature were simulated at each gauging station within the Grand River at Brantford catchment, for each timeline, to account for uncertainty associated with future climate projections. A temporal window of 14 days, block length of 10 days and interpolation coefficients of 0.9 are used while simulating both daily precipitation and temperature data. Choice of these parameters was made keeping in mind the recommendations made in King et al., (2012).

Simulated future daily precipitation and mean temperature timeseries is analysed to select variable combinations most likely to cause hydro-climatic extremes in future. This was done using the scatter-plot method. Scatter-plot diagrams and hydro-climatic extremes selected for 2050s and 2090s at one climate station (Apps Mills) is shown in Figure 20. Average daily precipitation and temperature values corresponding to fifty future realisations generated at Apps Mills for 2050s and 2090s are plotted. Realisations projecting hot-dry, cold-humid, hot-humid and cold-dry scenarios in future are picked using the generated scatter plot. In case of Apps Mills, realisations projecting hot-dry, cold-humid, hot-humid and cold-dry scenarios in 2050s have temperature and precipitation mean values of (12.021, 0.307), (10.775,2.363), (13.672, 2.372) and (10.077,1.877) respectively. Similar procedure is followed for all gauging stations lying within the catchment. A list of means of extreme future precipitation and temperature combinations selected at different climate stations lying within the Grand River at Brantford catchment for 2050s and 2090s is provided in Appendix F.

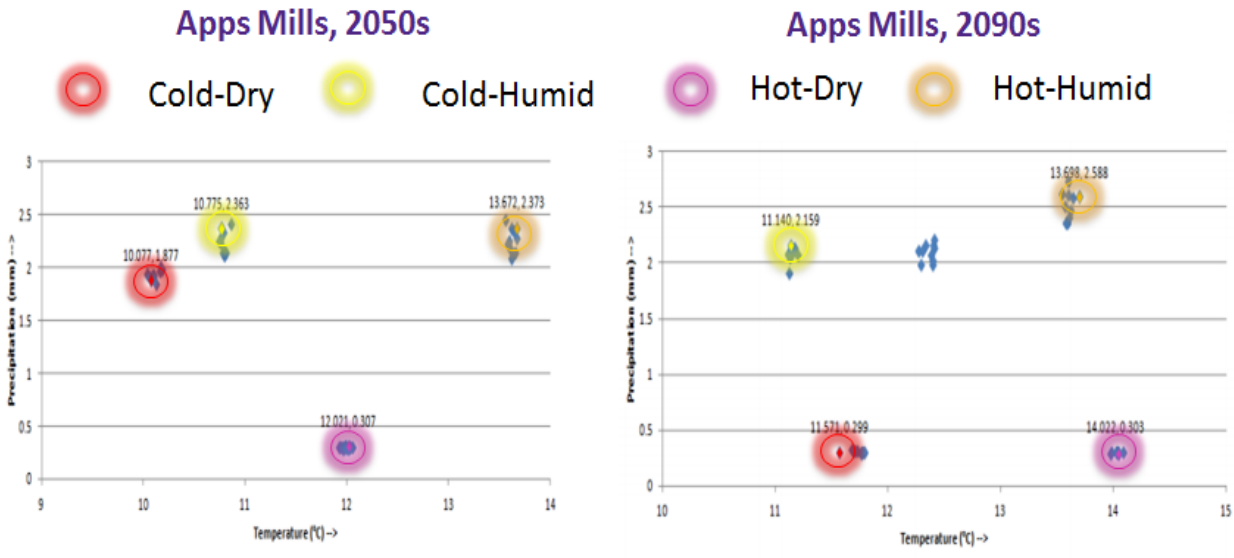


**Figure 190** Selection of future precipitation and temperature realisations most probable of causing hydro-climatic extremes for climate station: Apps Mills, for 2050s and 2090s

Future peak flows are determined by performing continuous hydrological modelling on selected extreme future realisations using semi-distributed hydrological model WATFLOOD. The model calibrated for Grand River basin for the period 2000-2005 is obtained from Dr. Nicholas Kouwen (Professor Emeritus, University of Waterloo). Using hourly climate data obtained from the GRCA, gridded precipitation and temperature datasets are developed for the period 1993-2000. Supplementary packages ragmet.exe and tmp.exe, made available with WATFLOOD, are used to do so. These gridded datasets are used in the calibrated model to validate the WATFLOOD model with respect to observed flow-series for the period 1993-2000 and satisfactory results are obtained. Coefficient of determination (R-square) values for modeled and observed flow series obtained at four discharge stations lying within the catchment are listed in Table 5. Once validated, the hydrologic model is used to generate flow series for future timelines.

**Table 5** Coefficient of determination values for daily and monthly historical flow series simulated by the hydrologic model

| Discharge stations | Daily series | Monthly series |
|---|---|---|
| Brantford | 0.675 | 0.795 |
| Galt | 0.767 | 0.900 |
| West Montrose | 0.832 | 0.921 |
| Shand dam | 0.952 | 0.995 |

Precipitation and temperature gridded data corresponding to eight combinations of hydro-climatic and variability scenarios are generated for each future timeline. For a particular combination, hourly temperature series are generated following the process outlined in section 2.2.2. Daily precipitation is internally disaggregated by the model. Hourly reservoir release information for most recent year (2012) is used and is considered constant over future timelines. Once all meteorological inputs and event files are ready, model calibrated on historical observed data is run with gridded future climate variable data to generate flow patterns for 2050s and 2090s.

Historical observed and generated future flow-series are used to obtain flood magnitude and return period relationships. In this study, POT method is employed to select flow peaks. Selection of independent peak discharge values is made using the software WETSPRO (Willems, 2009). The selection of independent flow peaks in WETSPRO is made using the following three criteria:

- Time between the two peaks should be greater than the recession constant $k$ (time in which flow becomes lower than 37% of its peak value).
- Minimum discharge between the two peaks should be less than a fraction $f$ of the peak discharge.
- Peak discharge should be greater than the threshold discharge value $q_{lim}$.

Values of parameters ‘k’ and ‘f’ have been chosen as 10 and 0.37 respectively. A reasonable estimate of threshold $q_{lim}$ is made for each flow-series following the guidelines mentioned in section 2.3. Mean exceedence above threshold vs. threshold value plots are

prepared for each flow-series to be analysed and the range of threshold domain is estimated. Plots generated to estimate the threshold domain for historically observed flows at Brantford is provided in Figure 21. To prepare these plots, mean exceedence value of flowseries crossing a particular threshold value is calculated and plotted against the threshold values. The process is repeated for several threshold values selected within the variable range. Values obtained for mean exceedence above threshold are plotted against mean threshold and region where a linear relationship exists between them is identified. An appropriate value of threshold is then decided within the threshold domain, so that total number of POT selections are above 3N (here, N denotes the number of years of available data) to satisfy the Poisson process criterion or for selected values to be randomly distributed over distribution space (described in section 2.3).

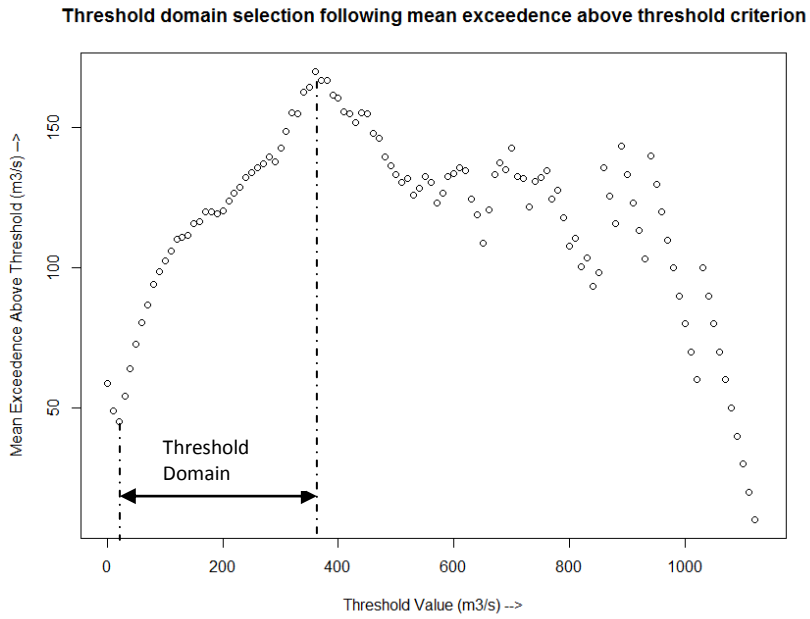


**Figure 201** Estimation of threshold domain for historically observed flows at Brantford

Selected flow peaks are used to fit a GPD and associated parameters are estimated using L-moments method. Flow quantiles corresponding to 2-year, 5-year, 10-year, 25-year, and 100-year return period floods are calculated. Results obtained for historically observed and future flow-series are compared thereafter, to estimate probable changes in peak flow return periods across Grand River at Brantford.

## 3.4 Results and discussion

Flood-magnitude and return period relationships are formulated for the catchment under study at three discharge locations: Brantford, Galt and West Montrose. The discharge station Brantford is located in the lower reaches of the catchment while Galt and West Montrose are located in the central regions of the catchment with West Montrose located north of Galt. Flow magnitude and return period relationships are formulated at these discharge stations for baseline and future timelines (2050s and 2090s) corresponding to all the scenarios formulated before. In the figures 22 to 24, *scenario 1-8* correspond to eight combinations of extreme hydro-climatic and temperature variability scenarios: *Max Temp Var & Cold and Dry*, *Max Temp Var & Cold and Humid*, *Max Temp Var & Hot and Dry*, *Max Temp Var & Hot and Humid*, *Min Temp Var & Cold and Dry*, *Min Temp Var & Cold and Humid*, *Min Temp Var & Hot and Dry* and *Min Temp Var & Hot and Humid* respectively. Also, historical simulation corresponds to the period 1961-2000.

Percent changes in flood quantiles obtained for future timelines at these three discharge stations are tabulated in Appendix G. A decreasing trend in peak flow quantiles is noted throughout the catchment, which might be linked to decreasing precipitation and increasing temperature trends projected for future across the catchment. However, magnitude of decrease varies with future scenarios considered for analysis. Anomalously high decreases are observed for scenarios projecting Hot and Dry climate in future. Relatively smaller and consistent decreases in flood quantiles are noted for other scenarios, which range between 30-60% of flood quantiles of the observed flow data.

Changes in the magnitude of flood quantiles are more significant for higher return period (25 or 100 year) events than that for lower return period events. This suggests that more significant impact of climate change can be expected on large extreme events than on lower extreme events.

Another notable point is that low precipitation scenarios (for example Hot and Dry, Cold and Dry) project significantly higher decreases in flood quantiles than high precipitation scenarios (for example Cold and Humid, Hot and Humid). However, the same is not always true for temperature scenarios. For example, scenarios Hot and Humid and Cold and Humid project

similar decreases in peak flow quantiles in both timelines. This suggests that changes in peak flow quantiles are more sensitive to changes in precipitation than to changes in temperature.

Peak flow quantiles are not found to be sensitive towards sub-daily scale temperature variability. From the results summarised in Appendix G, only minor changes (<1% in most cases) in flood quantiles are noted between scenarios considering or neglecting temperature variability on sub-daily scales. Therefore, it can be concluded that uncertainty associated with sub-daily temperature variability doesn't contribute significantly towards projected changes in future peak flow quantiles.

Rapid decreases in peak flow quantiles are observed till 2050s after which changes observed are more gradual, which suggest that the impacts gradually stabilize with time between the two future timelines.

With regards to spatial variability of changes in peak flow frequencies, higher decreases are simulated for downstream discharge station Brantford than for upstream stations Galt and West Montrose, which suggests that flow regimes will be affected to a greater extent in the southern regions of Grand River catchment than in the northern and central regions.

Figure 24 present the Cumulative Distribution Function (CDF) of historical observed and future projected peak flows at Brantford. It can be noted from the curves that return periods corresponding to a particular amount of flood increase in future. The increases are again, anomalously high for scenarios 3 and 7, which correspond to scenarios associated with hot and dry climate projections in future. Other scenarios are grouped close to each other and may be considered for making flow predictions in the catchment. Similar findings were noted for other discharge stations at Galt and West Montrose (refer to Appendix H for the results).

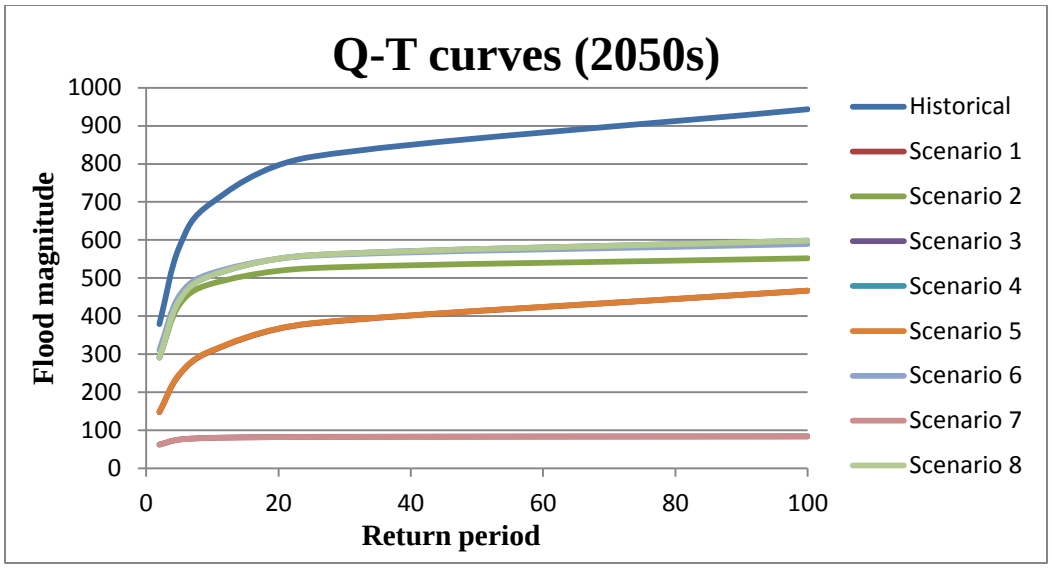


**Figure 212** Flood magnitude-return period curves for projected flows at Brantford in 2050s

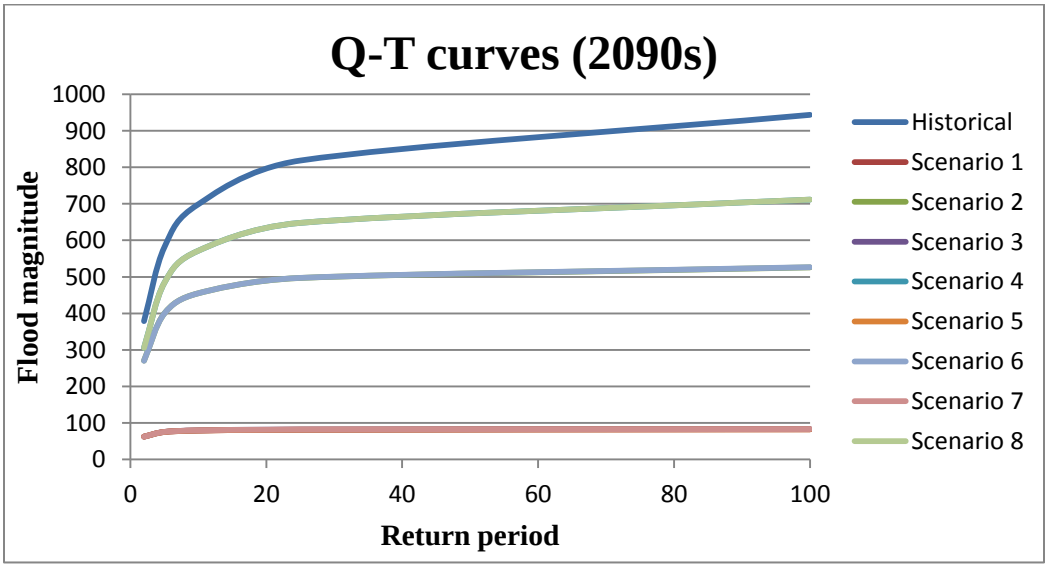


**Figure 23** Flood magnitude-return period curves for projected flows at Brantford in 2090s

Above findings suggest that flooding events will be decreasing throughout the catchment in future. On an average, 30-60% of changes in flood peaks are predicted. Southern regions of the catchment are expected to face more intense impacts than northern and central regions. Changes can be even worse if extreme hot and dry scenarios are realised in future.

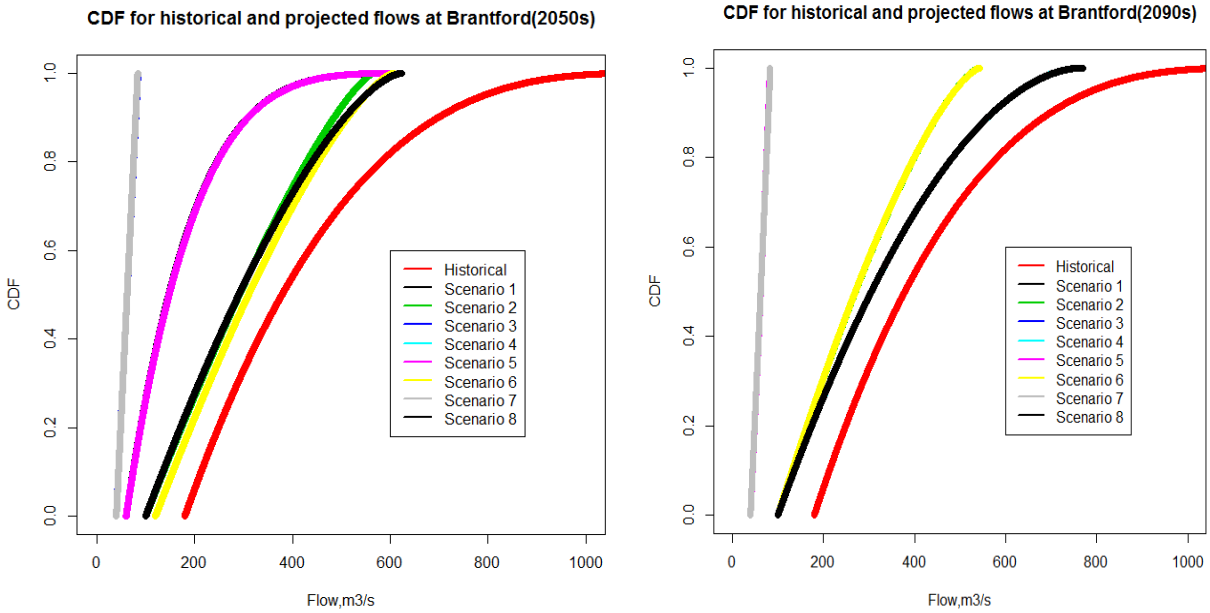


**Figure 24** Cumulative distribution function curves for historical and projected future flows at Brantford

# 4 CONCLUSION

This chapter describes the utility of proposed methodology in quantifying the impacts of climate change on return period of peak flows. Summary of results obtained from a case study performed on Grand River at Brantford is also provided. Lastly, some recommendations for future work in this direction are made.

## 4.1 Utility of proposed methodology

This research presents a methodology for performing Climate Change Impact Studies on flow regimes for a catchment. The proposed methodology focusses on addressing uncertainties inherent with future climate projections. Uncertainty associated with climate model selection has been identified as a major source of uncertainty in climate change impact studies. Therefore, significant efforts have been placed to select problem-specific GCMs for analysis. GCMs are ranked using different methodologies and most robust set of GCMs are chosen for analysis. From the obtained rankings, it is evident that a GCM skillfully projecting mean climatic conditions of a region may not necessarily project the extremes with equal skill. Therefore, methodologies like weighted bin factor approach, as proposed and used in this research, are helpful in selecting problem-specific GCMs for the region under study.

Plotting methodologies like percentile method and the scatter-plot method have been used in this study to encompass uncertainty associated with future climate projections. These methods are utilised in this study to select appropriate GCM-scenario combinations for analysis, and while selecting precipitation-temperature combinations likely to produce hydro-climatic extremes in future. These methods cover the projected uncertainty effectively by selecting only the extreme scenarios or specific quantiles of projections.

It is important to project entire distributions of climate variables accurately in future. The importance of doing so has been realised by the scientific community and latest methodologies for model evaluation, bias-correction and downscaling are focusing on projecting entire distributions of climate variables satisfactorily. Usage of such methodologies is necessary in climate change impact studies, especially when hydrologic extremes are being projected for

future. Analysis has been performed using Pdfs and CDFs for more realistic projection of whole distributions of climate variables in future.

Climate processes are analysed at high temporal resolution in this study. GCM evaluation and selection, bias-correction, and downscaling are performed on daily timescales. Additional scenarios based on sub-daily temperature variability are introduced and linked with four extreme hydro-climatic scenarios to generate a group of eight future scenarios. These eight scenarios cover the range of uncertainty inherent in climate variables at daily and sub-daily timescales. Formulation of such scenarios at high temporal scale is important while studying climate change impact on flow regimes to account for future uncertainty associated with physical processes operating at fine temporal scales.

Continuous hydrological modelling is performed using a semi-distributed hydrologic model to simulate future peak flows accurately. Peak Over Threshold (POT) model is used to develop relationship between peak flows and recurrence interval since the number of years of historical and future flow-series data is found to be small. A Generalised Pareto Distribution (GPD) is used to fit the flow peaks crossing a particular threshold. Method of L-moments is used to estimate parameters of GPD. These selections are made to simulate future flow patterns and analyse statistical differences between flood magnitude-return period relationships obtained for historical and future timelines.

In summary, methodology used in this study tries to capture climate related uncertainty associated with future streamflow projections. The importance of analysing changes in entire distributions of climate variables at fine temporal scales has been advocated. Available methodologies helpful in doing so have been explored and utilised to project changes in future peak flow return periods across the Grand River basin.

## 4.2 Results for the basin

Continual decreases in peak flows are observed at all three discharge stations selected for the analysis. Changes are more significant for higher return period events than lower return period events. Climate change impacts on peak flow return periods are found to be more intense in southern region of the catchment as compared to northern and central regions. Peak flow return

periods are projected to increase across the entire catchment, which means that the catchment will be more prone to droughts than to flooding events in future.

## 4.3 Future work

The analysis presented in this thesis can be further improved by making following considerations:

- While ranking GCMs, model evaluation is performed on sections showing distinct climate trends in the past. Identification of these sections is made subjectively by analysing plots showing historical climate trends across the province. Different clustering methodologies, for example as proposed by Mahlstein & Knutti, (2009) can be utilised in this regard to identify regions with distinct climatology in a more statistical manner.
- Streamflow projection made from this analysis can be further improved by taking into consideration other sources of uncertainty in addition to future climate projection uncertainty such as: uncertainties associated with hydrological model structure, hydrological parameters, downscaling techniques, bias correction techniques etc.
- Changes in land-use patterns may be considered while performing hydrological simulations for the catchment under study. Existing land-use has a significant role in simulating the flow response of catchment towards changes in climate variables. Projected future land-use datasets are available (for example, Hurtt et.al. 2009) and may be utilised while performing the hydrological modelling step.
- An attempt is made in this study to address uncertainty associated with sub-daily temperature variability. Efforts should be made to study sub-daily variability by taking into account changes in precipitation as well.
- The analysis presented in the thesis is performed using WRCP CMIP3 multi-model datasets. These datasets formed the basis of multi-model comparisons in IPCC, 2007. Datasets from the WRCP's CMIP5 project have been released in November, 2012. Results from the CMIP5 multi-model experiments will be discussed in the fifth assessment report of the IPCC (AR5) and are the most extensive and reliable multi-model datasets available currently (Taylor, Stouffer, & Meehl, 2012). These datasets should be preferred over CMIP3 datasets while performing climate change impact studies in future.

- Condition of non-stationarity is ignored while performing this analysis. Climate models are evaluated on present climate; bias-correction parameters obtained for historical record are directly applied to correct future climate variables; hydrological parameters have been kept constant between historical and future timelines; hydrological model calibrated for present climate conditions have been used to model future flows and so on. With rapidly changing climatic conditions across the globe, this assumption of non-stationarity is under scrutiny by the scientific community (Milly et al., 2008). Therefore, efforts should be made in the future to fulfill the condition of non-stationarity while undertaking climate change impact studies.

# REFERENCES

Alexander, L. V., Zhang, X., Peterson, T. C., Caesar, J., Gleason, B., Klein Tank, a. M. G., Haylock, M., et al. (2006). Global observed changes in daily climate extremes of temperature and precipitation. *Journal of Geophysical Research*, *111*(D5), D05109. doi:10.1029/2005JD006290

Anderson, E.A. 1973. National Weather Service River Forecast System-Snow Accumulation and Ablation Model. National Oceanographic and Atmospheric Administration, Silver Springs, Md., Tech. Memo NWS_HYDRO-17

Anandhi, A., Frei, A., Pierson, D. C., Schneiderman, E. M., Zion, M. S., Lounsbury, D., & Matonse, A. H. (2011). Examination of change factor methodologies for climate change impact assessment. *Water Resources Research*, *47*(3), W03501. doi:10.1029/2010WR009104

Baldwin, D. J. B., Desloges, J. R., and Band, L. E.: 2000, 'Physical Geography of Ontario', in Perera, A. H., Euler, D. E., and Thompson, I. D. (eds.), *Ecology of a Managed Terrestrial Landscape: Patterns and Processes of Forest Landscapes in Ontario*, University of British Columbia Press, Vancouver, B. C., pp. 141–162

Barrow E, B. Maxwell and P. Gachon (Eds), 2004. Climate Variability and Change in Canada: Past, Present and Future, ACSD Science Assessment Series No. 2, Meteorological Service of Canada, Environment Canada, Toronto, Ontario, 114p

Barrow, E., & Yu, G. (2005). CLIMATE SCENARIOS FOR ALBERTA A Report Prepared for the Prairie Adaptation Research Collaborative ( PARC ) in co-operation with Alberta Environment, (May), 1–73.

Berthet, L., Andréassian, V., Perrin, C., and Javelle, P.: How crucial is it to account for the Antecedent Moisture Conditions in flood forecasting? Comparison of event-based and continuous approaches on 178 catchments, Hydrol. Earth Syst. Sci. Discuss., 6, 1707-1736, doi:10.5194/hessd-6-1707-2009, 2009

Bingeman, A. K., Kouwen, N., Asce, M., & Soulis, E. D. (2006). Validation of the Hydrological Processes in a Hydrological Model, (October), 451–463.

Boyd, D., Cooke, S., Yerex, W., "Exploring Grand-Erie connections: Flow, quality and ecology", 9th Annual Grand River Watershed Water Forum. 18 September 2009. www.grandriver.ca/WaterForum/Boyd09.Pdf

Boyd, D., Smith, A. F., & Veale, B. (2000). Flood Management on the Grand River Basin, 1–26.

Brooks, G.R., S.G. Evans and J.J. Clague. (2001). "Flooding". *A Synthesis of Natural Geological Hazards in Canada*. G.R. Brooks (ed.). Ottawa: Geological Survey of Canada Bulletin 548. 101-143

Chen, C., Haerter, J. O., Hagemann, S., & Piani, C. (2011). On the contribution of statistical bias correction to the uncertainty in the projected hydrological cycle. *Geophysical Research Letters*, *38*(20), L20403. doi:10.1029/2011GL049318

Chin, D.A.,2006. Water-Resources Engineering.Prentice Hall, New Jersey

Cunnane, C., 1989. Statistical distributions for flood frequency analysis, Operational Hydrology Report no. 33, World Meteorological Organization, Geneva

Dankers, R., & Feyen, L. (2009). Flood hazard in Europe in an ensemble of regional climate scenarios. *Journal of Geophysical Research*, *114*(D16), D16108. doi:10.1029/2008JD011523

Das, S., & Simonovic, S. P. (2012). Assessment of Uncertainty in Flood Flows under Climate Change Impacts in the Upper Thames River Basin , Canada. *British Journal of Environment & Climate Change*, *2*(4), 318–338.

Debele, B., Srinivasan, R., & Yves Parlange, J. (2007). Accuracy evaluation of weather data generation and disaggregation methods at finer timescales. *Advances in Water Resources*, *30*(5), 1286–1300. doi:10.1016/j.advwatres.2006.11.009

Decker, M., Brunke, M. a., Wang, Z., Sakaguchi, K., Zeng, X., & Bosilovich, M. G. (2012). Evaluation of the Reanalysis Products from GSFC, NCEP, and ECMWF Using Flux Tower Observations. *Journal of Climate*, *25*(6), 1916–1944. doi:10.1175/JCLI-D-11-00004.1

Déry, S. J. (2005). Decreasing river discharge in northern Canada. *Geophysical Research Letters*, *32*(10), L10401. doi:10.1029/2005GL022845

Dessai, S. (2005). Limited sensitivity analysis of regional climate change probabilities for the 21st century. *Journal of Geophysical Research*, *110*(D19), D19108. doi:10.1029/2005JD005919

Ehret, U., Zehe, E., Wulfmeyer, V., Warrach-Sagi, K., & Liebert, J. (2012). *HESS Opinions* "Should we apply bias correction to global and regional climate model data?" *Hydrology and Earth System Sciences*, *16*(9), 3391–3404. doi:10.5194/hess-16-3391-2012

Environment Canada. 2004. Threats to Water Availability in Canada. National Water Research Institute, Burlington, Ontario. NWRI Scientific Assessment Report Series No. 3 and ACSD Science Assessment Series No. 1. 128 p

Farwell, J., Boyd, D., & Ryan, T. (2008). Making Watersheds More Resilient to Climate Change A Response in the Grand River Watershed , Ontario Canada.

Fowler, H. and Kilsby, C.: Using regional climate model data to simulate historical and future river flows in northwest England, Climatic Change, 80, 337–367, doi:10.1007/s10584-006-9117-3,2007

Garraway, M. (2011). Guide for Assessment of Hydrologic Effects of Climate Change in Ontario & Future Climate Change Data Sets, 1–19.

Gosling, S. N., Taylor, R. G., Arnell, N. W., & Todd, M. C. (2011). A comparative analysis of projected impacts of climate change on river runoff from global and catchment-scale hydrological models. *Hydrology and Earth System Sciences*, *15*(1), 279–294. doi:10.5194/hess-15-279-2011

Graham, L. P., J. Andréasson, and B. Carlsson (2007), Assessing climate change impacts on hydrology from an ensemble of regional climate mod- els, model scales and linking methods—A case study on the Lule River basin, Clim. Change, 81(S1), 293–307, doi:10.1007/s10584-006-9215-2

Grand River Conservation Authority, 2005. Establishing Environmental Flow Requirements for Selected Streams in the Grand River Watershed. Prepared by the Ontario Ministry of the Environment

Groisman, P.Y., S. Bomin, R.S. Vose, J.H. Lawrimore, P.H. Whitfield, E. F ørland, I. Hannssen-Baur, M.C. Serreze, V.N. Razuvaev and G.V. Alekseev, 2003: "Contemporary climate changes in high latitudes of the northern hemisphere: daily time resolution". Proceedings of the 14th Symposium on Global Change and Climate Variations

Haerter, J. O., Hagemann, S., Moseley, C., & Piani, C. (2011). Climate model bias correction and the role of timescales. *Hydrology and Earth System Sciences*, *15*(3), 1065–1079. doi:10.5194/hess-15-1065-2011

Hagemann, S., Chen, C., Haerter, J. O., Heinke, J., Gerten, D., & Piani, C. (2011). Impact of a Statistical Bias Correction on the Projected Hydrological Changes Obtained from Three GCMs and Two Hydrology Models. *Journal of Hydrometeorology*, *12*(4), 556–578. doi:10.1175/2011JHM1336.1

Hirabayashi Y., Shinjiro kanae, Seita emori, Taikan Oki & Masahide Kimoto (2008): Global projections of changing risks of floods and droughts in a changing climate, Hydrological Sciences Journal, 53:4, 754-772

Hosking, J.R.M., Wallis, J.R., 1997. Regional frequency analysis: an approach based on L-moments. Cambridge University Press, Cambridge.

Huber, M., & Knutti, R. (2011). Anthropogenic and natural warming inferred from changes in Earth's energy balance. *Nature Geoscience*, *5*(1), 31–36. doi:10.1038/ngeo1327

Ines, A. V. M., & Hansen, J. W. (2006). Bias correction of daily GCM rainfall for crop simulation studies. *Agricultural and Forest Meteorology*, *138*(1-4), 44–53. doi:10.1016/j.agrformet.2006.03.009

IPCC, 2012: Managing the Risks of Extreme Events and Disasters to Advance Climate Change Adaptation. A Special Report of Working Groups I and II of the Intergovernmental Panel on Climate Change [Field, C.B., V. Barros, T.F. Stocker, D. Qin, D.J. Dokken, K.L. Ebi, M.D. Mastrandrea, K.J. Mach, G.-K. Plattner, S.K. Allen, M. Tignor, and P.M. Midgley (eds.)]. Cambridge University Press, Cambridge, UK, and New York, NY, USA, 582 pp

IPCC, 2007: Climate Change 2007: The Physical Science Basis. Contribution of Working Group I to the Fourth Assessment Report of the Intergovernmental Panel on Climate Change[Solomon, S., D. Qin, M. Manning, Z. Chen, M. Marquis, K.B. Averyt, M. Tignor and H.L. Miller (eds.)]. Cambridge University Press, Cambridge, United Kingdom and New York, NY, USA, 996 pp

IPCC, 2001:Climate Change 2001: The Scientific Basis. Contribution of Working Group I to the Third Assessment Report of the Intergovernmental Panel on Climate Change [Houghton, J.T., Y. Ding, D.J. Griggs, M. Noguer, P.J. van der Linden, X. Dai, K. Maskell, and C.A. Johnson (eds.)]. Cambridge University Press, Cambridge, United Kingdom and New York, NY, USA, 881pp

IPCC, 2000 - Nebojsa Nakicenovic and Rob Swart (Eds.). IPCC Special Report on Emission Scenarios. Cambridge University Press, UK. pp 570

Jakob Themeßl, M., Gobiet, A., & Leuprecht, A. (2011). Empirical-statistical downscaling and error correction of daily precipitation from regional climate models. *International Journal of Climatology*, *31*(10), 1530–1544. doi:10.1002/joc.2168

Jung, I.-W., Chang, H., & Moradkhani, H. (2011). Quantifying uncertainty in urban flooding analysis considering hydro-climatic projection and urban development effects. *Hydrology and Earth System Sciences*, *15*(2), 617–633. doi:10.5194/hess-15-617-2011

Kalnay, E., M. Kanamitsu, R. Kistler, W. Collins, D. Deaven, L. Gandin, M. Iredell, S. Saha, G. White, J. Woollen, Y. Zhu, M. Chelliah, W. Ebisuzaki, W. Higgins, J. Janowiak, K. C. Mo, C. Ropelewski, J. Wang, A. Leetmaa, R. Reynolds, R. Jenne, and D. Joseph, 1996: The NMC/NCAR 40-Year Reanalysis Project". *Bull. Amer. Meteor. Soc.*, 77, 437-471

Kay, a. L., Davies, H. N., Bell, V. a., & Jones, R. G. (2009). Comparison of uncertainty sources for climate change impacts: flood frequency in England. *Climatic Change*, *92*(1-2), 41–63. doi:10.1007/s10584-008-9471-4

Khakbaz, B., Imam, B., Hsu, K., & Sorooshian, S. (2012). From lumped to distributed via semi-distributed: Calibration strategies for semi-distributed hydrologic models. *Journal of Hydrology*, *418-419*, 61–77. doi:10.1016/j.jhydrol.2009.02.021

Kiktev, D., Sexton, D. M. H., Alexander, L., & Folland, C. . (2003). Comparison of Modeled and Observed Trends in Indices of Daily Climate Extremes. *Journal of Climate*, *16*, 3560–3571.

King, L. M. (2012). Application of a K-nearest neighbour weather generator for simulation of historical and future climate variables in the Upper Thames River basin.

King, L. M., Mcleod, A. I., & Simonovic, S. P. (2012). Simulation of historical temperatures using a multi-site , multivariate block resampling algorithm with perturbation. doi:10.1002/hyp

Kingston, D. G., & Taylor, R. G. (2010). Sources of uncertainty in climate change impacts on river discharge and groundwater in a headwater catchment of the Upper Nile Basin, Uganda. *Hydrology and Earth System Sciences*, *14*(7), 1297–1308. doi:10.5194/hess-14-1297-2010

Knutti, R., Furrer, R., Tebaldi, C., Cermak, J., & Meehl, G. a. (2010). Challenges in Combining Projections from Multiple Climate Models. *Journal of Climate*, *23*(10), 2739–2758. doi:10.1175/2009JCLI3361.1

Kouwen, N., Soulis, E. D., Pietroniro, A., Donald, J., & Harrington, R. A. (1993). Grouped Response Units For Distributed Hydrological Modeling. *Journal of Water Resource Planning and Management*, *119*(3), 289–305.

Labat, D., Godd, Y., Probst, J. L., & Guyot, J. L. (2004). Evidence for global runoff increase related to climate warming. *Advances in water resources*, *27*(6), 631–642.

Lang, M., & Bobe, B. (1999). Towards operational guidelines for over-threshold modeling. *Journal of Hydrology*, *225*, 103–117.

Lapp, S., Sauchyn, D., & Wheaton, E. (2008). Institutional Adaptations to Climate Change Project : Future Climate Change Scenarios for the South Saskatchewan River Basin, (November).

Lemmen, D.S.,Warren, F.J., Lacroix, J., and Bush, E., editors (2008): From Impacts to Adaptation: Canada in a Changing Climate 2007; Government of Canada, Ottawa, ON, 448 p

Mahlstein, I., & Knutti, R. (2009). Regional climate change patterns identified by cluster analysis. *Climate Dynamics*, *35*(4), 587–600. doi:10.1007/s00382-009-0654-0

Maraun, D., & Wetterhall, F. (2010). Precipitation downscaling under climate change: Recent developments to bridge the gap between dynamical models and the end user. *Reviews of Geophysics*, (2009), 1–34. doi:10.1029/2009RG000314.

Maxino, C. C., Mcavaney, B. J., Pitman, A. J., & Perkins, S. E. (2008). Ranking the AR4 climate models over the Murray-Darling Basin using simulated maximum temperature , minimum temperature and precipitation, *1112*(August 2007), 1097–1112. doi:10.1002/joc

Mearns, L. O., W. J. Gutowski, R. Jones, L.-Y. Leung, S. McGinnis, A. M. B. Nunes, and Y. Qian: A regional climate change assessment program for North America. *EOS*, Vol. 90, No. 36, 8 September 2009, pp. 311-312

Meehl, G. a., Covey, C., Taylor, K. E., Delworth, T., Stouffer, R. J., Latif, M., McAvaney, B., et al. (2007). THE WCRP CMIP3 Multimodel Dataset: A New Era in Climate Change Research. *Bulletin of the American Meteorological Society*, *88*(9), 1383–1394. doi:10.1175/BAMS-88-9-1383

Mesinger, F., DiMego, G., Kalnay, E., Mitchell, K., Shafran, P. C., Ebisuzaki, W., Jović, D., et al. (2006). North American Regional Reanalysis. *Bulletin of the American Meteorological Society*, *87*(3), 343–360. doi:10.1175/BAMS-87-3-343

Milly, P. C. D., Betancourt, J., Falkenmark, M., Hirsch, R. M., Zbigniew, W., Lettenmaier, D. P., & Stouffer, R. J. (2008). Stationarity Is Dead : Whither Water Management ?, (February), 573–574.

Mortsch, L. (2011). Climate change scenarios for Mon application in water resources impact and adaptation assessments The challenge for water resources practitioners :

Muerth, M. J., Gauvin St-Denis, B., Ricard, S., Velázquez, J. a., Schmid, J., Minville, M., Caya, D., et al. (2012). On the need for bias correction in regional climate scenarios to assess climate change impacts on river runoff. *Hydrology and Earth System Sciences Discussions*, *9*(9), 10205–10243. doi:10.5194/hessd-9-10205-2012

Pathiraja, S., Westra, S., & Sharma, a. (2012). Why continuous simulation? The role of antecedent moisture in design flood estimation. *Water Resources Research*, *48*(6), W06534. doi:10.1029/2011WR010997

Perkins, S. E., Pitman, a. J., Holbrook, N. J., & McAneney, J. (2007). Evaluation of the AR4 Climate Models' Simulated Daily Maximum Temperature, Minimum Temperature, and Precipitation over Australia Using Probability Density Functions. *Journal of Climate*, *20*(17), 4356–4376. doi:10.1175/JCLI4253.1

Piani, C. and J. O. Haerter (2012), Two dimensional bias correction of temperature and precipitation copulas in climate models., *Geophys. Res. Lett.*, doi:10.1029/2012GL053839, in press

Piani, C., Haerter, J. O., & Coppola, E. (2009). Statistical bias correction for daily precipitation in regional climate models over Europe. *Theoretical and Applied Climatology*, *99*(1-2), 187–192. doi:10.1007/s00704-009-0134-9

Piani, C., Weedon, G. P., Best, M., Gomes, S. M., Viterbo, P., Hagemann, S., & Haerter, J. O. (2010). Statistical bias correction of global simulated daily precipitation and temperature for the application of hydrological models. *Journal of Hydrology*, *395*(3-4), 199–215. doi:10.1016/j.jhydrol.2010.10.024

Pierce, D. W., Barnett, T. P., Santer, B. D., & Gleckler, P. J. (2009). Selecting global climate models for regional climate change studies. *Proceedings of the National Academy of Sciences of the United States of America*, *106*(21), 8441–6. doi:10.1073/pnas.0900094106

R Development Core Team (2008). R: A language and environment for statistical computing. R Foundation for Statistical Computing, Vienna, Austria. ISBN 3-900051-07-0, URL http://www.R-project.org.

Raje, D., & Mujumdar, P. P. (2011). A comparison of three methods for downscaling daily precipitation in the Punjab region. *Hydrological Processes*, *25*(23), 3575–3589. doi:10.1002/hyp.8083

Report of the Expert Panel on Climate Change Adaptation (2009). Adapting to Climate Change in Ontario. Retrieved from http://www.ene.gov.on.ca/stdprodconsume/groups/lr/@ene/@resources/documents/resource/std01_079212.Pdf

Rojas, R., Feyen, L., Dosio, a., & Bavera, D. (2011). Improving pan-european hydrological simulation of extreme events through statistical bias correction of RCM-driven climate simulations. *Hydrology and Earth System Sciences Discussions*, *8*(2), 3883–3936. doi:10.5194/hessd-8-3883-2011

Schmidli, J., Frei, C., & Vidale, P. L. (2006). Downscaling from GCM precipitation: a benchmark for dynamical and statistical downscaling methods. *International Journal of Climatology*, *26*(5), 679–689. doi:10.1002/joc.1287

Shabbar, A. and B. Bonsal, 2003: As assessment of changes in winter cold and warm spells over Canada. Natural Hazards, 29, 173-188

Sharma, D., Das Gupta, a., & Babel, M. S. (2007). Spatial disaggregation of bias-corrected GCM precipitation for improved hydrologic simulation: Ping River Basin, Thailand. *Hydrology and Earth System Sciences Discussions*, *4*(1), 35–74. doi:10.5194/hessd-4-35-2007

Shrubsole,D. and others (2003). "An assessment of flood risk management in Canada". ICLR Research Paper Series – No. 28. ISBN 0-9732213-6-4

Stadnyk-Falcone, T. A. (2008). Mesoscale Hydrological Model Validation and Verification using Stable Water Isotopes : The isoWATFLOOD Model. Doctrate of Philosophy disseration.

Swainson, B. (2009). Rivers at Risk :The Status of Environmental Flows in Canada.

Taylor, K. E., Stouffer, R. J., & Meehl, G. a. (2012). An Overview of CMIP5 and the Experiment Design. *Bulletin of the American Meteorological Society*, *93*(4), 485–498. doi:10.1175/BAMS-D-11-00094.1

Taylor, K., "IPCC Coupled Model Output For Working Group 1", IPCC Working Group I Fourth Assessment Report First Lead Authors Meeting. 26-29 September 2004, Trieste, Italy

Tebaldi, C. (2004). Regional probabilities of precipitation change: A Bayesian analysis of multimodel simulations. *Geophysical Research Letters*, *31*(24), L24213. doi:10.1029/2004GL021276

Teutschbein, C., & Seibert, J. (2012). Is bias correction of Regional Climate Model (RCM) simulations possible for non-stationary conditions? *Hydrology and Earth System Sciences Discussions*, *9*(11), 12765–12795. doi:10.5194/hessd-9-12765-2012

Vannitsem, S. (2011). Bias correction and post-processing under climate change. *Nonlinear Processes in Geophysics*, *18*(6), 911–924. doi:10.5194/npg-18-911-2011

Watanabe, S., Kanae, S., Seto, S., Yeh, P. J.-F., Hirabayashi, Y., & Oki, T. (2012). Intercomparison of bias-correction methods for monthly temperature and precipitation simulated by multiple climate models. *Journal of Geophysical Research*, *117*(D23), D23114. doi:10.1029/2012JD018192

Whitfield, P. H., & Cannon, A. J. (2000). Recent Variations in Climate and Hydrology in Canada, (1).

Wilby, R. L., & Harris, I. (2006). A framework for assessing uncertainties in climate change impacts: Low-flow scenarios for the River Thames, UK. *Water Resources Research*, *42*(2), W02419. doi:10.1029/2005WR004065

Willems, P. (2009). Environmental Modelling & Software A time series tool to support the multi-criteria performance evaluation of rainfall-runoff models. *Environmental Modelling and Software*, *24*(3), 311–321. doi:10.1016/j.envsoft.2008.09.005

Young, K. C. (1993).A multivariate chain model for simulating climatic parameters from daily data, Journal of Applied Meteorology, 33, 661-671.

# APPENDICES

## Appendix A: Schematic diagram of SRES scenarios with their descriptions

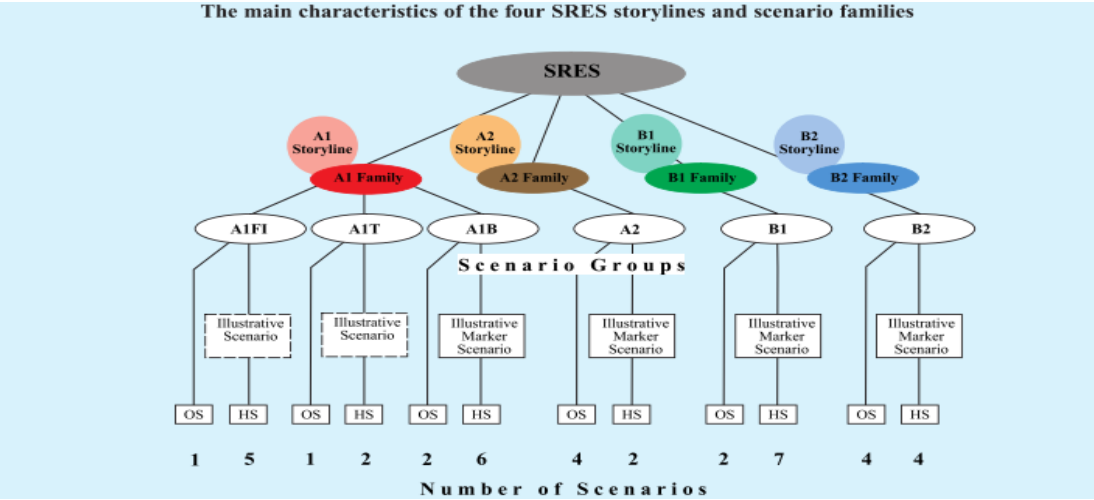


**Figure 225** The hierarchy of SRES scenarios (taken from IPCC, 2000)

**Table 6**.Description of four underlying storylines of SRES scenarios

| Storyline | Description |
|---|---|
| *A1* | Rapid technological and demographic growth till mid 21st century after which global population decreases and energy efficient systems are introduced. Underlying theme is equality among regions and increased social and cultural interactions. This storyline branches out into three scenario groups: A1F1, A1T and A1B based on the society's inclination towards fossil, non-fossil and a balanced use of both fuels for technological development |
| *A2* | Presents a very heterogeneous world with continuously increasing population. The underlying theme is self-preservance and local development |
| *B1* | Rapid demographic growth till mid 21st century after which it decreases. Focus thereafter is on the usage of resource-efficient technologies and towards building an environmentally sustainable world, however, without any additional climate initiatives |
| *B2* | Presents a world with continuously increasing population (at a rate lower than A2). Overall emphasis is towards building a environmentally and culturally sustainable environment, but only at regional or local levels |

# Appendix B: Gauging stations lying within the Grand River at Brantford catchment

**Table 7** Gauging stations where historical observed daily climate data is extracted

| Station Name | Long(degrees) | Lat(degrees) | Elevation |
|---|---|---|---|
| Apps mill | -80.383 | 43.133 | 230.1 |
| Arthur | -80.567 | 43.817 | 452 |
| Ayr | -80.45 | 43.283 | 289.6 |
| Blue acton | -80.05 | 43.6 | 365.8 |
| Blue corwhin | -80.117 | 43.533 | 350.5 |
| Blue rockwood | -80.117 | 43.583 | 350.5 |
| Blue scout | -80.083 | 43.617 | 342.9 |
| Blue springs creek | -80.117 | 43.633 | 373.4 |
| Brantford morell | -80.283 | 43.15 | 198.1 |
| Burford | -80.433 | 43.1 | 259.1 |
| Cambridge galt moe | -80.317 | 43.33 | 268.2 |
| Cambridge-stewart | -80.3 | 43.35 | 289 |
| Canning | -80.45 | 43.183 | 259.1 |
| Cathcart | -80.567 | 43.117 | 269.7 |
| Crewsons corners | -80.1 | 43.617 | 358.1 |
| Damascus | -80.483 | 43.917 | 487.7 |
| Drumbo | -80.55 | 43.233 | 304.8 |
| Drumbo harrington | -80.517 | 43.233 | 281.9 |
| Elmira | -80.533 | 43.6 | 350.5 |
| Elora automatic climate station | -80.417 | 43.65 | 376.4 |
| Elora rcs | -80.417 | 43.65 | 376.4 |
| Elora research stn | -80.417 | 43.65 | 376.4 |
| Falkland | -80.45 | 43.133 | 262.1 |
| Fergus moe | -80.38 | 43.702 | 396.2 |
| Fergus shand dam | -80.331 | 43.735 | 417.6 |
| Glen allan | -80.711 | 43.684 | 400 |
| Grand valley wpcp | -80.333 | 43.883 | 464.8 |
| Guelph arboretum | -80.217 | 43.55 | 327.7 |
| Guelph oac | -80.233 | 43.517 | 333.8 |

| | | | |
|---|---|---|---|
| Guelph oac physics dept | -80.267 | 43.55 | 340.5 |
| Guelph turfgrass cs | -80.217 | 43.55 | 325 |
| Haysville | -80.633 | 43.35 | 320 |
| Hillsburgh | -80.167 | 43.767 | 427 |
| Kitchener | -80.5 | 43.433 | 320 |
| Kitchener city eng 1 | -80.483 | 43.45 | 320 |
| Kitchener city eng 2 | -80.483 | 43.45 | 281.9 |
| Kitchener owrc | -80.433 | 43.4 | 321.6 |
| Kitchener/waterloo | -80.379 | 43.461 | 342.9 |
| Millers lake | -80.383 | 43.283 | 304.8 |
| Monticello | -80.4 | 43.967 | 481.6 |
| Morriston | -80.117 | 43.467 | 304.8 |
| Newton | -80.9 | 43.583 | 373.4 |
| Newton | -80.883 | 43.583 | 382 |
| Paris | -80.45 | 43.183 | 266.7 |
| Preston | -80.417 | 43.4 | 291.1 |
| Preston wpcp | -80.35 | 43.383 | 272.8 |
| Salem | -80.47 | 43.71 | 430 |
| Waldemar | -80.283 | 43.883 | 449.6 |
| Waterloo fire hall | -80.517 | 43.467 | 317 |
| Waterloo wellington a | -80.383 | 43.45 | 317 |
| Waterloo wellington 2 | -80.383 | 43.45 | 313.6 |
| Waterloo wpcp | -80.517 | 43.483 | 327.7 |

# Appendix C: Description of climate models considered in the analysis

**Table 8** Climate models and number of realizations of historical data considered in the analysis

| S.No | Model | Number of realisations of historical data considered | Atmospheric component resolution | |
|---|---|---|---|---|
| | | | *Horizontal(lat x lon)* | *Vertical (levels)* |
| 1 | BCCR-BCM2.0, 2005 | 1 | 1.9º x 1.9º | L31 |
| 2 | CGCM3.1(T47), 2005 | 5 | 2.8º x 2.8º | L31 |
| 3 | CGCM3.1(T63), 2005 | 1 | 1.9º x 1.9º | L31 |
| 4 | CNRM-CM3, 2004 | 1 | 1.9º x 1.9º | L45 |
| 5 | CSIRO-MK3.0, 2001 | 3 | 1.9º x 1.9º | L18 |
| 6 | CSIRO-MK3.5, 2005 | 3 | 1.9º x 1.9º | L18 |
| 7 | GFDL-CM2.0, 2005 | 1 | 2.0ºx 2.5º | L24 |
| 8 | GFDL-CM2.1, 2005 | 1 | 2.0º x 2.5º | L24 |
| 9 | GISS-AOM, 2004 | 1 | 3ºx 4º | L12 |
| 10 | GISS-EH, 2004 | 1 | 4º x 5º | L20 |
| 11 | GISS-ER, 2004 | 1 | 4º x 5º | L20 |
| 12 | FGOALS-g1.0, 2004 | 3 | 2.8º x 2.8º | L26 |
| 13 | ECHAM4/MPI-OM, 2005 | 1 | 1.9º x 1.9º | L18 |
| 14 | INM-CM3.0, 2004 | 1 | 4º x 5º | L21 |
| 15 | IPSL-CM4, 2005 | 2 | 2.5° x 3.75° | L19 |
| 16 | MIROC3.2(hires), 2004 | 1 | 1.1º x 1.1º | L56 |
| 17 | MIROC3.2(medres), 2004 | 2 | 2.8º x 2.8º | L20 |
| 18 | ECHO-G, 1999 | 3 | 3.9ºx 3.9º | L19 |
| 19 | ECHAM5/MPI-OM, 2005 | 2 | 1.9º x 1.9º | L31 |
| 20 | MRI-CGCM2.3.2, 2003 | 5 | 2.8º x 2.8º | L30 |
| 21 | CCSM3, 2005 | 7 | 1.4º x 1.4º | L26 |
| 22 | PCM, 1998 | 3 | 2.8º x 2.8º | L26 |
| 23 | UKMO-HadCM3, 1997 | 1 | 2.5º x 3.75º | L19 |

* Model UKMO-HadGEM1 contained only monthly precipitation data and hence was disregarded from the analysis

# Appendix D: Stations at which hourly precipitation data is obtained from the GRCA

**Table 9** Stations at which hourly precipitation data is obtained from the GRCA

| Station_ID | Station_Name | Easting | Northing |
|---|---|---|---|
| 1 | Proton Station | 538657 | 4890504 |
| 2 | Monticello | 546796 | 4870194 |
| 3 | Grand Valley WPCP | 553569 | 4859138 |
| 4 | Fergus Shand Dam | 553704 | 4842478 |
| 5 | Elora RCS | 547057 | 4833173 |
| 6 | Mount Forest (AUT) | 520063 | 4870059 |
| 7 | Glen Allan | 522851 | 4836748 |
| 8 | Elmira | 537659 | 4831262 |
| 9 | Waterloo Wellington | 549910 | 4810980 |
| 10 | Preston | 547252 | 4805408 |
| 11 | Guelph Turfgrass | 563292 | 4822199 |
| 12 | Cambridge Galt MOE | 555396 | 4797843 |
| 13 | Stratford MOE | 500013 | 4801541 |
| 14 | Roseville | 543238 | 4799828 |
| 15 | Woodstock | 520352 | 4773808 |
| 16 | Scotland | 547562 | 4760987 |
| 17 | Brantford MOE | 562370 | 4775914 |
| 18 | Valens | 570216 | 4803756 |
| 19 | Middleport | 578658 | 4774231 |
| 20 | Hagersville | 576132 | 4757543 |
| 21 | Dunville Pumping stn. | 613076 | 4743243 |

# Appendix E: GCM rankings across three sections of Ontario

**Table 10** Comparison of GCM rankings obtained for precipitation and temperature at all three sections of Ontario

| Section 1 (Precipitation) | | | | | | |
|---|---|---|---|---|---|---|
| **Models** | **Observed data+traditional approach** | | **Observed data+bin scores approach** | | **Observed and Reanalysis data+skill scores approach** | |
| | *Skill score (out of 1)* | *Rank* | *Skill score (x10-5)* | *Rank* | *Skill score (x10-5)* | *Rank* |
| bccr_bcm2_0 | 0.899 | 10 | 2.523 | 19 | 2.853 | 18 |
| cccma_cgcm3_1 | 0.9 | 9 | 2.832 | 11 | 3.127 | **3** |
| cccma_cgcm3_1_t63 | 0.907 | 8 | 2.752 | 14 | 2.984 | 12 |
| cnrm_cm3 | 0.836 | 19 | 2.599 | 18 | 2.941 | 14 |
| csiro_mk3_0 | 0.887 | 12 | 2.657 | 15 | 3.006 | 11 |
| csiro_mk3_5 | 0.947 | **2** | 3.056 | 8 | 3.084 | 10 |
| gfdl_cm2_0 | 0.896 | 11 | 2.963 | 10 | 3.195 | **1** |
| gfdl_cm2_1 | 0.936 | **3** | 2.813 | 12 | 2.955 | 13 |
| giss_aom | 0.914 | **6** | 2.621 | 17 | 2.906 | 15 |
| giss_model_e_h | 0.568 | 22 | 3.167 | **6** | 2.699 | 22 |
| giss_model_e_r | 0.686 | 21 | 3.331 | **3** | 2.87 | 17 |
| iap_fgoals1_0_g | 0.883 | 14 | 2.481 | 21 | 2.798 | 20 |
| ingv_echam4 | 0.848 | 16 | 3.194 | **5** | 3.144 | **2** |
| inmcm3_0 | 0.839 | 18 | 3.237 | **4** | 3.111 | **5** |
| ipsl_cm4 | 0.861 | 15 | 3.058 | 7 | 3.085 | 9 |
| miroc3_2_medres | 0.913 | 7 | 2.645 | 16 | 2.895 | 16 |
| miub_echo_g | 0.845 | 17 | 2.793 | 13 | 3.087 | 8 |
| mpi_echam5 | 0.947 | **1** | 3.56 | **1** | 3.091 | 7 |
| mri_cgcm2_3_2a | 0.924 | **5** | 3.0272 | 9 | 3.111 | **4** |
| ncar_ccsm3_0 | 0.885 | 13 | 2.497 | 20 | 2.840 | 19 |
| ncar_pcm1 | 0.831 | 20 | 2.398 | 22 | 2.750 | 21 |
| ukmo_hadcm3 | 0.935 | **4** | 3.402 | **2** | 3.110 | **6** |

| Section 2 (Precipitation) | | | | | | |
|---|---|---|---|---|---|---|
| **Models** | **Observed data+traditional approach** | | **Observed data+bin scores approach** | | **Observed and Reanalysis data+skill** | |
| | *Skill score (out of 1)* | *Rank* | *Skill score (x10-5)* | *Rank* | *Skill score (x10-5)* | *Rank* |
| bccr_bcm2_0 | 0.926 | **6** | 2.508 | 19 | 2.593 | 19 |
| cccma_cgcm3_1 | 0.898 | 11 | 2.819 | 12 | 2.904 | 11 |
| cccma_cgcm3_1_t63 | 0.905 | 10 | 2.739 | 14 | 2.823 | 14 |
| cnrm_cm3 | 0.808 | 20 | 2.627 | 17 | 2.669 | 18 |
| csiro_mk3_0 | 0.907 | 9 | 2.643 | 15 | 2.728 | 15 |
| csiro_mk3_5 | 0.955 | **1** | 3.042 | 8 | 3.127 | 8 |
| gfdl_cm2_0 | 0.896 | 12 | 2.950 | 10 | 3.035 | 10 |
| gfdl_cm2_1 | 0.928 | **5** | 2.799 | 13 | 2.882 | 12 |
| giss_aom | 0.881 | 13 | 2.607 | 18 | 2.692 | 17 |
| giss_model_e_h | 0.587 | 22 | 3.710 | **2** | 3.255 | **6** |
| giss_model_e_r | 0.679 | 21 | 3.874 | **1** | 3.420 | **3** |
| iap_fgoals1_0_g | 0.871 | 14 | 2.467 | 21 | 2.552 | 21 |
| ingv_echam4 | 0.847 | 16 | 3.276 | **6** | 3.277 | **5** |
| inmcm3_0 | 0.843 | 17 | 3.378 | **5** | 3.332 | **4** |
| ipsl_cm4 | 0.848 | 15 | 3.064 | 7 | 3.140 | 7 |
| miroc3_2_medres | 0.930 | **4** | 2.631 | 16 | 2.717 | 16 |
| miub_echo_g | 0.840 | 18 | 2.819 | 11 | 2.860 | 13 |
| mpi_echam5 | 0.949 | **2** | 3.598 | **3** | 3.660 | **1** |
| mri_cgcm2_3_2a | 0.932 | **3** | 3.013 | 9 | 3.098 | 9 |
| ncar_ccsm3_0 | 0.910 | 8 | 2.483 | 20 | 2.568 | 20 |
| ncar_pcm1 | 0.837 | 19 | 2.384 | 22 | 2.469 | 22 |
| ukmo_hadcm3 | 0.922 | 7 | 3.432 | **4** | 3.494 | **2** |

| Section 3 (Precipitation) | | | | | | |
|---|---|---|---|---|---|---|
| **Models** | **Observed data+traditional approach** | | **Observed data+bin scores approach** | | **Observed and Reanalysis data+skill** | |
| | *Skill score (out of 1)* | *Rank* | *Skill score (x10-5)* | *Rank* | *Skill score (x10-5)* | *Rank* |
| bccr_bcm2_0 | 0.833 | 14 | 2.463 | 19 | 2.568 | 19 |
| cccma_cgcm3_1 | 0.884 | 9 | 2.774 | 12 | 2.878 | 12 |
| cccma_cgcm3_1_t63 | 0.912 | **5** | 2.694 | 14 | 2.788 | 14 |
| cnrm_cm3 | 0.741 | 18 | 2.585 | 17 | 2.688 | 16 |
| csiro_mk3_0 | 0.901 | 7 | 2.598 | 15 | 2.703 | 15 |
| csiro_mk3_5 | 0.927 | **3** | 2.997 | 8 | 3.082 | 8 |
| gfdl_cm2_0 | 0.871 | 12 | 2.905 | 10 | 3.009 | 10 |
| gfdl_cm2_1 | 0.913 | **4** | 2.754 | 13 | 2.816 | 13 |
| giss_aom | 0.797 | 17 | 2.562 | 18 | 2.667 | 18 |
| giss_model_e_h | 0.617 | 22 | 4.033 | **2** | 3.939 | **2** |
| giss_model_e_r | 0.666 | 21 | 4.197 | **1** | 4.103 | **1** |
| iap_fgoals1_0_g | 0.823 | 15 | 2.422 | 21 | 2.519 | 21 |
| ingv_echam4 | 0.835 | 13 | 3.246 | **6** | 3.351 | **6** |
| inmcm3_0 | 0.689 | 20 | 3.374 | **5** | 3.474 | **5** |
| ipsl_cm4 | 0.879 | 10 | 3.021 | 7 | 3.113 | 7 |
| miroc3_2_medres | 0.908 | **6** | 2.586 | 16 | 2.677 | 17 |
| miub_echo_g | 0.810 | 16 | 2.777 | 11 | 2.880 | 11 |
| mpi_echam5 | 0.955 | **1** | 3.553 | **3** | 3.658 | **3** |
| mri_cgcm2_3_2a | 0.871 | 11 | 2.968 | 9 | 3.072 | 9 |
| ncar_ccsm3_0 | 0.937 | **2** | 2.438 | 20 | 2.542 | 20 |
| ncar_pcm1 | 0.726 | 19 | 2.339 | 22 | 2.443 | 22 |
| ukmo_hadcm3 | 0.895 | 8 | 3.387 | **4** | 3.491 | **4** |

| Section 1 (Temperature) | | | | | | |
|---|---|---|---|---|---|---|
| **Models** | **Observed data+traditional approach** | | **Observed data+bin scores approach** | | **Observed and Reanalysis data+skill** | |
| | *Skill score (out of 1)* | *Rank* | *Skill score (x10-3)* | *Rank* | *Skill score (x10-3)* | *Rank* |
| bccr_bcm2_0 | 0.899 | 10 | 6.193 | 18 | 5.563 | 18 |
| cccma_cgcm3_1 | 0.9 | 9 | 7.372 | **1** | 6.450 | **1** |
| cccma_cgcm3_1_t63 | 0.907 | 8 | 6.531 | 11 | 5.735 | 14 |
| cnrm_cm3 | 0.836 | 19 | 6.553 | 8 | 5.671 | 15 |
| csiro_mk3_0 | 0.887 | 12 | 6.535 | 10 | 5.924 | 7 |
| csiro_mk3_5 | 0.947 | **2** | 6.492 | 13 | 5.831 | 11 |
| gfdl_cm2_0 | 0.896 | 11 | 0.688 | 22 | 5.583 | 17 |
| gfdl_cm2_1 | 0.936 | **3** | 6.662 | **5** | 6.003 | **4** |
| giss_aom | 0.914 | **6** | 6.888 | **3** | 5.990 | **5** |
| giss_model_e_h | 0.568 | 22 | 6.856 | **4** | 6.006 | **3** |
| giss_model_e_r | 0.686 | 21 | 6.500 | 12 | 5.770 | 12 |
| iap_fgoals1_0_g | 0.883 | 14 | 6.330 | 16 | 5.558 | 19 |
| ingv_echam4 | 0.848 | 16 | 6.568 | 7 | 5.974 | **6** |
| ipsl_cm4 | 0.839 | 18 | 6.295 | 17 | 5.643 | 16 |
| miroc3_2_hires | 0.861 | 15 | 6.546 | 9 | 5.903 | 8 |
| miroc3_2_medres | 0.913 | 7 | 6.460 | 14 | 5.848 | 10 |
| miub_echo_g | 0.845 | 17 | 6.186 | 19 | 5.359 | 20 |
| mpi_echam5 | 0.947 | **1** | 7.372 | **2** | 6.446 | **2** |
| mri_cgcm2_3_2a | 0.924 | **5** | 6.603 | **6** | 5.762 | 13 |
| ncar_ccsm3_0 | 0.885 | 13 | 5.945 | 21 | 5.335 | 21 |
| ncar_pcm1 | 0.831 | 20 | 6.008 | 20 | 5.280 | 22 |
| ukmo_hadcm3 | 0.935 | **4** | 6.403 | 15 | 5.848 | 9 |

| Section 2 (Temperature) | | | | | | |
|---|---|---|---|---|---|---|
| **Models** | **Observed data+traditional approach** | | **Observed data+bin scores approach** | | **Observed and Reanalysis data+skill** | |
| | *Skill score (out of 1)* | *Rank* | *Skill score (x10-3)* | *Rank* | *Skill score (x10-3)* | *Rank* |
| bccr_bcm2_0 | 0.849 | 16 | 6.533 | 15 | 7.034 | 12 |
| cccma_cgcm3_1 | 0.863 | 13 | 7.778 | **1** | 7.972 | **1** |
| cccma_cgcm3_1_t63 | 0.882 | 8 | 6.911 | 8 | 7.055 | 11 |
| cnrm_cm3 | 0.842 | 17 | 6.658 | 14 | 6.892 | 14 |
| csiro_mk3_0 | 0.879 | 10 | 6.786 | 13 | 7.332 | **2** |
| csiro_mk3_5 | 0.761 | **22** | 6.118 | 22 | 6.736 | 21 |
| gfdl_cm2_0 | 0.916 | 2 | 7.001 | **5** | 6.880 | 15 |
| gfdl_cm2_1 | 0.908 | **4** | 7.001 | **6** | 7.001 | 13 |
| giss_aom | 0.892 | **7** | 7.124 | **3** | 7.135 | 8 |
| giss_model_e_h | 0.861 | 15 | 6.876 | 10 | 7.259 | **3** |
| giss_model_e_r | 0.900 | 6 | 7.052 | **4** | 7.158 | **5** |
| iap_fgoals1_0_g | 0.880 | 9 | 6.877 | 9 | 7.108 | **9** |
| ingv_echam4 | 0.810 | 19 | 6.494 | 16 | 7.156 | **6** |
| ipsl_cm4 | 0.870 | 12 | 6.801 | 12 | 6.846 | 17 |
| miroc3_2_hires | 0.810 | 20 | 6.493 | 17 | 7.065 | 10 |
| miroc3_2_medres | 0.775 | 21 | 6.207 | 21 | 6.873 | 16 |
| miub_echo_g | 0.878 | 11 | 6.972 | 7 | 6.832 | 18 |
| mpi_echam5 | 0.999 | **1** | 7.326 | **2** | 7.217 | **4** |
| mri_cgcm2_3_2a | 0.862 | **14** | 6.838 | 11 | 7.144 | 7 |
| ncar_ccsm3_0 | 0.905 | 5 | 6.356 | 19 | 6.813 | 20 |
| ncar_pcm1 | 0.910 | 3 | 6.324 | 20 | 6.518 | 22 |
| ukmo_hadcm3 | 0.835 | **18** | 6.368 | 18 | 6.816 | 19 |

| Section 3 (Temperature) | | | | | | |
|---|---|---|---|---|---|---|
| **Models** | **Observed data+traditional approach** | | **Observed data+bin scores approach** | | **Observed and Reanalysis data+skill** | |
| | *Skill score (out of 1)* | *Rank* | *Skill score (x10-3)* | *Rank* | *Skill score (x10-3)* | *Rank* |
| bccr_bcm2_0 | 0.838 | 16 | 6.947 | 16 | 7.054 | 16 |
| cccma_cgcm3_1 | 0.867 | 11 | 7.238 | 10 | 7.347 | 10 |
| cccma_cgcm3_1_t63 | 0.866 | 13 | 7.154 | 12 | 7.226 | 12 |
| cnrm_cm3 | 0.830 | 18 | 7.014 | 15 | 7.173 | 14 |
| csiro_mk3_0 | 0.867 | 12 | 7.230 | 11 | 7.363 | 9 |
| csiro_mk3_5 | 0.769 | 22 | 6.567 | 19 | 6.689 | 19 |
| gfdl_cm2_0 | 0.871 | 10 | 7.091 | 13 | 7.068 | 15 |
| gfdl_cm2_1 | 0.910 | **5** | 7.596 | **5** | 7.616 | **5** |
| giss_aom | 0.875 | 8 | 7.388 | 7 | 7.510 | 7 |
| giss_model_e_h | 0.910 | **4** | 7.705 | **3** | 7.826 | **3** |
| giss_model_e_r | 0.913 | **3** | 7.713 | **2** | 7.842 | **2** |
| iap_fgoals1_0_g | 0.915 | **2** | 7.648 | **4** | 7.734 | **4** |
| ingv_echam4 | 0.780 | 21 | 6.489 | 21 | 6.586 | 21 |
| ipsl_cm4 | 0.879 | 7 | 7.289 | 8 | 7.332 | 11 |
| miroc3_2_hires | 0.838 | 17 | 7.052 | 14 | 7.224 | 13 |
| miroc3_2_medres | 0.813 | 20 | 6.845 | 17 | 7.010 | 17 |
| miub_echo_g | 0.854 | 14 | 7.268 | 9 | 7.375 | 8 |
| mpi_echam5 | 0.930 | **1** | 7.879 | **1** | 7.995 | **1** |
| mri_cgcm2_3_2a | 0.893 | **6** | 7.509 | **6** | 7.582 | **6** |
| ncar_ccsm3_0 | 0.874 | 9 | 6.557 | 20 | 6.681 | 20 |
| ncar_pcm1 | 0.842 | 15 | 6.161 | 22 | 6.283 | 22 |
| ukmo_hadcm3 | 0.813 | 19 | 6.715 | 18 | 6.724 | 18 |

# Appendix F: Selected future extreme precipitation-temperature combinations

**Table 11** . Extreme precipitation-temperature combinations selected for gauging stations within the Grand River at Brantford catchment (2050s)

| Station | Cold-Dry | | Hot-Humid | | Hot-Dry | | Cold-Humid | |
|---|---|---|---|---|---|---|---|---|
| | *PPT* | *Tmean* | *PPT* | *Tmean* | *PPT* | *Tmean* | *PPT* | *Tmean* |
| Apps mill | 1.877 | 10.077 | 2.373 | 13.672 | 0.290 | 12.021 | 2.363 | 10.775 |
| Arthur | 2.433 | 8.452 | 2.951 | 12.000 | 0.395 | 10.317 | 3.050 | 9.118 |
| Ayr | 1.882 | 9.954 | 2.499 | 13.581 | 0.297 | 11.946 | 2.421 | 10.699 |
| Blue acton | 1.652 | 9.591 | 2.336 | 13.123 | 0.281 | 11.473 | 2.227 | 10.312 |
| Blue corwhin | 1.682 | 9.667 | 2.388 | 13.202 | 0.289 | 11.604 | 2.199 | 10.360 |
| Blue rockwood | 1.754 | 9.616 | 2.384 | 13.150 | 0.289 | 11.490 | 2.365 | 10.339 |
| Blue scout | 1.639 | 9.575 | 2.267 | 13.140 | 0.291 | 11.484 | 2.183 | 10.247 |
| Blue springs creek | 0.324 | 10.712 | 2.766 | 12.462 | 0.343 | 10.797 | 2.767 | 9.586 |
| Brantford morell | 1.804 | 9.974 | 2.474 | 13.551 | 0.276 | 11.968 | 2.337 | 10.675 |
| Burford | 1.771 | 10.111 | 2.529 | 13.667 | 0.293 | 12.060 | 2.331 | 10.799 |
| Cambridge galt moe | 2.243 | 9.063 | 2.845 | 12.596 | 0.342 | 10.968 | 2.867 | 9.751 |
| Cambridge-stewart | 2.255 | 9.890 | 2.897 | 13.447 | 0.348 | 11.811 | 2.855 | 10.601 |
| Canning | 1.832 | 9.926 | 2.596 | 13.486 | 0.277 | 11.878 | 2.575 | 10.667 |
| Cathcart | 1.766 | 10.076 | 2.535 | 13.639 | 0.277 | 12.085 | 2.515 | 10.835 |
| Crewsons corners | 0.319 | 11.356 | 2.668 | 13.127 | 0.325 | 11.462 | 2.631 | 10.273 |
| Damascus | 1.857 | 9.173 | 2.531 | 12.714 | 0.312 | 11.084 | 2.437 | 9.857 |
| Drumbo | 1.919 | 10.003 | 2.506 | 13.570 | 0.304 | 13.600 | 2.421 | 10.690 |
| Drumbo harrington | 0.309 | 11.887 | 2.565 | 13.653 | 0.315 | 11.992 | 2.580 | 10.770 |
| Elmira | 0.314 | 11.174 | 2.984 | 12.901 | 0.326 | 11.239 | 2.606 | 10.033 |
| Elora automatic climate station | 1.840 | 8.995 | 2.563 | 12.515 | 0.292 | 10.863 | 2.622 | 9.686 |
| Elora rcs | 1.791 | 9.532 | 2.453 | 13.133 | 0.456 | 11.510 | 2.385 | 10.271 |
| Elora research stn | 0.312 | 10.587 | 2.514 | 12.249 | 0.332 | 10.687 | 2.745 | 9.458 |
| Falkland | 0.301 | 11.955 | 2.534 | 13.689 | 0.296 | 12.033 | 2.525 | 10.761 |
| Fergus moe | 2.245 | 9.240 | 2.888 | 12.741 | 0.344 | 11.164 | 3.000 | 9.932 |
| Fergus shand dam | 2.330 | 7.481 | 2.828 | 11.010 | 0.371 | 9.390 | 3.125 | 8.192 |
| Glen allan | 2.408 | 7.673 | 3.141 | 11.228 | 0.402 | 9.613 | 3.215 | 8.385 |
| Grand valley wpcp | 0.338 | 9.909 | 2.502 | 11.648 | 0.334 | 9.948 | 2.607 | 8.775 |
| Guelph arboretum | 2.103 | 8.758 | 2.515 | 12.362 | 0.327 | 10.684 | 2.657 | 9.494 |
| Guelph oac | 1.771 | 9.594 | 2.319 | 13.205 | 0.289 | 11.570 | 2.283 | 10.330 |
| Guelph oac physics dept | 0.307 | 10.884 | 2.607 | 12.636 | 0.326 | 10.993 | 2.732 | 9.758 |
| Guelph turfgrass cs | 1.714 | 9.631 | 2.334 | 13.233 | 0.287 | 11.605 | 2.349 | 10.364 |
| **Station** | **Cold-Dry** | | **Hot-Humid** | | **Hot-Dry** | | **Cold-Humid** | |

| | *PPT* | *Tmean* | *PPT* | *Tmean* | *PPT* | *Tmean* | *PPT* | *Tmean* |
|---|---|---|---|---|---|---|---|---|
| Hillsburgh | 1.800 | 8.888 | 2.480 | 12.499 | 0.290 | 10.818 | 2.536 | 9.721 |
| Kitchener city eng 1 | 1.864 | 9.859 | 2.429 | 13.473 | 0.306 | 11.842 | 2.458 | 10.598 |
| Kitchener city eng 2 | 0.320 | 11.764 | 2.741 | 13.516 | 0.335 | 11.859 | 2.881 | 10.640 |
| Kitchener owrc | 1.786 | 9.766 | 2.479 | 13.371 | 0.296 | 11.745 | 2.362 | 10.502 |
| Kitchener/waterloo | 0.369 | 11.197 | 2.917 | 12.882 | 0.368 | 11.242 | 2.857 | 10.047 |
| Millers lake | 1.843 | 9.657 | 2.669 | 13.282 | 0.299 | 11.625 | 2.646 | 10.381 |
| Monticello | 2.594 | 6.852 | 3.173 | 10.384 | 0.416 | 8.763 | 3.396 | 7.579 |
| Morriston | 1.845 | 9.695 | 2.612 | 13.247 | 0.288 | 11.646 | 2.433 | 10.431 |
| Newton | 0.317 | 10.831 | 2.577 | 12.588 | 0.325 | 10.939 | 2.512 | 9.700 |
| Newton | 1.738 | 9.498 | 2.250 | 13.125 | 0.282 | 11.466 | 2.277 | 10.285 |
| Paris | 0.291 | 11.937 | 2.429 | 13.647 | 0.297 | 12.028 | 2.372 | 10.755 |
| Preston | 2.166 | 9.840 | 2.898 | 13.429 | 0.336 | 11.750 | 3.126 | 10.555 |
| Preston wpcp | 0.388 | 10.515 | 3.024 | 12.248 | 0.385 | 10.611 | 3.051 | 9.372 |
| Salem | 1.807 | 9.374 | 2.499 | 12.933 | 0.283 | 11.309 | 2.524 | 10.122 |
| Waldemar | 0.339 | 9.808 | 2.938 | 11.592 | 0.341 | 9.905 | 3.040 | 8.705 |
| Waterloo fire hall | 1.798 | 9.892 | 2.406 | 13.406 | 0.306 | 11.798 | 2.427 | 10.560 |
| Waterloo wellington 2 | 1.800 | 9.778 | 2.477 | 13.385 | 0.296 | 11.757 | 2.366 | 10.514 |
| Waterloo wellington A | 0.341 | 10.427 | 2.751 | 12.133 | 0.343 | 10.478 | 2.837 | 9.275 |
| Waterloo wpcp | 2.335 | 9.850 | 2.861 | 13.440 | 0.354 | 11.810 | 2.873 | 10.567 |

**Table 12** Extreme precipitation-temperature combinations selected for gauging stations within the Grand River at Brantford catchment (2090s)

| Station | Cold-Dry | | Hot-Humid | | Hot-Dry | | Cold-Humid | |
|---|---|---|---|---|---|---|---|---|
| | *PPT* | *Tmean* | *PPT* | *Tmean* | *PPT* | *Tmean* | *PPT* | *Tmean* |
| Apps mill | 0.299 | 11.571 | 2.588 | 13.698 | 0.288 | 14.046 | 2.159 | 11.140 |
| Arthur | 0.394 | 10.039 | 3.200 | 12.032 | 0.413 | 12.313 | 2.844 | 9.455 |
| Ayr | 0.316 | 11.588 | 2.690 | 13.607 | 0.310 | 13.902 | 2.172 | 11.033 |
| Blue acton | 0.284 | 11.127 | 2.365 | 13.179 | 0.279 | 13.447 | 1.999 | 10.587 |
| Blue corwhin | 0.296 | 11.236 | 2.449 | 13.259 | 0.291 | 13.588 | 2.046 | 10.666 |
| Blue rockwood | 0.294 | 11.183 | 2.377 | 13.206 | 0.286 | 13.441 | 2.066 | 10.615 |
| Blue scout | 0.291 | 11.113 | 2.404 | 13.165 | 0.292 | 13.432 | 2.048 | 10.575 |
| Blue springs creek | 0.332 | 10.467 | 2.904 | 12.405 | 0.340 | 12.723 | 2.520 | 9.911 |
| Brantford morell | 0.303 | 11.644 | 2.459 | 13.570 | 0.291 | 13.982 | 2.028 | 11.054 |
| Burford | 0.299 | 11.784 | 2.661 | 13.666 | 0.296 | 14.070 | 2.064 | 11.143 |
| Cambridge galt moe | 0.370 | 10.542 | 2.949 | 12.673 | 0.356 | 12.963 | 2.509 | 10.096 |
| Cambridge-stewart | 0.366 | 11.495 | 3.133 | 13.408 | 0.355 | 13.775 | 2.694 | 10.930 |
| Canning | 0.301 | 11.574 | 2.543 | 13.559 | 0.304 | 13.900 | 2.161 | 10.978 |
| Cathcart | 0.298 | 11.817 | 2.699 | 13.683 | 0.283 | 14.063 | 2.130 | 11.156 |
| Crewsons corners | 0.341 | 11.184 | 2.577 | 13.167 | 0.323 | 13.434 | 2.362 | 10.580 |
| Damascus | 0.322 | 10.783 | 2.628 | 12.766 | 0.332 | 13.000 | 2.210 | 10.196 |
| Drumbo | 0.312 | 11.665 | 2.590 | 13.624 | 0.305 | 13.957 | 2.185 | 11.049 |
| Drumbo harrington | 0.336 | 11.687 | 2.892 | 13.679 | 0.324 | 14.013 | 2.490 | 11.131 |
| Elmira | 0.345 | 10.898 | 2.711 | 12.926 | 0.329 | 13.222 | 2.403 | 10.355 |
| Elora automatic climate station | 0.320 | 10.544 | 2.641 | 12.500 | 0.309 | 12.918 | 2.138 | 9.999 |
| Elora rcs | 0.425 | 11.031 | 2.489 | 13.165 | 0.316 | 13.457 | 2.140 | 10.586 |
| Elora research stn | 0.343 | 10.329 | 2.696 | 12.274 | 0.339 | 12.701 | 2.319 | 9.792 |
| Falkland | 0.329 | 11.709 | 2.696 | 13.621 | 0.307 | 14.096 | 2.162 | 11.133 |
| Fergus moe | 0.374 | 10.842 | 3.053 | 12.768 | 0.363 | 13.155 | 2.586 | 10.263 |
| Fergus shand dam | 0.409 | 9.030 | 2.898 | 11.096 | 0.375 | 11.327 | 2.601 | 8.529 |
| Glen allan | 0.422 | 9.332 | 2.938 | 11.226 | 0.412 | 11.585 | 2.803 | 8.734 |
| Grand valley wpcp | 0.351 | 9.671 | 2.780 | 11.686 | 0.341 | 11.918 | 2.532 | 9.105 |
| Guelph arboretum | 0.327 | 10.398 | 2.684 | 12.396 | 0.327 | 12.674 | 2.331 | 9.808 |
| Guelph oac | 0.304 | 11.093 | 2.498 | 13.131 | 0.297 | 13.511 | 2.106 | 10.642 |
| Guelph oac physics dept | 0.322 | 10.675 | 2.681 | 12.665 | 0.329 | 12.999 | 2.297 | 10.074 |
| Guelph turfgrass cs | 0.292 | 11.127 | 2.467 | 13.201 | 0.288 | 13.548 | 2.072 | 10.674 |
| Haysville | 0.321 | 11.641 | 2.778 | 13.593 | 0.310 | 13.927 | 2.347 | 11.022 |
| Hillsburgh | 0.321 | 10.531 | 2.778 | 12.527 | 0.310 | 12.788 | 2.347 | 9.933 |
| Kitchener | 0.324 | 11.362 | 2.689 | 13.399 | 0.316 | 13.793 | 2.165 | 10.917 |
| Kitchener city eng 1 | 0.323 | 11.362 | 2.684 | 13.399 | 0.316 | 13.793 | 2.162 | 10.917 |
| Kitchener city eng 2 | 0.339 | 11.588 | 2.973 | 13.441 | 0.334 | 13.874 | 2.511 | 10.985 |

| Station | Cold-Dry | | Hot-Humid | | Hot-Dry | | Cold-Humid | |
|---|---|---|---|---|---|---|---|---|
| | *PPT* | *Tmean* | *PPT* | *Tmean* | *PPT* | *Tmean* | *PPT* | *Tmean* |
| Kitchener owrc | 0.296 | 11.265 | 2.513 | 13.403 | 0.299 | 13.695 | 2.136 | 10.817 |
| Kitchener/waterloo | 0.383 | 10.942 | 2.972 | 12.872 | 0.376 | 13.237 | 2.673 | 10.375 |
| Millers lake | 0.322 | 11.387 | 2.923 | 13.251 | 0.329 | 13.645 | 2.242 | 10.734 |
| Monticello | 0.437 | 8.447 | 3.474 | 10.408 | 0.448 | 10.701 | 2.882 | 7.903 |
| Morriston | 0.297 | 11.330 | 2.608 | 13.323 | 0.299 | 13.623 | 2.123 | 10.730 |
| Newton | 0.339 | 10.578 | 2.542 | 12.534 | 0.334 | 12.901 | 2.234 | 10.065 |
| Newton | 0.303 | 11.226 | 2.460 | 13.152 | 0.286 | 13.480 | 2.168 | 10.585 |
| Paris | 0.303 | 11.735 | 2.611 | 13.614 | 0.300 | 14.015 | 2.177 | 11.098 |
| Preston | 0.356 | 11.336 | 3.033 | 13.411 | 0.343 | 13.760 | 2.619 | 10.891 |
| Preston wpcp | 0.417 | 10.282 | 3.137 | 12.209 | 0.405 | 12.584 | 2.803 | 9.722 |
| Salem | 0.311 | 11.028 | 2.506 | 12.985 | 0.311 | 13.315 | 2.205 | 10.410 |
| Waldemar | 0.367 | 9.576 | 3.233 | 11.618 | 0.364 | 11.840 | 2.633 | 9.036 |
| Waterloo fire hall | 0.326 | 11.347 | 2.576 | 13.383 | 0.314 | 13.767 | 2.224 | 10.903 |
| Waterloo wellington 2 | 0.295 | 11.278 | 2.524 | 13.417 | 0.299 | 13.710 | 2.135 | 10.830 |
| Waterloo wellington A | 0.332 | 10.237 | 2.936 | 12.112 | 0.352 | 12.490 | 2.667 | 9.608 |
| Waterloo wpcp | 0.388 | 11.450 | 2.971 | 13.366 | 0.352 | 13.759 | 2.656 | 10.889 |

# Appendix G: Percent changes in flood quantiles projected for future timelines

**Table 13** Percent changes in 2, 5, 10, 25 and 100 year return period flood quantiles projected for 2050s and 2090s (Results have been rounded off to nearest the whole number)

| Scenarios(2050s) | Brantford | | | | | Galt | | | | | West Montrose | | | | |
|---|---|---|---|---|---|---|---|---|---|---|---|---|---|---|---|
| | 2 | 5 | 10 | 25 | 100 | 2 | 5 | 10 | 25 | 100 | 2 | 5 | 10 | 25 | 100 |
| Max Temp Var+Cold and Dry | -61 | -58 | -56 | -54 | -51 | -59 | -65 | -68 | -72 | -76 | -40 | -59 | -62 | -60 | -48 |
| Max Temp Var+Cold and Humid | -23 | -26 | -31 | -36 | -42 | -30 | -41 | -48 | -55 | -62 | -9 | -40 | -51 | -60 | -67 |
| Max Temp Var+Hot and Dry | -84 | -87 | -89 | -90 | -91 | -73 | -80 | -83 | -86 | -89 | -40 | -60 | -67 | -72 | -77 |
| Max Temp Var+Hot and Humid | -23 | -24 | -27 | -32 | -37 | -33 | -43 | -49 | -56 | -63 | -12 | -44 | -55 | -63 | -70 |
| Min Temp Var+Cold and Dry | -61 | -58 | -56 | -53 | -51 | -59 | -65 | -68 | -72 | -76 | -31 | -53 | -62 | -68 | -74 |
| Min Temp Var+Cold and Humid | -18 | -22 | -27 | -32 | -38 | -30 | -41 | -48 | -55 | -62 | -15 | -41 | -52 | -60 | -67 |
| Min Temp Var+Hot and Dry | -84 | -87 | -89 | -90 | -91 | -73 | -80 | -83 | -86 | -89 | -40 | -60 | -67 | -72 | -77 |
| Min Temp Var+Hot and Humid | -23 | -24 | -27 | -32 | -37 | -33 | -43 | -49 | -56 | -63 | -12 | -44 | -55 | -63 | -70 |
| **Scenarios (2090s)** | **Brantford** | | | | | **Galt** | | | | | **West Montrose** | | | | |
| | 2 | 5 | 10 | 25 | 100 | 2 | 5 | 10 | 25 | 100 | 2 | 5 | 10 | 25 | 100 |
| Max Temp Var+Cold and Dry | -84 | -87 | -89 | -90 | -91 | -70 | -79 | -83 | -86 | -89 | -40 | -60 | -67 | -72 | -77 |
| Max Temp Var+Cold and Humid | -29 | -31 | -35 | -39 | -44 | -44 | -53 | -58 | -64 | -69 | -24 | -47 | -56 | -63 | -70 |
| Max Temp Var+Hot and Dry | -84 | -87 | -89 | -90 | -91 | -73 | -80 | -83 | -86 | -89 | -40 | -60 | -67 | -72 | -77 |
| Max Temp Var+Hot and Humid | -19 | -17 | -18 | -21 | -25 | -33 | -39 | -43 | -48 | -54 | -14 | -42 | -53 | -61 | -68 |
| Min Temp Var+Cold and Dry | -84 | -87 | -89 | -90 | -91 | -73 | -80 | -83 | -86 | -89 | -40 | -60 | -67 | -72 | -77 |
| Min Temp Var+Cold and Humid | -29 | -31 | -35 | -39 | -44 | -44 | -53 | -58 | -64 | -69 | -24 | -47 | -56 | -63 | -70 |
| Min Temp Var+Hot and Dry | -84 | -87 | -89 | -90 | -91 | -73 | -80 | -83 | -86 | -89 | -40 | -60 | -67 | -72 | -77 |
| Min Temp Var+Hot and Humid | -19 | -17 | -18 | -21 | -25 | -33 | -39 | -43 | -48 | -54 | -23 | -44 | -53 | -60 | -67 |

# Appendix H: CDFs of historical and projected future flows at Galt and West Montrose

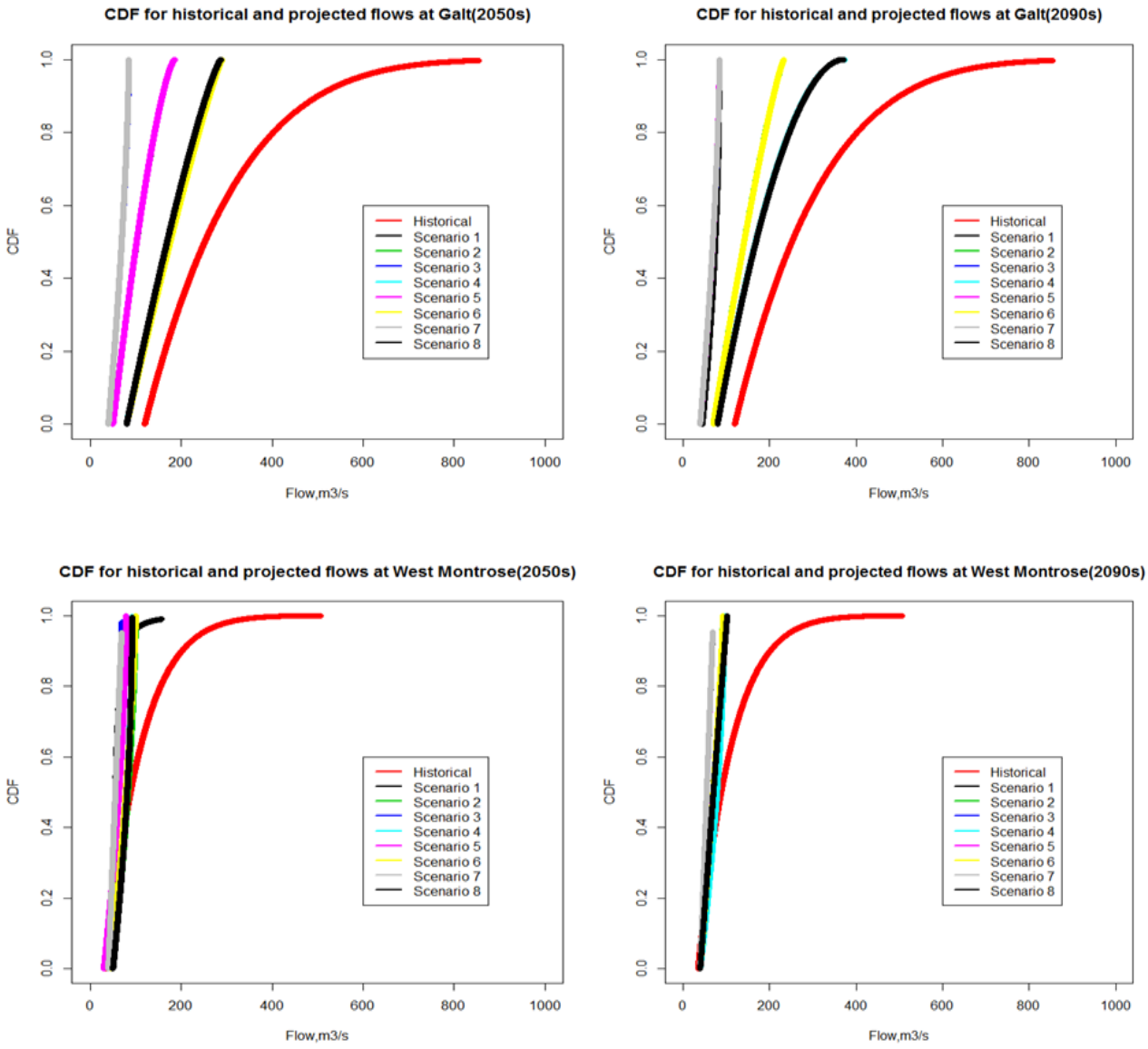


**Figure 236** CDFs of historical and projected future flows at Galt and West Montrose

# CURRICULUM VITAE

| | |
|---|---|
| **Name:** | Abhishek Gaur |
| **Post-secondary Education and Degrees:** | National Institute of Technology<br>Durgapur, West Bengal, India<br>2006-2010 B-Tech. |
| **Related Work Experience** | Teaching Assistant<br>Western University<br>2011-2013 |